UNIVERSIDAD CARLOS III DE MADRID
ESCUELA POLITÉCNICA SUPERIOR

INGENIERÍA DE TELECOMUNICACIONES

PROYECTO FIN DE CARRERA

Evaluating the Effective Diversity Gain on Laptop Antennas

Autora: Laura Cañizares Lozano
Tutores: Daniel Segovia Vargas y Kent Rosengren

27 de febrero de 2008

EVALUATING THE EFFECTIVE DIVERSITY GAIN ON LAPTOP ANTENNAS

Laura Cañizares Lozano

Supervisor: Kent Rosengren (Ethertronics)
Examiner: Prof. Per-Simon Kildal

CHALMERS

Antenna Group
Department of Signals and Systems
CHALMERS UNIVERSITY OF TECHNOLOGY
Göteborg, Sweden
&
ETHERTRONICS Sweden AB
Kalmar, Sweden

ethertronics
shaping antenna technology™

A mis padres y mi hermano,
por quererme tanto…

Con el tiempo uno aprende...
(J. L. Borges)

Abstract

In the past few years the demand of high data transmission rates for video, image and other communications has increased. Therefore, a lot of research has been done to improve the link budget between mobile and base station. Multiple Input and Multiple Output (MIMO) systems have been introduced in the recent years using the decorrelation of signals coming from the overall multipath environment. In such systems, the capacity in communication links depends on signal to noise ratio and also on signal correlation when many antennas receive the transmitted signal. The correlation also plays a large role in diversity schemes but the radiation efficiency is often the main limiting factor of the effective diversity gain.

The aim of the thesis is to study the influence of the radiation efficiency and correlation on the effective diversity gain between the antenna elements by varying the source impedance. The source impedance is altered within practical limits and the effective diversity gain is calculated for these source impedances. Support simulations have been performed using CST Microwave Studio and analyzed using a software called Multi-Port Antenna evaluator (MPA) developed in CHASE. Several examples are successively treated, starting from two parallel dipoles to prove the correct performance of the MPA software. Thereafter five and three antenna configurations are considered on a laptop.

For our proposed laptop example, firstly one antenna port will be designed to fulfil an antenna specification for the W-CDMA plus WLAN bands. Later on, this dual band antenna will be added in a realistic laptop model done with CST in order to build it later and to compare it to simulated results. Two simulated cases are covered. In the first one, five antenna ports separated 2.8 cm is studied. In this case, a real laptop model including the designed antennas will be built and measured using a network analyzer and a reverberation chamber. In the second case, just three antenna ports are included and the spacing between them is only 1 cm, to increase the coupling between the ports.

We propose a method in which we vary the source impedance and show that this can improve the effective diversity systems. The method is also applicable when designing antennas for MIMO-systems since radiation efficiency and correlation are design parameters also here.

Index

List of Figures

Figures from Appendix A:

Figures from Appendix B:

Figures from Appendix C:

List of Tables

Preface

This Master Thesis was born at Chalmers University of Technology in Göteborg, while attending the antenna course given by Professor Per-Simon Kildal. Although I was just an Erasmus student for one year, when this opportunity arouse, I felt the need of staying more in Sweden to make the most of it. This thesis was a proposed project on Multiple Input Multiple Output (MIMO) terminals by Flextronics Antenna Design in Kalmar within Chalmers Antenna Systems Excellence centre[1] (CHASE). During the development of this thesis, the Flextronics Antenna Technology group was totally acquired by Ethertronics Sweden AB. It entailed many changes to the office and fortunately, Ethertronics maintained my project and I was able to finish it within 6 months during the autumn and winter 2007.

I moved to Kalmar in September 2007 and I had started to work on this thesis every day at the office. At the beginning, some literature reading was done in order to acquire information about important previously published results necessary to develop this thesis. During the first weeks, and after being familiarized with the CST Studio Design Software [1], the laptop model was designed. Following a real example, a simulated laptop design was implemented in order to perform simulations on it when placing the antennas on it.

The first prototypes of antennas were done and simulations were performed for more than a month using CST, prior to construction. Later on, with the inestimable help of my supervisor, Kent Rosengren, the real laptop started to be modified in order to implement real antennas on it. The implementation of the antennas took me a couple of weeks, to adjust them to the desired frequency bands and to obtain some measurements results of their performance using a network analyzer. In the model we included 5 antenna elements separated by 2.8 cm and using all the available space on top of the laptop, as we expected to have a high coupling between them and thus, a high correlation too. However, the performance differed from our initial expectations.

The simulated antennas were improved to make them equal to the real ones. The simulated results were taken as initial values and later on, we studied how the source impedance of all antenna ports could influence the performance of our diversity system.

[1] CHASE is a VINN Excellence centre within antenna systems at Chalmers University of Technology (Sweden). The centre covers the research areas such as antennas, signals, systems, electromagnetic computations, medical engineering and biological effects of microwaves. Not only Chalmers participates actively in CHASE projects, but also 15 Swedish companies in market areas such as wireless communications, satellite communications, medical technology and sensing.

During those initial months, I had been trying to use simulation results from CST imported to the Multi-Port Analyzer (MPA) and the Circuit Simulator (CircSim). As it was the first time all the programs were used together, some unexpected results and errors were found. However, thanks to Kristian Karlsson and Jan Carlsson from SP [2], the interaction between the programs and the complete evaluation of MPA was performed after three months. Firstly, two parallel dipoles were taken as initial example. Their performance was studied and compared to previously published results as in [3], [4] and [5]. Several simulations were done to study different parameter influences on them.

It has to be mentioned that we had problems to get the optimizer tool provided by MPA working properly and we were not able use it to add lumped components to our design cases.

Later on, after the laptop simulations had been performed, we obtained real results for our real model. As mentioned before, some measurements were taken from the network analyzer and the model was also measured in the reverberation chamber that Ethertronics has in its facilities to obtain the total radiation efficiency, the power correlation and the diversity gain between the antennas. The measured values were compared to the simulated ones. All the measurements and mock-up building took us a month.

As we were not able to make use of MPA to optimize the model by adding lumped components, we decided to use our own optimization procedure and we made a study of the source impedance influence in our model. Varying the source impedance, we studied the impact it had in our antenna specifications. This approach was just followed for simulations, because in practice, an impedance transformation will be added to the antenna ports in the real laptop model.

Opposite to what we expected, the obtained simulated and measured correlation was extremely low. So we tried to increase the coupling between our antenna elements with a second simulated example. We located closely just three antennas in our model, separated by 1 cm. As expected, the coupling between them was higher and consequently, the effective diversity gain was worse. We also studied the influence of the source impedance in this three-antenna case.

During all the thesis time, we had several CHASE meetings in different places in Sweden. We presented our objectives and intermediate results in all of them, showing the evolution of the thesis. Participants in our group, subgroup 2.2, helped us also to clarify our following steps on the evolution of the project.

Acknowledgments

I cannot miss the opportunity to thank all the people that somehow made this thesis possible because all of them are part of me and therefore, part of it too.

Firstly, I would like to thank Professor Per-Simon Kildal for his motivating antenna course and because he transmitted me his interest in antennas as no other could have done it. He also gave me the opportunity to participate in this thesis project. I recall with particular gratitude the guidance, time and encouragement of my supervisor, Kent Rosengren, who assisted me in this thesis. He has been so helpful, patient and incredibly enthusiastic and he always had great suggestions and corrections. Tack så mycket! And of course, to my coordinator at Madrid, Daniel Segovia, for all his help during the exchange.

Thanks to all my Ethertronics (and Flex) workmates for the great atmosphere at the company. They gave me their time and their knowledge when I needed it. Thanks especially to Carmen, more than just a workmate. Thanks for her sincere friendship, her energy and her altruistic help in everything. My appreciation to Kristian Karlsson and Jan Carlsson for helping me with MPA and CircSim so kindly. And also to Laurent Desclos for all his time and valuable comments which helped me so much. Thanks to my Endesa workmates that encouraged me during the last stage of my degree.

Thanks to all my friends from Carlos III University who helped me through the most difficult years of my degree in Madrid and also when I came to Sweden. They transformed our stressful days into days of laughs. Especially to Patri, David, Myriam, María, Vicky and Blanca for their encouragement and our good moments.

Thanks to all my friends from Chalmers University who shared the incredibly Erasmus experience with me. It was not just one more year! Thanks to Laura and Natalia, for their support, for listening to me so many times and for the friendship they have given to me. Thanks to all the Högsbo family, especially to Guzmán, Miguel and Dominik, for their happiness. And to Fabien for the moments and the friendship.

I would like to thank all my friends for every single moment that we have spent together and for sharing so much with me. You are so nice! Especially to Lucía, who was close to me since kindergarten for her company all these years and for being so friendly. And also to Mamen for her words, her amity and for being so kind always.

I must thank David for his patience, insight, tenderness and motivation. He always believed in me and supported me along this way. Meeting him has been a gift.

Last but not least, my truthful gratitude to my beloved parents, Piedad and Manuel, because they taught me all! I am filled with admiration at their example, for being so loving, supportive and protective. They gave me everything and there are not words to convey my gratitude. Thanks to my wonderful brother Víctor, always so generous, sincere and kind-hearted. And in general to my whole family, for their affection and constant support and especially to my grandparents.

… Because I would not have done it without all you and I would not be who I am…
¡Gracias de corazón a todos!

1. Initial description

As mentioned in the abstract, we will see how the effective diversity gain can be influenced by our proposed method. The correlation between different antenna ports situated on a laptop will be also minimized. However, the limiting factor for the effective diversity gain will be proved to be the radiation efficiency in the provided example. Both simulations and measurements will be performed. The procedure that will be followed consists in a variation of the source impedance that will influence the total radiation efficiency, the correlation and the effective diversity gain.

The covered frequency bands that will be studied are W-CDMA (1920-2170 MHz) and WLAN (2.4 GHz). As specifications for this thesis, both of them must have a return loss better than 6 dB, radiation efficiency higher than 50% and a correlation coefficient approximately of 0.05.

This thesis is organized as follows: in chapter 2 of this report, a theoretical background is included. It will cover the most important theory aspects used for this thesis as well as the basic antennas that will be modified to develop the objectives of this thesis. An explanation of the frequency bands that will be considered is also included in this part.

A brief explanation of the software used can be seen in chapter 3. It includes a brief description of CST Microwave Studio and of the Multiport Analyzer (MPA) provided by CHASE. Besides, two parallel dipoles are used as a simple application example. Several simulations of a two parallel dipoles case are performed to compare them with previously published results in order to see the correct performance of the MPA. Using MPA, the radiation efficiency, the magnitude of the complex correlation and the diversity gain of our antennas will be computed. The influence of the source impedance in this particular case will be studied too.

Not only simulation results will be obtained, but also some measured results to prove the correct performance of our design. For this purpose, a network analyzer and a reverberation chamber will be used. A brief description of the reverberation chamber is included in chapter 4. In chapter 5, the explanation about measurements setup is included. The designed antennas are explained there as well as the measurements that will be performed within that design. In that chapter, our proposed method will be clearly explained with a simple graph that will show the simulation procedure that we have followed. A brief list of the main instrumentation used is also included.

The results are included in chapter 6. We will add simulated results from CST and MPA. Measurement results obtained not only with the network analyzer but also using the reverberation chamber are included. However, all the comments on the measurements and some conclusions will be included in chapter 7. It also includes a brief discussion on how the performance of the initial model can be improved by using our proposed method. Chapter 8 includes some suggestions for future work.

2. Theoretical Background

Mobile wireless terminal, such as phones and laptops, are evolving continuously to provide more services and high data rates. This increasingly demand should imply maintenance of the wireless channel, considering signal fading, Inter-Symbol Interference (ISI) and co-channel interference. The use of multiple antennas will not only provide higher data rates but also enforce the channel against channel fading and interference.

In wireless communications, the transmitted waves can be propagated in three different modes: ground waves, sky waves or line-of-sight (LOS). Normally around transmitter and receiver there exist natural reflectors that will create multiple paths for a transmitted signal. Therefore, the received signal is affected by fading that distorts the transmitted modulated signal. Multipath propagation is one of the main causes of fading in the environment. As a consequence, the propagated signal follows different paths and arrives to the receiver at different times with different amplitude and phase. Hence, the received signal is the superposition of multiple copies and each of them is affected by attenuation, inherent noise, distortion and dispersion in the channel and by the rest of transmitted signals.

Besides, when designing antennas for mobile terminals, the actual tendency is to build them with the small volume as possible and with a total radiation efficiency and a bandwidth optimized to achieve the specified performance. Therefore, a compromise between all these objectives has to be found.

As all antennas, the ones that will be designed for the aim of this thesis have to fulfil certain specifications in terms of return loss, radiation efficiency, effective diversity gain and correlation between them, included in section 2.1.2.

2.1 THEORY CONCEPTS

2.1.1 Rayleigh fading

In antenna transmissions there is always a power loss between transmitter and receiver. It can be caused by free-space attenuation, absorption in the atmosphere and signal fading [6]. There are two types of fading that characterize mobile communications. First of all, large-scale fading that represents the path loss due to movement over large areas. In contrast, small-scale fading refers to the amplitude and phase variations due to changes smaller than half-wavelength in the separation between transmitter and receiver. Small scale fading is also called Rayleigh fading.

Rayleigh fading will statistically model the propagation environment where there is no line-of-sight between transmitter and receiver. There are three main contributions in the environment that will affect the signal propagation: large smooth objects may cause reflection, whereas the edges of large objects can cause diffraction and small objects will cause scattered waves. Therefore, if the number of incoming waves is large, that is, there are many scattered waves then the channel impulse response will be modelled accordingly to a normally distributed Gaussian process. At receiving side, the multipath environment can be characterized by several independent waves, with different amplitude, phase, polarization and angle of arrival. The amplitude of the signal sum is described by a Rayleigh distribution, which includes deep fading dips. The movement of the terminal causes a variable attenuation that can be high at some points, causing fading dips and dropped calls.

We use diversity to avoid deep fading levels and to increase the SNR. We can use different antennas for each signal and the combination of them will give us a better signal-to-noise ratio (SNR) that will increase the channel capacity. If two or more receiving antennas are used, the performance can be improved because there is a lower probability that both antennas are located in a deep fading dip at the same time. Besides, using several antennas we can also establish many communication channels through the multipath environment. This is the main principle of multiple-input multiple-output (MIMO) systems that will increase the data throughput and the channel capacity of the link without varying the needed transmitted power or the bandwidth. From [7], it can be seen that the radiation efficiency has a much larger influence on the channel capacity than correlation. However, both parameters will be taken into account in this thesis.

2.1.2 Antenna Basics

To have good antennas, they have to be resonant for the desired frequency and matched to the radio-block. It can be done measuring the characteristic impedance. The impedance matching shows how much power is transmitted to the antenna from the input port and it is represented using the Voltage Standing-Wave Ratio (VSWR) or Return Loss (RL). Due to mismatching, some power is reflected back to the radio-block. The VSWR indicates how much power is reflected back and it should be kept low. In our case, the VSWR should be kept less than 3:1 to indicate a good matching, because it means that less than 25% power is reflected at the antenna port. The RL also describes the reduction in the amplitude of the reflected power, as compared to the forwarded power. It should be kept below –6 dB, which corresponds approximately to a VSWR 3:1.

To have a perfectly resonating antenna, the impedance should be purely resistive at a certain frequency. As mentioned before, we will take into account the return loss, the radiation efficiency, the diversity gain and the correlation between the antennas as a measurement of the performance of the system. Besides, the bandwidth of the antenna is the frequency range in which it operates. Therefore, the bandwidth will be defined by the RL, which is 6 dB at the frequency limits, corresponding to approximately VSWR $\leq$ 3:1.

We cannot forget that the desire of having mobile terminals with a reduced size implies also a reduction on the volume of the antennas that can be used. Bringing the antennas closer together causes an increase in mutual coupling that can affect considerably the performance of the system. It will affect the gain, the bandwidth and the input impedance of the antenna elements. Besides, the mutual coupling between the elements will cause signal correlation and will influence too the radiation efficiency. As it was mentioned in [8], the mutual coupling between the individual antennas of the MIMO system must be taken into account. The coupling can reduce the correlation between the received signals on the individual antennas but it also can reduce the radiation efficiency and thus, reduces the capacity of the system.

Many of these parameters will be studied using the 3D-radiation patterns of the designed antennas. The radiation pattern of an antenna is a representation of the distribution of the power radiated or received by an antenna, in the case of a transmitting or receiving antenna respectively, as a function of the direction angles.

All the antenna specifications for this thesis are summarized in Table 2.1:

		TCH	[MHz]	Return Loss RL (S_{11}) [dB]	Efficiency η [%]	Correlation ρ
UMTS band 1 1.92-2.17 GHz	**Tx**	9750	1950.0	>6	>50	0.05
	Rx	10700	2140.0	>6	>50	0.05
WLAN 2.4 GHz			2400.0	>6	>50	0.05
			2483.0	>6	>50	0.05

Table 2.1: Antenna specifications

2.1.3 Return Loss

One of the parameters that are taken into account in the design of our antennas is the return loss (RL). It describes the reduction in amplitude of the reflected energy, as compared to the forwarded energy. The two main causes of RL are discontinuities and principally impedance mismatches. The relationship between VSWR and return loss is shown as:

$$RL(dB) = 20\log_{10}\frac{VSWR}{VSWR-1} \tag{2.1}$$

$$RL(dB) = -10\log_{10}|S_{11}|^2 \tag{2.2}$$

Where S_{11} is the complex S-parameter at the antenna port.

As this parameter indicates the reflected power at the antenna port, we will consider that the designed antennas will have a return loss better than 6 dB as specified in Table 2.1.

2.1.4 Diversity

Thanks to the random nature of radio propagation we can have independent or highly uncorrelated signal paths for communication. Therefore, to increase signal performance, diversity techniques can be used and both long-term and short-term fading can be reduced [6].

Thus, having the antennas far from each other (spatial diversity) or with a low coupling between them (polarization or pattern diversity) we can implement diversity. The received signal will be different on all the antennas and there is a low probability of having a fading dip simultaneously on all the antennas. Therefore, using diversity techniques we can obtain an increase in the signal-to-noise ratio (SNR) that can be used to improve the channel capacity [7].

As mentioned before, there are several diversity techniques that can be implemented. Spatial diversity separates the antennas by a fixed number of wavelengths. This distance is chosen to maximize the reception of a given antenna when the other one is at its minimum. Temporal diversity aligns multiple signals and selects the one with best-expected time of arrival. When we take into account the dependence of the phase cancellation with the frequency, we can implement frequency diversity. Another important type of diversity is polarization diversity, where the antennas may have orthogonal polarizations. And finally, angle diversity where directional antennas differentiate between angle spaces.

Nevertheless, for practical implementations, just spatial, polarization and angle diversity are considered because frequency and time diversity require base station transmissions specifically for these diversity methods. Besides, using the concept of spatial diversity, the probability of having a fading under a reference level decreases exponentially with the number of antenna elements used [9].

There are many different schemes to combine the received signals such as selection combining (SEC) that selects the strongest signal, switched combining (SWC), equal gain combining (EGC) or maximum ratio combining (MRC).

2.1.4.1 Characterization of diversity performance

The correlation coefficient represents how different the fading between the antennas is. A lower correlation will give us better diversity gain. This correlation coefficient between two antennas is a function of the antenna radiation patterns, the separation between the antennas and the incoming multipath wave distribution. As it is one of the parameters that will be considered to improve the diversity performance, it will be defined later on in this theoretical part of the report, in section 2.1.7.

Another parameter that will be used to study the diversity performance is the diversity gain. As published in [10], plotting the cumulative probability density function, it can be seen that the received power level in a multipath environment with no LOS is distributed as a Rayleigh function, represented in Figure 2.1. This is also the curve that an ideal reference antenna with 100% radiation efficiency follows. Taking the same published example of two parallel dipoles separated 15 mm at 900 MHz, the

received power of each of them follows the previous theoretical curve, but shifted to the left due to their lower radiation efficiency. Using a selection-combining scheme, the cumulative power distribution for the combined case is located to the right of the curves for both branches. Therefore, looking at Figure 2.1, we can define the Effective Diversity Gain as the difference between the reference antenna and the combined signal at some desirable probability level. The Apparent Diversity Gain is the difference between the cumulative distribution function of the combined signal and the one at the port with the strongest average signal levels. The effective diversity gain was also defined also in [8] and it represents the gain over a single ideal reference antenna, impedance-matched to the transmission line feeding without ohmic losses, with no additional antenna close to it.

In our case, we will take 1% as probability level. It will indicate that if in our system we allow a fading margin of 20 dB in order to receive with sufficient quality 99% of the time, the fading margin can be reduced a value equal to the effective diversity gain using this diversity scheme. The theoretical maximum effective diversity gain is approximately 10 dB at 1% probability level, using selection combining [10].

Giving some equations, the apparent diversity gain at 1% cumulative probability level for selection combining is approximately, as in [11]:

$$G_{app} = 10\sqrt{1-0.99\left|\rho\right|^2} \tag{2.3}$$

Thus, the effective diversity gain is:

$$G_{eff} = \eta G_{app} \tag{2.4}$$

Where η is the efficiency of the strongest antenna branch.

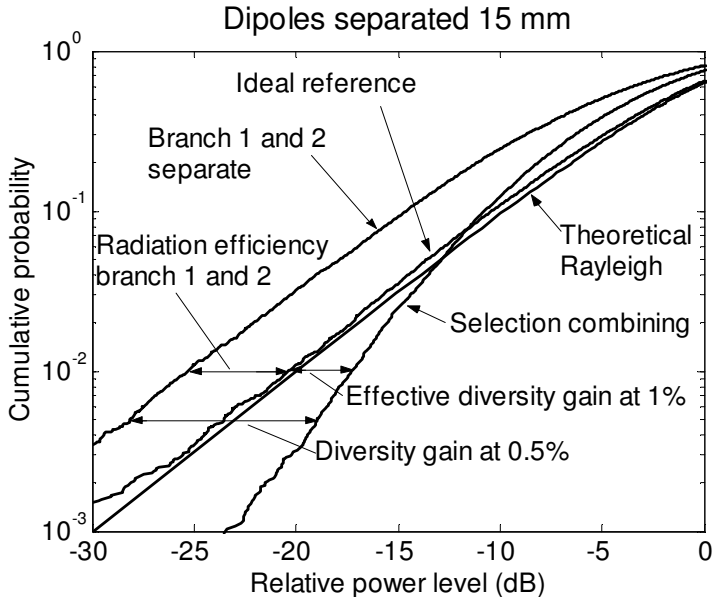

Figure 2.1: Cumulative density function of two parallel dipoles with 0.045λ spacing, located in the reverberation chamber

However, if the total radiation efficiency of the two antenna elements is quite different, we cannot apply the equations (2.3) and (2.4) directly. If the fading between several diversity branches is not independent, using [12], we can represent the effect of correlation in fading among diversity branches by equation (2.5):

$$\Pr(\gamma < x) = 1 - \exp\left(-\frac{x}{\Gamma_1}\right) Q\left(\sqrt{\frac{2x}{\Gamma_2\left(1-|\rho|^2\right)}}, |\rho|\sqrt{\frac{2x}{\Gamma_1\left(1-|\rho|^2\right)}}\right) - \exp\left(-\frac{x}{\Gamma_2}\right)\left[1 - Q\left(|\rho|\sqrt{\frac{2x}{\Gamma_2\left(1-|\rho|^2\right)}}, \sqrt{\frac{2x}{\Gamma_1\left(1-|\rho|^2\right)}}\right)\right] \tag{2.5}$$

Where Γ_1 is the total radiation efficiency of first branch, Γ_2 the total radiation efficiency of second branch and ρ is the correlation between them. The Q-function was also defined in [12].

2.1.5 Multiple Input Multiple Output (MIMO)

As mentioned before, if we use several antennas we can establish many communication channels through the multipath environment. In Multiple-Input Multiple-Output (MIMO) systems, the transmitted signal is distributed among different channels and combined after reception making the overall channel capacity maximum [7]. These systems will increase the data throughput and the capacity of the link without varying the needed transmitted power or the bandwidth.

In MIMO systems, each of the signals received by the different antennas is processed incoherently to optimize system performance. However, if the antenna elements are too closely located they will be electromagnetically coupled and the capacity will be reduced due to the high correlation and the reduction in radiation efficiency. Besides, in MIMO systems, we will treat each antenna as being independently excited. The radiation efficiency at each port and the correlation between all of them can be determined by the far-field patterns of the corresponding embedded elements or using a reverberation chamber, as seen in [7].

The quality of a MIMO system in a fading multipath environment is characterized by the maximum available capacity. The capacity of MIMO systems heavily depends on the available channel state at receiver or transmitter, the channel Signal-to-Noise Ratio (SNR) and the correlation between the channel gains on each antenna element. Therefore, the instantaneous maximum capacity of the MIMO system:

$$C = \log_2\left(\det\left(I_{MxN} + \frac{SNR}{M} H_{MxN} H^*_{MxN}\right)\right) \quad [b/s/Hz] \tag{2.6}$$

Where M is the number of transmitters and N is the number of receivers in the MIMO system. I_{MxN} is a unit matrix, H_{MxN} is a normalized complex channel matrix and H^*_{MxN} is the complex conjugate transpose of H_{MxN} [13].

In equation (2.6), as explained in [8], the coupling between the antennas is included. Moreover, if we normalize the channel matrix H to a reference level, the radiation efficiency and mutual coupling are also included in equation (2.6). In this case, the correlation due to the embedded pattern is just a part of the total correlation. If we measure the correlation in a reverberation chamber, as the wall antennas are uncorrelated, we will just obtain the correlation due to embedded pattern.

It was also shown in [8] that the largest average capacity will be obtained if the fading between the channels is independent, so the correlation between the received signals is low. However, if the transmitters or receivers are not sufficiently spaced, the correlation should be considered and it can considerably decrease the capacity of the MIMO system. Antenna correlation varies as a function of the scattering environment, the distance between transmitter and receiver and the antenna far-field patterns. This correlation will affect the capacity of the system, as well as SNR and the radiation efficiency of antennas in the MIMO system. As studied in [8], the radiation efficiency is the parameter that will affect the most to the capacity of our system.

We do not explicitly characterize MIMO systems in this work. However, the radiation efficiency and the correlation also play an important role in channel capacity. Therefore, the source variation method proposed in our particular diversity method can be useful to study the variation of the correlation for MIMO systems too.

2.1.6 Embedded Radiation Efficiency

In classical array analysis, the radiation pattern of a single element is calculated when all the other ports are not excited, and they are simply terminated with loads representing the source impedance on their ports. However, the embedded element pattern is preferred in MIMO analysis. In multipath environment, the received signal on each port is detected independently of on the others, so each port receives signals through their embedded element patterns. Thus, the radiation efficiency at each port is determined by its embedded element pattern, as well as the correlation between signals on all ports [7].

As it was done in [3], to calculate the total radiation efficiency of an embedded element on a multiport antenna I will study the case of two parallel dipoles. Using the analysis in [3], we have that the input impedance Z_{in} is:

$$Z_{in} = Z_{d1} + \frac{Z_{12} I_2}{I_1} = Z_{d1} - \frac{Z_{12}^2}{Z_{d2} + Z_L^t} \tag{2.7}$$

Where Z_L^t is the transformed impedance seen at port of dipole 2.

The reflection coefficient at the input of port 1 and the reflection efficiency:

$$\Gamma = \frac{Z_a - Z_c}{Z_a + Z_c} \qquad \text{and} \qquad e_{refl} = 1 - |\Gamma|^2 \tag{2.8}$$

Where Z_c is the characteristic line impedance.

We can easily calculate the radiation efficiency as indicated in [3], using previous equations:

$$e_{rad} = e_{refl} e_{abs} \tag{2.9}$$

Where:

$$e_{abs} = \frac{P_{rad}}{P_{acc}} = \frac{P_{acc} - P_2}{P_{acc}} = 1 - \frac{R_{L2}\left|I_2\right|^2}{\mathrm{Re}\{Z_{in}\}\left|I_1\right|^2} \tag{2.10}$$

With P_{acc} as the total power accepted by port 1, P_2 as the absorbed power in the load on port 2 and P_{rad} as the radiated power.

This definition of the radiation efficiency includes impedance mismatch, losses in the antenna itself and losses in the near-in environment. As an example, taking the obtained results in [8] and looking at Figure 2.1 in section 2.1.4.1, the radiation efficiency is the difference between the cumulative probability distributions of the two dipoles of the branches in the diversity antenna and the one of the ideal reference. In that mentioned case, as we have coupling antennas, the radiation efficiency will be degraded due to absorption in neighbouring antennas and the impedance mismatch at the antenna terminals.

2.1.7 Complex correlation coefficient

If the received signals are correlated to some degree, we can study its correlation with the complex correlation coefficient. It can be calculated either from scattered parameters or radiation patterns. It depends on the propagation environment and the far-field radiation pattern of the antennas, and for two ports it can be calculated as the normalised coupling between the corresponding embedded element radiation field functions, expressed as in [3]:

$$\rho = \frac{\iint_{4\pi} G_{emb}^{1} G_{emb}^{2^*} d\Omega}{\sqrt{\iint_{4\pi} G_{emb}^{1} G_{emb}^{1^*} d\Omega} \sqrt{\iint_{4\pi} G_{emb}^{2} G_{emb}^{2^*} d\Omega}} \tag{2.11}$$

And it can be evaluated taking pairs of antennas in the MIMO system.

The envelope correlation coefficient can be calculated in a uniform scattering environment using the scattering S-parameters too. Nevertheless, for the aim of our thesis we will rely on equation (2.11) as MPA does.

In [14], three different forms to express the correlation are shown. We can differentiate between complex signal correlation (ρ_s), envelope correlation (ρ_e) and power correlation coefficient (ρ_p). As mentioned in [14], in Rayleigh fading environments, $|\rho_s|^2 \approx \rho_e$, and also $\rho_e = \rho_p$.

It has to be noted that the reverberation chamber in Ethertronics Design in Kalmar provides the power correlation, whereas the MPA computes the magnitude of the complex correlation coefficient.

To sum up, as correlation is one of the parameters that have to be optimized in this Thesis, we can conclude that the lower correlation coefficient, the higher diversity gain will be achieved, because the apparent diversity gain will be lowered faster with high correlation values. As a thumb rule, the correlation should be lower than 0.7 or 0.5 in diversity systems.

2.1.8 Scattering Parameters

The scattering parameters are fixed properties of the circuit, which describe how the complex voltage waves couples between each pair of ports. Therefore, using these S-parameters, many electrical properties of our antennas will be expressed such reflection coefficients, return loss and voltage standing wave ratio.

Taking the simple example of a 2-port scattering matrix, the four obtained S-parameters represent:

- S_{11} is the input port voltage reflection coefficient; reflected wave at port 1
- S_{12} is the reverse voltage gain
- S_{21} is the forward voltage gain
- S_{22} is the output port voltage reflection coefficient; transmitted wave at port 2

2.2 TYPES OF ANTENNAS

In order to design our new antennas, some basic antennas are taken as initial examples: monopoles/dipoles and Inverted-F Antennas.

2.2.1 Monopoles and Dipoles

A monopole antenna is a half of a dipole antenna placed in half space with a perfectly conducting, infinite ground plane. However, if the ground plane is large enough, the monopole acts as dipole. In this case, the image theorem can be applied. Therefore, the input impedance is half of the input impedance of the dipole, and the radiation pattern above the infinite ground plane is the same as the upper half of the radiation pattern of the mentioned dipole [15]. In practice, a ground plane cannot be infinite, but the approximation can be done if the ground plane has a radius approximately the same as the monopole's length.

The dipole is the basic antenna, consisting of a straight piece of wire that is fed with a balanced generator near the centre of the wire. This kind of antenna consists of two

aligned quarter wavelength long cylinders, separated by a feed gap where the generator is located. It is resonant at the frequency were the two wire length is a half wavelength, and in this case, the reactive part of the input impedance is close to zero. For a vertical dipole, the radiation pattern is completely rotational symmetric. As mentioned in [13], the radiation pattern of a dipole, as the one represented in Figure 2.2, depends on its length and thickness.

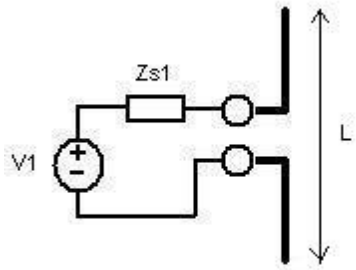

Figure 2.2: Dipole representation

Note that many of the references used in this thesis include several studies on dipoles. Many of those results will be used and mentioned later on, in our particular dipole example in section 3.3.

2.2.2 Inverted-F Antenna (IFA)

The Inverted-F Antenna is a variation on the transmission line antenna or monopole antenna that includes an offset feed. The geometry obtained is similar to a letter F rotated facing the ground plane. One of the legs will be connected to that plane, whereas the other one will be connected to the feeding port. The configuration is treated as a small loop inductor [16].

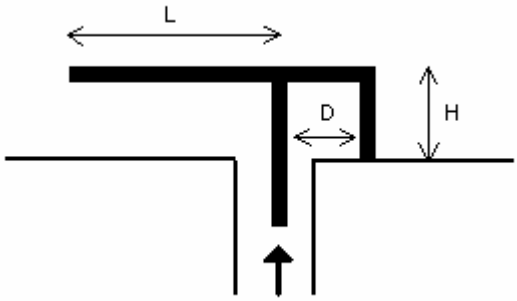

Figure 2.3: Inverted F-Antenna

The magnitudes and phases on the currents in vertical wires, see Figure 2.3, are constant and the charge is stored in the capacitance between the horizontal segments [16]. Therefore, those wires act as ideal monopole radiators. Besides, the horizontal wires and the vertical one connected to ground can be seen as a bent monopole of resonant length with an offset feed located at a given distance. It is also known that if the distance between the feed line and the short-circuit stub is decreased, the resonant

frequency will increase as well as the input resistance at resonance. Normally, the sum of L and H affects the resonant frequency. In case of having a low height, a capacitive coupling between the ground plane and the upper part of the antenna occurs, and the sum $T = H + L \approx \lambda/4$ can be reduced. The distance D between the vertical parts of the antenna has just effect on the input impedance, not on the resonant frequency and therefore, this configuration is used to tune the input impedance of the antenna.

Due to its many advantages, the IFA is widely used in antenna designs. It has a reduced size and it is very compact. However, the biggest disadvantage is its narrow bandwidth.

A proposed solution to solve this problem was to construct a Planar Inverted-F Antenna (PIFA). These kinds of antennas are made by replacing the top horizontal arm with a surface parallel to the ground plane and a vertical short circuit plate. As the width of the short circuit plate is smaller than the width of the horizontal plate, an inductance is introduced and the effective length of the current flow becomes longer. Thus, the resonant frequency will be lowered.

2.3 WIRELESS SYSTEMS AND STANDARDS

2.3.1 W-CDMA

Mobile users can use multiple access schemes to share simultaneously the radio spectrum and hence it can be achieved a higher capacity of the communications system. Those access techniques can be divided in narrowband and wideband, depending on how the spectrum is divided between users. The antennas designed in this Thesis have to work in the W-CDMA frequency range, and it is considered as a wideband system. The transmission bandwidth of a single channel is larger that the coherence bandwidth of the channel, and therefore, multipath fading does not affect so much the received signal [6].

The data to be transmitted is encoded using a spreading code that varies depending on the different users. In Code Division Multiple Access (CDMA) every user will be allocated the entire spectrum all the time and codes will be used to identify the different connections. CDMA uses spread-spectrum technology and the coded signal has a higher bandwidth than the data. It also supports multipath to combine all the signals and to obtain a stronger one at the receiver.

Wideband Code Division Multiple Access (W-CDMA) is the radio access scheme used for third generation mobile terminals nowadays. It uses Direct-Sequence spreading, combining the baseband information to high chip rate binary code. The spreading factor is the ratio between the chip rate and the data rate. It provides support for many services with a 5MHz channel bandwidth. Using this bandwidth it has the capacity to carry over 100 simultaneous voice calls, or able to carry data speeds up to 2 Mbps. Due to its wide bandwidth, it is considered as a wideband CDMA.

There are currently six bands specified for use of WCDMA, but the ones that will be used in this thesis are the bands between 1920-1980 MHz and 2110-2170 MHz.

2.3.2 WLAN

Due to the increase in digital wireless and mobile communications, an indoor standard for operating at 2.4 GHz has been developed. Wireless Local Area Network (WLAN) is a communication system, which basics are specified in the IEEE 802.11 standard, especially suitable for high-rate applications. It uses spread-spectrum or Orthogonal Frequency Division Multiplexing (OFDM) modulation technology based on radio waves that allows users to have a higher mobility and to transmit large amounts of digital data. OFDM splits the radio signal into multiple smaller sub signals, and then transmits them simultaneously at different frequencies to the receiver. WLAN systems use Time-Division Duplex (TDD), where the same frequency is used for transmission and reception.

Although the IEEE 802.11 standard includes many different specifications, in our case we will use the WLAN standard frequencies for USA and EU: 2.4-2.4835 GHz, and that is the range that will be considered in this thesis. The entire band is divided in different channels, depending on the country, and a WLAN receiver can use any of these channels, changing from one to another if interference appears. The Bluetooth protocol operates in this band and it is used nowadays as a common way of connecting personal devices such as laptops, mobile phones or digital cameras, among others.

3. Software

3.1 CST STUDIO SUITE 2006 B

In order to design the complete system, the CST STUDIO SUITE was used. This software is designed for the efficient and accurate 3D electromagnetic simulations of high frequency problems. The laptop model as well as the antennas was firstly simulated using this program to study their performance.

Thanks to this software, broadband calculation of S-parameters as well as the radiation patterns of the antennas was performed. It offers different solvers such as the Time and the Frequency Domain solvers. It includes multi signal functionality to simulate various excitations. I took advantage of the post processing abilities that the software provides, to obtain important far-field calculations such as directivity gain, E-field patterns and many other antenna parameters.

I have also made use of the autoregressive (AR) filtering for the fast time domain calculations of resonant structures and of the Perfect Boundary Approximation (PBA) that gave an accurate and fast computation of arbitrarily shaped objects [1]. Besides, thanks to mesh generation the studied domain can be divided in small cells to obtain better results.

As input for antenna calculations, we should select the units, set the background material, the desired frequency range and the boundary conditions. We define the excitation ports and we set the far-field monitors and the post processing results that want to be shown. After all those steps have been done, we can start the transient solver and when it finishes, the results can be analyzed.

The design procedure that has been followed was:

- Design of the laptop that will include the antennas, accordingly to a real model
- Design of an independent antenna element
- Import the laptop in the antenna design and include the antenna on the top of screen
- Simulation of the performance of the whole system until an acceptable solution is achieved. All laptop components are considered for simulation and for the boundary conditions, but not for meshing, that just the upper metal parts and the antennas will be considered. Several tries were made to achieve an acceptable performance.

- Include more antennas to the design and study its performance and the obtained results. Improvement in performance while adding more antennas has to be shown. The performance of the complete system will be studied.

The antenna design has to be chosen in order to give maximal coverage in the bands of interest and accordingly to the specifications mentioned in section 2.1.2. Two different examples are included in this thesis. A laptop with 5 antennas separated from each other by 2.8 cm and a laptop with 3 antennas placed closer to each other, with a separation of 1 cm.

3.1.1 Laptop design with CST

The designed CST-model was done following a real DELL laptop model. Thus, simulation results compare acceptable to reality. The model was designed using CST STUDIO SUITE. The real DELL laptop was modified later on to include the antennas on it to perform measurement results.

The laptop is divided in two separated parts: the upper part, made mainly of plastic and the lower one, of metal. Both parts are joined via a plastic cylinder. In the lower part, a plastic keyboard was included too. The upper part includes the screen, made of Plexiglas, a metal border around it with a thin metal surface attached to it. The antennas are placed on small plastic blocks that for simulation purposes have a relative dielectric constant equal to 2.1. The upper part includes also a plastic edge that will cover our antennas. A final CST-model design of the laptop can be seen in Figure 3.1.

Figure 3.1: Laptop design using CST

For simulations and for boundary conditions of CST, all components are considered. Nevertheless, just upper metal parts are considered for meshing the problem. The desire of a faster simulation motivates this decision.

The designed antennas will be included in this laptop design to simulate their performance. They will be attached in the upper part of the screen and a space in the plastic cover of the laptop was specially made for this purpose. The laptop model will be used for different antenna designs for the aim of this thesis. In Figure 3.2 a representation of the metal parts considered for the antenna performance evaluation can be seen. Besides, the antennas for the two different cases studied are also included in the mentioned figure.

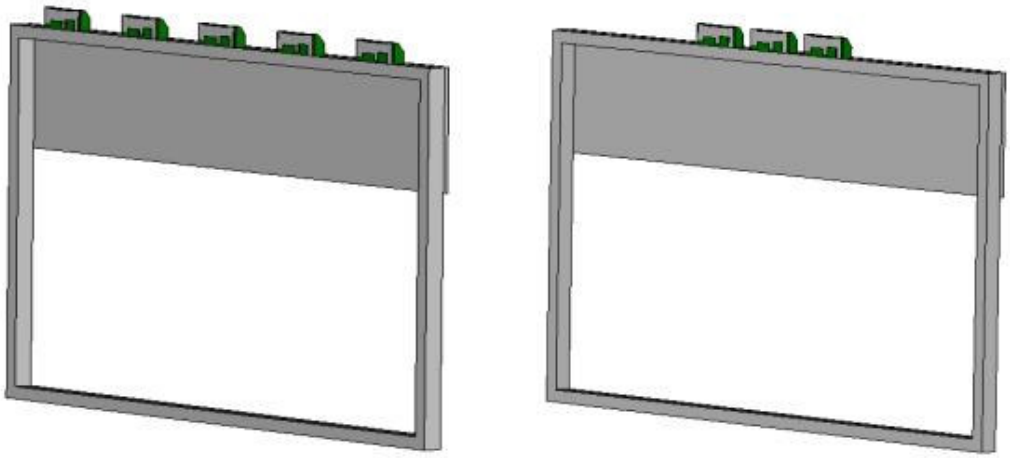

Figure 3.2: Laptop PEC surfaces considered for meshing and antennas included in both cases of study

3.2 MULTIPORT ANALYZER TOOL DESIGN IN CHASE (MPA)

As it was mentioned before, this thesis is a project proposed by Ethertronics that arise within the CHASE project. Besides, within this centre, a software was provided to develop methods so that new antenna solutions and system technologies for mobile terminals can be efficiently evaluated and optimized. Thanks to Multi-Port Antenna Evaluator (MPA), developed by Kristian Karlsson at SP [2], we can calculate many of the characteristics of our multi-port antenna for arbitrary loading and excitation conditions [4]. This software offers different optimizations to improve the performance of some antenna examples and circuit layouts. The MPA optimizer uses its own generic fitness function and more information about it can be found in [4]. Nevertheless, we will not make use of this function due to the reasons mentioned in the preface of this thesis.

The embedded element patterns and the S-parameter port responses from the full wave simulator (CST) as well as a circuit simulator (CircSim) are imported by the MPA. The computations are done much faster than using any other additional full wave simulator.

Thus, using the embedded element patterns, a representation of the individual antenna port excitation when the others are terminated is obtained. As the port currents

computed in the circuit simulator are also used, the total field for the general case is figured out making use of this weighting. Therefore, the radiation pattern from our dual band antenna for any excitation and loading condition can be computed. It should be mentioned that a uniform signal propagation environment is simulated with MPA.

The MPA software can compute the total radiated power, radiation pattern, near field functions, efficiency, correlation, MEG, apparent diversity gain and other antenna characteristics as mutual coupling, isolation and impedance. It should be mentioned that the program allows both short-circuit embedded element patterns and matched embedded element patterns.

The version used of MPA is still a trial version and it can use the imported embedded element patterns from CST, WSAP, EMDS, IE3D and MicroStripes. As circuit simulator, the software uses CircSim that was developed specially for the MPA by Jan Carlsson at SP [2]. A brief description of it is included in next section.

No comments on the way of operation of this new software are included in this thesis. Just brief mention to the obtained parameters will be done.

3.2.1 CircSim

Using port S-parameter responses determined by full wave simulations combined with lumped circuit models, the port responses for arbitrary loading and excitation can be calculated. CircSim is a software that presents an easy interface to obtain circuit layouts and to obtain probe files for MPA. It computes in time- or frequency-domain.

This circuit simulator program uses “Modified Nodal Approach” (MNA) and therefore, the impedance matrix, Z-matrix, is needed. Performing N full wave simulations, the matrix representing the N-port responses as a function of frequency is obtained. The MNA replaces the branch currents of all current defining elements in the circuit, such as in conductors, resistors or current sources, by their characteristic equation, and all branch voltages by node voltages. Making some calculations, the node voltages and the currents through sources and inductors are obtained [17].

3.2.2 Software interaction

When using the MPA, several files are needed, as can be seen in the graphical interaction provided by Figure 3.3. First of all, we need to obtain the far-field patterns of the embedded elements in CST, for all the ports in the design. Note that the ports must have a S-parameter source type and 50 Ω reference impedance.

The field monitors have to be defined as Farfield/RCS. After this establishment, a simulation can take place and afterwards, we can export as ASCII files the far-field patterns, one for each port. As for our asked specifications we need more than one field monitor, we will export the far-field patterns for all the ports and for each of the monitoring frequencies, as ‘.txt’ files. In our case, we defined field monitors at the frequency band limits and at the central frequency of each of our bands. Note that the

far-field patterns have to be plotted as E-fields, in linear scaling, using as reference distance 1m and without using far-field approximation. It will make possible to export the complex far-field, in amplitude and phase in [V/m] units. Besides, the angle step width to represent the far-field patterns is recommended to be 5 degrees, as it will generate more data to obtain a better accuracy when importing those files to MPA.

We also export the S-parameters as a Touchstone file, with '.sNp' extension, where N indicates the amount of ports that the design has.

The desired circuit layout will be made using CircSim. It has to be taken into account, that the circuit model uses Z-parameters to compute responses. Consequently, we firstly convert the Touchstone S-parameter file into Z-Matrix file using CircSim too. Due to the mode of operation of the MPA, just a frequency response can be analyzed each time. Thus, using the interpolation utility provided by CircSim, the desired frequency for the field monitor is selected, and the 'ZMatrix.dat' file will be modified, leaving just this frequency value. This new file is imported into the circuit model. Afterwards, we save the circuit model with '.ckt' extension and a probe file for MPA will be directly saved to help it to identify the circuit components.

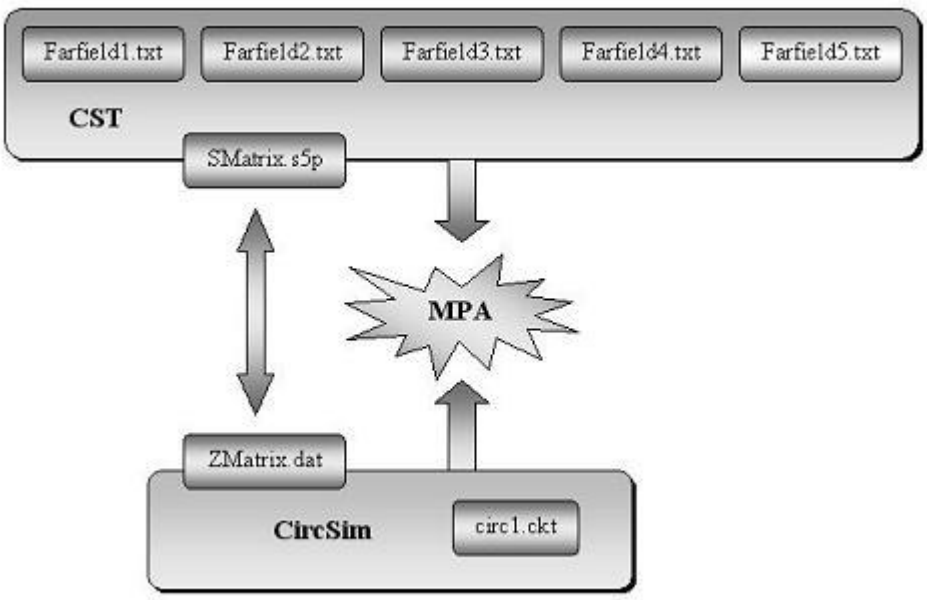

Figure 3.3: Interaction between software used for simulations

3.3 EXAMPLE: TWO PARALLEL DIPOLES

First of all, two dipoles will be used as an example to prove the correctly performance of the MPA. The same example was carried out in [4], but there the dipoles were not simulated using CST, but by using analytical dipole equations. I will use this example to obtain the far-field patterns to import them to MPA and to study their radiation efficiency, their correlation and their diversity gain to make a comparison with some results obtained in [4] and [18].

The mutual coupling between the elements will cause signal correlation. As in [3], the mutual impedance Z_{12} between two parallel dipoles influences both the correlation and the radiation efficiency.

A theoretical representation of the two parallel dipoles implemented is shown in the upper part of Figure 3.4. Besides, the equivalent circuit for classical analysis of two parallel diversity dipoles with independent sources V_1 and V_2 is included in the lower part of Figure 3.4. The embedded element pattern of port 1 is obtained by setting V_2=0 and correspondingly V_1=0 for port 2. We assume Z_{s1}=Z_{s2} and Z_{d1}=Z_{d2}, see [5].

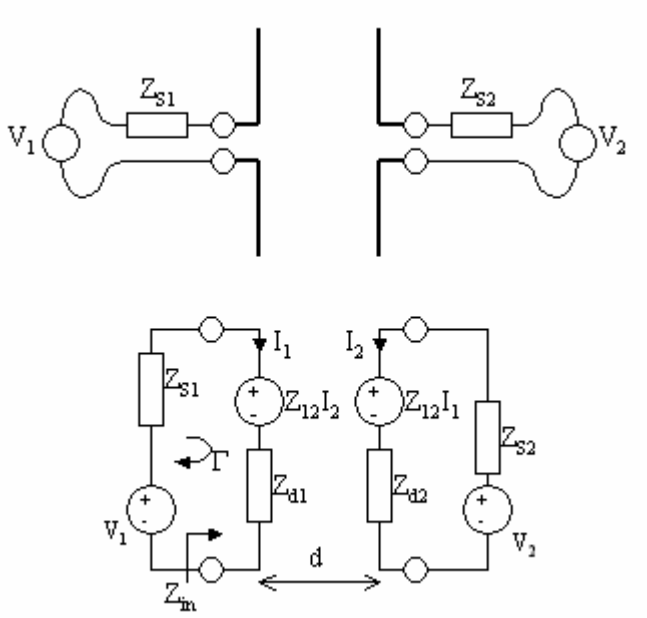

Figure 3.4: Theoretical representation of two parallel diversity dipoles (upper) and equivalent circuit (lower) for classical analysis with independent sources V_1 and V_2

The input impedance of the embedded element at port 2 is:

$$Z_{in} = Z_{d1} + \frac{Z_{12} I_2}{I_1} \tag{3.1}$$

The simulations will be performed using CST, and the two electric dipoles will have a length of 0.94 λ/2, to have the imaginary part of the input impedance of the dipoles approximately equal to zero. The radius of the dipoles is 1 mm. A discrete port is used

to define an excitation in the middle of each dipole. Initially, to study the performance of our system, a far-field monitor at 900 MHz is also included. However, some other far-field monitors will be included later at different frequencies to study several performance cases.

The two dipoles are separated just 15 mm at the defined antenna frequency of 900 MHz to have a high coupling and a high correlation between them. As can be seen in [11], the correlation increases as spacing between the monopoles is decreasing. Besides, as shown in the same paper, if the correlation increases, the diversity gain will be degraded. Also, some other spacing values will be simulated to study their performance.

The initial CST design can be seen in Figure 3.5:

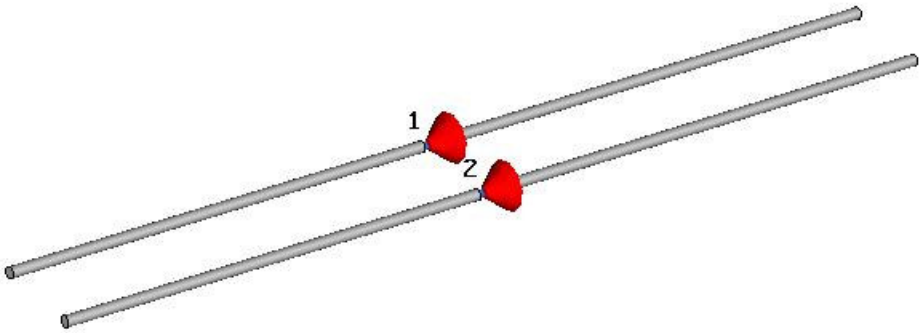

Figure 3.5: Representation of dipoles using CST

As the structure has small PEC elements, the CST meshing properties of the model were redefined. Increasing the number of mesh lines per wavelength and the refinement factor at PEC edges, the accuracy is improved.

The circuit that will be used to study the desired characteristics is done using CircSim and is shown in Figure 3.6:

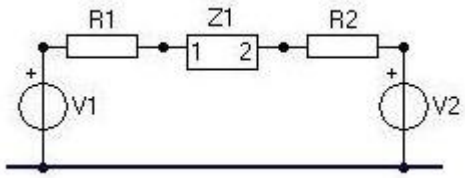

Figure 3.6: CircSim circuit to simulate the performance of dipoles

In the above circuit, the impedances R1 and R2 are 50 Ω, whereas the sources V1 and V2 are chosen as 14.14 V to emulate the 1 W sources in CST, and to be able to compare both results. Those source impedances will be modified also later on.

After simulating the initial model, with 50 Ω impedances, the results are imported to MPA. Computation of the radiation efficiency and of the correlation of our antenna is performed.

On one hand, using CST, the efficiency that is obtained for this model is equal to 0.4436 that corresponds to –3.53 dB. Computing then the desired antenna characteristics with MPA without any extra components, it can be seen that the efficiency obtained is 0.44, corresponding to –3.56 dB, and the correlation obtained using MPA was 0.8239. On the other hand, calculating the theoretical correlation coefficient using equation (2.11) by using the far-field patterns obtained with CST and a Matlab code to compute the mentioned equation was 0.82. And the radiation efficiency previously published in [18], was approximately –3.5 dB.

Even though no optimization will be performed, we will study the influence of different parameters in the dipoles example to see how the antenna characteristics are modified.

Some other simulations were performed varying the conditions to study the performance of the system. See as reference [18].

First of all, if we consider different source impedances, R1 and R2 in Figure 3.6, the total radiation efficiency should vary as seen in Figure 3.7, using theory from [5]. In our case, we will first consider just real source impedances. Therefore, the expected theoretical efficiency can be seen in Figure 3.8, where the curve is part of Figure 3.7 along the imaginary value of 0 Ω.

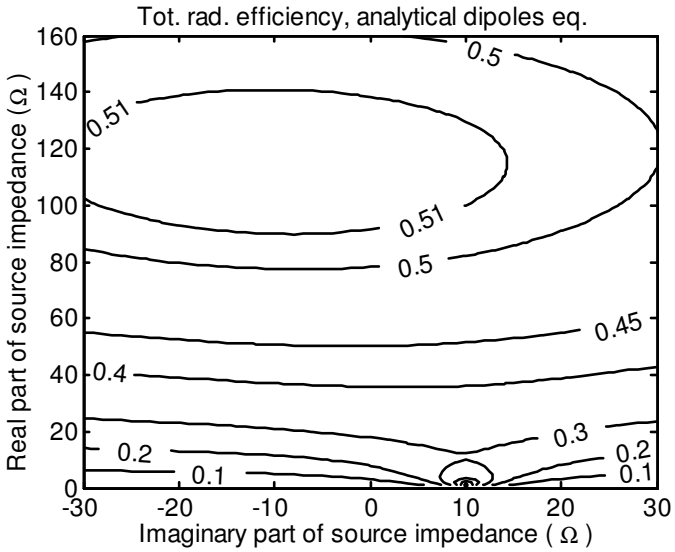

Figure 3.7: Total radiation efficiency as a function of source impedance

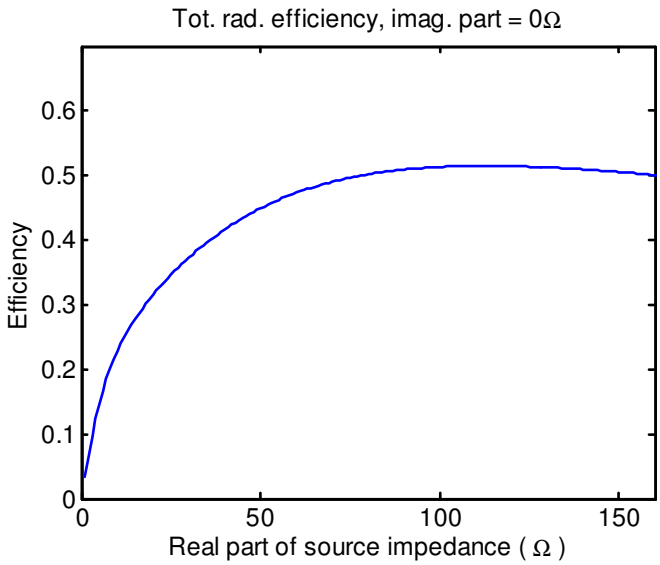

Figure 3.8: Theoretical Total Radiation Efficiency as function of the real part of source impedance

Computing the total radiation efficiency with MPA, the obtained values are shown in Table 3.1 and in Figure 3.9. As expected, the simulated total radiation efficiency is equal to the theoretical one.

Real part of source impedance [Ohms]	Total Radiation Efficiency using MPA [-]
0	0
10	0.2125
20	0.3001
30	0.3579
40	0.4039
50	0.4395
60	0.4672

Table 3.1: Total radiation efficiency for different real values of source impedance

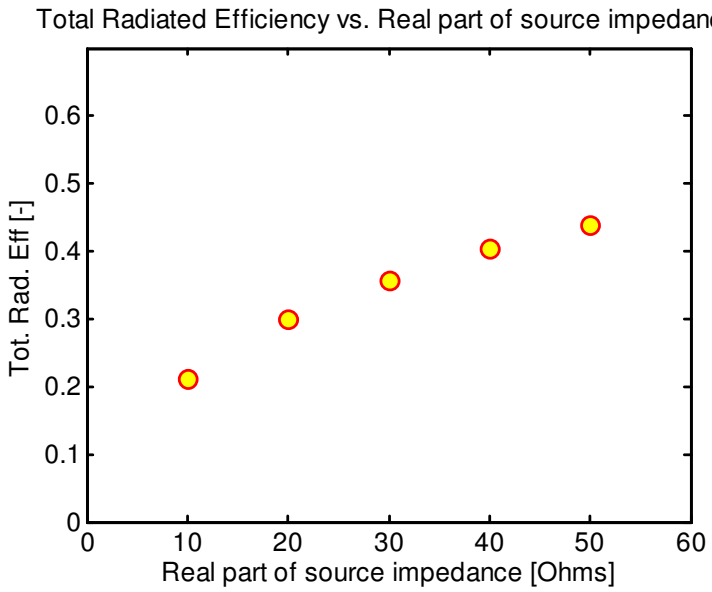

Figure 3.9: Total Radiation Efficiency vs. Real part of source impedance for two parallel dipoles

We can now consider that the source impedance can have not only real part, but also an imaginary part. In this second analysis case, we will study not only the efficiency, but also the correlation and the effective diversity gain. As was seen in [5], the effective diversity gain plot for 15 mm spacing between the dipoles is shown in Figure 3.10.

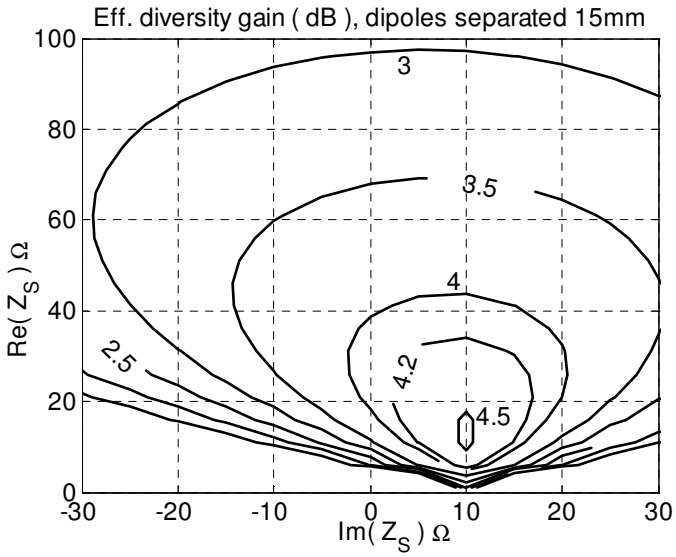

Figure 3.10: Effective Diversity Gain of two parallel dipoles separated 15 mm depending on the source impedance

To include the imaginary part of the source impedance R1 and R2 in CircSim, a text file has to be imported to it. In this file, the first column includes the frequency in Hz, the second one includes the real part of the source impedance and the third column is the imaginary part. Computing on MPA using different source impedances, we obtain Table 3.2:

Source impedance [Ohms]	Efficiency [-,dB]	Correlation	Effective Diversity Gain [dB]
50	0.44 (-3.56 dB)	0.8239	3.9
20	0.30 (-5.23 dB)	0.50936	4.1
20+10i	0.31 (-5.09 dB)	0.42171	4.4
15+10i	0.29 (-5.38 dB)	0.21526	4.5
10+10i	0.29 (-5.38 dB)	0.1053	4.6

Table 3.2: Effective diversity gain using different source impedances for two parallel dipoles

Therefore, looking at the values obtained above (Table 3.2) and comparing them with the theoretical results that can be seen on Figures 3.7 and 3.10, we conclude that the performance of MPA compares good with results in [5] for different source impedances.

Afterwards, we performed some simulations varying the spacing between the dipoles. In this case, looking at Table 3.3, it can be seen that there are some differences on the efficiency computed using CST and MPA. They can be due to the far-field pattern resolution because whereas CST calculates the efficiency from losses in the computation volume, MPA calculates the efficiency as an integration of the far-field pattern.

As expected, when we increment the distance between the two dipoles, the coupling will be reduced and therefore, the efficiency of our antennas will be higher and the correlation between them lower.

	Total Radiation Efficiency			Correlation	
Distance [mm]	**CST**	**MPA Port 1**	**MPA Port 2**	**MPA**	**Equation 2.11**
15	0.4436	0.43957	0.4401	0.8239	0.82
30	0.5885	0.5543	0.55437	0.48992	0.43
42	0.7008	0.65102	0.65023	0.29472	0.19
83	0.8666	0.83588	0.83316	0.063936	0.03

Table 3.3: Total Radiation Efficiency and Correlation for different spacing between dipoles

Finally, some simulations using different far-field monitors were performed. The selected spacing between the dipoles will be again 15 mm. We studied the frequency variation of the total radiation efficiency and the correlation of our dipoles.

As can be seen in the figure below (Figure 3.11), the total radiation efficiency calculated using the MPA is almost the same as the one given by the CST. Therefore, the MPA performance in terms of efficiency has been proved to work properly.

	Total Radiation Efficiency				Total Radiation Efficiency		
freq [MHz]	**CST**	**MPA Port 1**	**MPA Port 2**	**freq [MHz]**	**CST**	**MPA Port 1**	**MPA Port 1**
800	0.2935	0.2779	0.2795	**910**	0.4414	0.4319	0.434
820	0.3397	0.3256	0.3274	**920**	0.4354	0.4271	0.4286
860	0.4149	0.4032	0.4062	**930**	0.4257	0.4191	0.4198
870	0.4272	0.4159	0.4189	**940**	0.4129	0.4083	0.4083
880	0.4363	0.4251	0.4283	**960**	0.3813	0.3809	0.3797
890	0.4418	0.4309	0.4339	**980**	0.3471	0.3503	0.3484
900	0.4436	0.4332	0.4359	**1000**	0.3149	0.3206	0.3184

Table 3.4: Total radiation efficiency for the dipoles obtained with CST and MPA

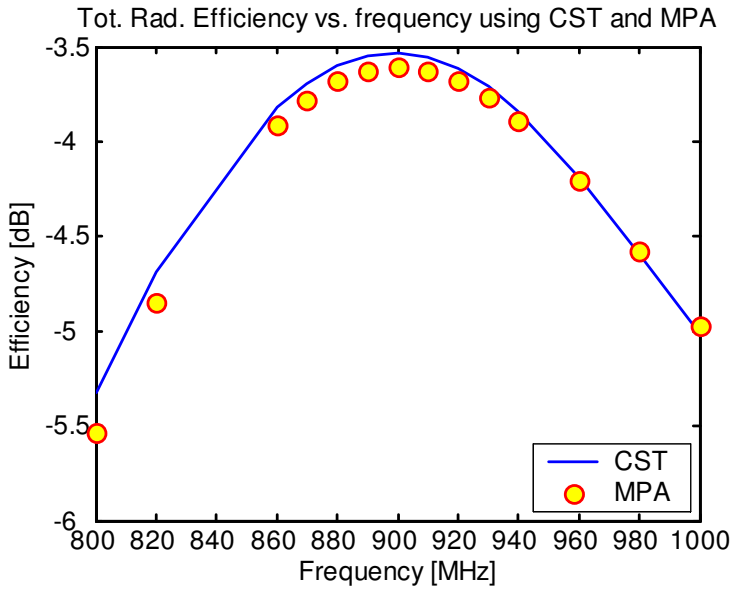

Figure 3.11: Total Radiation Efficiency calculated using CST simulations and MPA

The correlation of the dipoles within different frequencies has been also studied using MPA. Their performance is shown in Figure 3.12. As the dipoles are placed too closely (just 15 mm apart one from each other), there is a high correlation between them in the whole range of frequencies.

	Correlation		Correlation
freq [MHz]	**MPA**	**freq [MHz]**	**MPA**
800	0.95121	**910**	0.80622
820	0.93973	**920**	0.79169
860	0.8975	**930**	0.78144
870	0.88121	**940**	0.77595
880	0.86286	**960**	0.7778
890	0.84332	**980**	0.78971
900	0.82392	**1000**	0.80337

Table 3.5: Correlation between the dipoles computed with MPA

The graphical representation of this correlation values depending on the frequency can be seen in Figure 3.12. The correlation varies in the surroundings of our desired frequency.

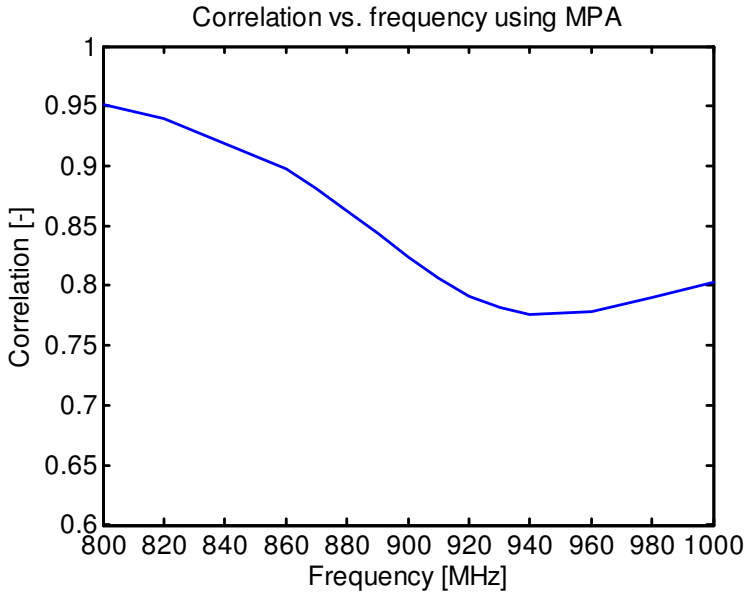

Figure 3.12: Correlation envelope vs. frequency computed using MPA

4. Reverberation Chamber

The measurements of the system performance will be made in the reverberation chamber from Bluetest AB [19] that Ethertronics has in its facilities in Kalmar.

This measurement instrument is used as an accurate method to measure the characteristics of the desired radiation of small antennas and active mobile terminals, especially those that will be used in Rayleigh fading environment such as wireless communications environments. Therefore, the uniform multipath environment, in which all directions of arrival over the whole unit sphere are equally probable [11], can be generated artificially in a reverberation chamber. In real environments, the Rayleigh distribution can be reproduced too, but it has many disadvantages compared to our proposed measurement method.

In the case of reverberation chambers, they will provide a repeatable laboratory-produced environment for characterizing our mobile device and its antennas. They can measure radiation efficiency, diversity gain, radiated power, MIMO system capacity, total radiated power and receiver sensitivity. As we can repeat exactly the same environment as many times as we want, only one single channel receiver will be used, avoiding to measure simultaneously the two channels and the single isolated antenna reference, as happened in the real environment case. Besides, real environment measurements are really time-consuming while our proposed measuring method is very fast.

In reverberation chambers, a minimum of absorption of electromagnetic energy occurs. Wall losses, leakage, lossy objects as well as the antennas affect the Q factor of the chamber and this value can be used to control the average power level of the transfer function. If the cavity resonators have a high Q factor, they can be used for electromagnetic compatibility (EMC) test methods. However, if the Q is lower they can be used for testing mobile terminals designed for using them in fading environments as in our case. With a lower Q-value, more cavity modes will be excited and the number of independent samples will increase too. To improve accuracy, some stirrers were included in the reverberation chambers. These stirrers are metal plate reflectors that can be used to simulate different boundary conditions while situating them in different orientations [18].

The stirring capabilities of the chamber as indicated in [8],[13] are:

- Mechanical stirring: Achieved by the movement of the two-plate stirrings along a complete wall or along the ceiling.

- Polarization stirring: It can be achieved switching between the three orthogonal wall-fixed antennas.

- Platform stirring: The antenna under test is located on a rotatable platform that moves the antenna to different positions.

- Frequency stirring: Averaging S_{21} or $|S_{21}|^2$ over a frequency band during the processing of the results.

A simple scheme of the reverberation chamber used, from [19]**,** is included below, see Figure 4.1. This basic measurement setup is used not only for measuring passive antenna performance but also for calibration. In the drawing, the head phantom is included and it is used to load the chamber for more excited mode. The antennas and the head phantom are located on a rotatable platform and rotated inside the chamber, giving us platform stirring. Moreover, the chamber makes use not only of this stirring type, but also of frequency stirring, to obtain a sufficient number of independent field contributions and polarization and mechanical stirring to improve even more the accuracy [8]. The head phantom and the device including the antennas are located far enough so they do not affect on the radiation efficiency of the antennas. The chamber is equipped with two mechanical plate-shaped stirrers [8].

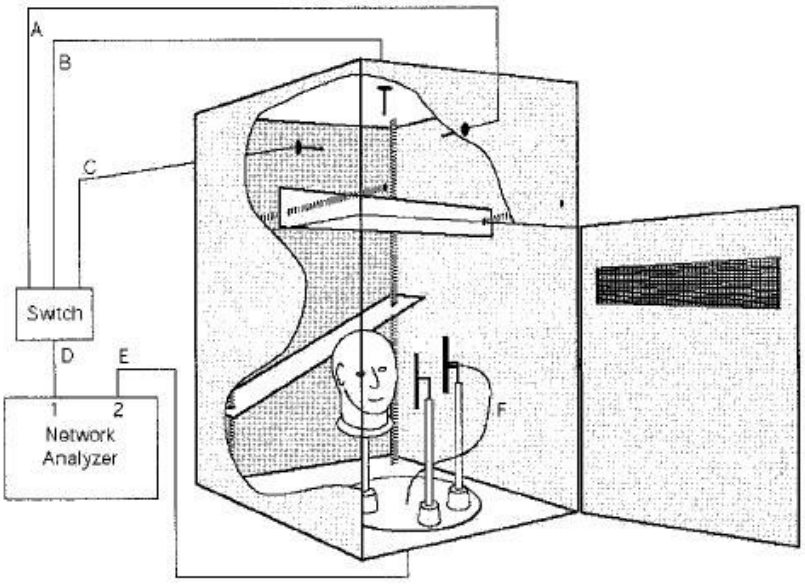

Figure 4.1: Schematic drawing of the reverberation chamber used in measurements. The chamber is available from Bluetest AB [19]

A network analyzer is used to acquire transmission samples S_{21} between the wall mounted antennas and the test antenna. Comparing the transmission samples to a known reference dipole, we can calculate the radiation efficiency of the antenna, which will be included in the calculation of the effective diversity gain. The level of the reference antenna must be measured in the same chamber under the same conditions as the AUT.

The radiation efficiency measured in the reverberation chambers that is defined in [8], includes impedance mismatch, losses in the antenna itself and losses in the near-in environment, such as the head phantom. In this case, the network analyzer is connected to the antenna under test (AUT) and through a switch, to the orthogonally placed receiving antennas. The S-parameter samples are measured between wall antennas and test antennas for each stirrer position and on the three switched receive antennas. It is also known that the average transfer function of the chamber is proportional to the radiation efficiency of the antennas.

A real photo of the chamber used can be seen in Figure 4.2. It has the dimensions 1.0m x 1.6m x 1.6m (depth, width, height). For more information about stirrer positions and other chamber parameters, see [19].

Figure 4.2: Real photo of the reverberation chamber used for measurements

The measurements in the reverberation chamber will be the apparent diversity gain and the effective diversity gain at 1% cumulative probability, the mean radiation efficiency over frequency band for antenna 1 and for antenna 2 and also the correlation coefficient between the two antennas. Those measurement results will be compared to the simulated ones in section 6 of this report. The combining method used by the reverberation chamber is Selection Combining (SEC).

5. Measurement setup and scenario

Not only simulated but also real results will be included in this thesis. For both measurements, the antennas will be placed in the upper part of a laptop. The measurements will be performed in a laptop design following a real laptop model.

Prior to explain the measurement setup, the generic method that will be followed to perform the simulations in this thesis is explained. A clarifying graph can be seen in Figure 5.1. As can be seen, after designing our laptop model, the single antenna element will be defined accordingly to the frequency requirements, depending on the bands that want to be covered. More antenna elements will be added and they will be located equally spaced. When placing all of them, some little adjustments should be done in order to maintain frequency specifications. Varying the source impedance, we will obtain several plots representing the variation of the total radiation efficiency, the correlation and the effective diversity gain. The results will be analyzed and an acceptable source impedance interval will be manually found for all the antennas for each frequency band. All the results will be included in section 6. Several antenna spacing will be studied.

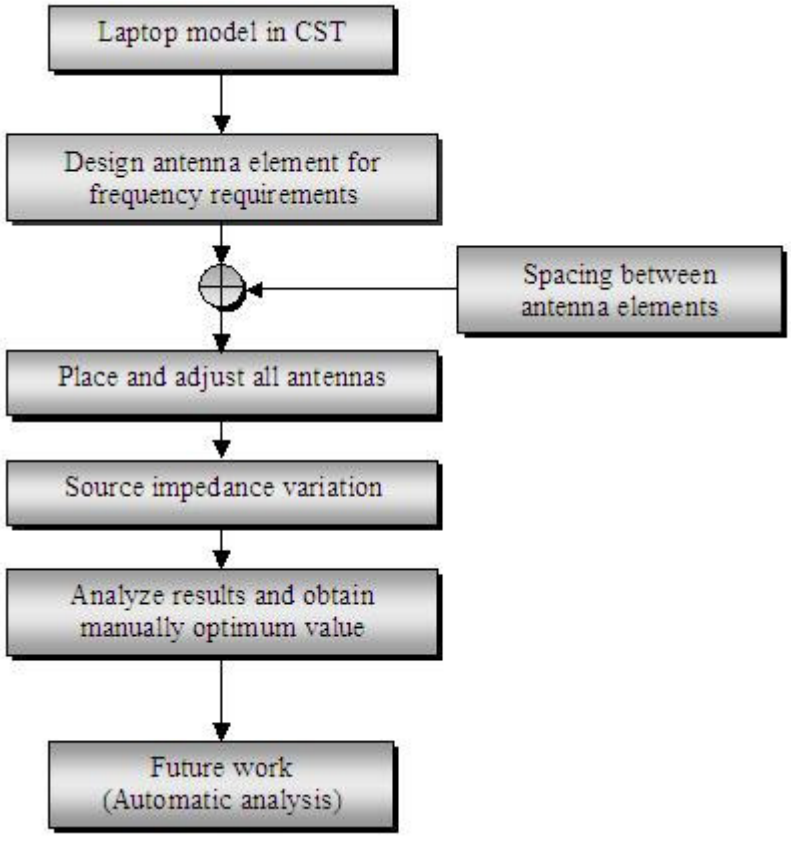

Figure 5.1: Graph representing a generic method to optimize antennas varying the source impedance for different frequency bands and a given antenna spacing

To start with the simulated design, we took into account the real laptop that we will use for measurements. The laptop used was a DELL Computer and due to its characteristics, the antennas will be placed on the upper part of the screen. Besides, we will use plastic blocks as the ones shown in Figure 5.2 that will fit perfectly in the space provided. The dimensions of the original plastic blocks were 2.5cm x 4.8cm x 10cm. Those plastic blocks have a chamfer edge and thereupon, the geometry of the used plastic blocks is not altogether rectangular.

First of all, the simulations of our design will be performed using CST and MPA software. The design of our antennas in CST is included in Figure 5.2. They were constructed just for laboratory purposes and they have no commercial value.

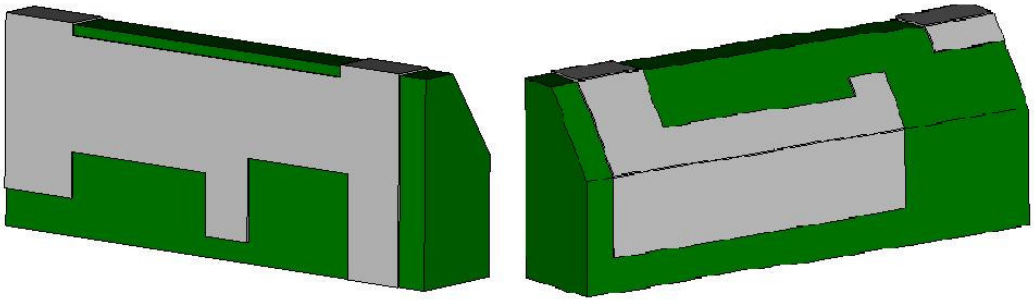

Figure 5.2: Antenna element design made using CST. Front (a) and back view (b)

As mentioned before in this thesis, two different measurement setups will be studied. First of all, 5 antenna elements will be located in the upper part of the screen and later on just 3 antennas located closely, will be simulated. Simulation results will be provided varying the source impedance for different spacing between the antenna elements.

After designing a single antenna element for the given band, I included 5 antenna elements in the laptop design. All the simulated antennas will be equal. The spacing between the five antennas will be 2.8 cm. A second case will be covered. In the three-antenna case the spacing between the elements will be just 1 cm, in order to increase the coupling between the antennas. They will be placed on the upper part of the laptop, already shown in section 3.1.1. The spacing of 2.8 cm was not chosen by chance, as it was the minimum spacing between the antennas that gave us acceptable coupling, according to the given specifications.

The complete model used to obtain the simulation results is shown below, in Figure 5.3, but not including the plastic cover as in Figure 3.1. The figure also includes the antenna elements used in our two cases of study.

Figure 5.3: Laptop design including both antenna cases

A detailed image of the metal upper parts considered for simulation as well as the element antennas was already seen in Figure 3.2.

The measurement results will be obtained just for the first case of study (5 antenna elements). The first step was to construct a real model that will be measured. I used the real DELL laptop mentioned before which I took into pieces in order to find a place in the upper part of it to place the antennas. In that upper part, I fixed a band of copper tape that plays the role of the metal surface included in the simulations in CST. Afterwards, I fixed five plastic blocks to include the copper tape later on them and to implement the antenna design previously simulated. The antennas will be made of adhesive copper tape over the designed plastic blocks. Each antenna must be adjusted in order to obtain the RL of each of them within the desired frequency bands. Figure 5.4 is a real representation of the designed antennas used in measurements.

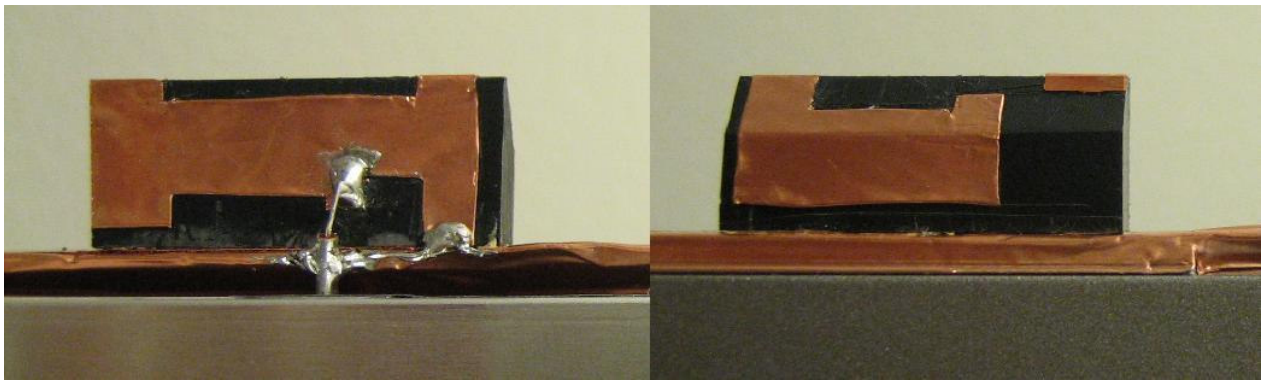

Figure 5.4: Front (a) and back (b) view of a real designed antenna element

The built real model can be seen Figure 5.5. The real laptop was modified, as previously explained and 5 antennas were included on the top part.

Figure 5.5: Real laptop model used for measurements

For the aim of this Thesis, different instrumentation was used. First of all, we used a personal computer to design the laptop and the antennas and to obtain the simulated results. As already mentioned in part 3, CST, CircSim, MPA and Matlab are used, as this is the software needed to obtain all the simulation results. Besides, a network analyzer will be used to perform real measurements of the coupling and the return loss of the antennas. Moreover, using a reverberation chamber we will obtain the antenna characteristics already mentioned in section 4.

To sum up, the procedure that was followed:

- Simulations of our 5-antenna case in CST
- Simulation of our 5-antenna case using MPA
- Implementation of 5 antennas on a real laptop
- Measurements in the lab using a network analyzer
- Measurements in reverberation chamber
- Modify the input impedance in our 5-antenna case using MPA, to obtain new simulated results, studying the influence of this parameter in all our desired antenna characteristics
- Simulation of our 3-antenna case in CST
- Simulation of our 3-antenna case using MPA
- Modify the input impedance in our 3-antenna case using MPA, to obtain new simulated results, studying the influence of this parameter in all our desired antenna characteristics

5.1 MEASURING ANTENNAS IN REVERBERATION CHAMBER

The AUT, our laptop including the 5-antennas, should be located inside the chamber but separated more than 0.5 wavelengths from the walls and mechanical stirrers [8]. Located far enough to avoid coupling, there should be a single reference antenna with known radiation efficiency. One of the AUT ports is connected to the network analyzer and the rest of the ports and the reference antenna will be terminated in 50 Ohms. The S-parameters are obtained between the port and the three-wall mounted antennas for all positions of the platform and the mechanical stirrers and for all frequency points. This procedure will be repeated for all our 5 antennas. The terminations on the rest of the unconnected ports will be of 50 Ohms. We will save the results for every stirrer position and frequency point. Due to the properties of the chamber and its stirrers, we can assume that the field environment inside is exactly the same when measuring all ports.

In our case, the reference antenna will be a dipole. The measurement procedure that will be followed is the same one as in [11]. Using platform stirring, moving the AUT in a circular path, we will obtain a higher number of independent samples, as studied in [20].

6. Results

In this chapter are included the simulation results obtained with CST and MPA, and also the measurement results obtained using the network analyzer and the reverberation chamber. The simulated results are performed for our two cases of study, with 3 and 5 antennas. However, the measurements results are obtained only for the 5-antenna port example, as it was the real model that we have implemented. In the Appendices A, B and C of this report, all the simulated results can be seen. More comments on the obtained results are included in chapter 7.

6.1 SIMULATION RESULTS

In this section, the results from the simulations using CST and MPA are presented. It has to be mentioned that the antennas were designed using CST and in order to fulfil the desired frequency specifications, they were tuned with the asked requirements. One single antenna element was designed and later on, it was copied to study our proposed cases with 3 or 5 antennas.

Thereafter, when the model was designed, the far-field patterns and the S-parameters obtained from CST were imported to the MPA to compare the efficiency results and to obtain the correlation and the apparent diversity gain between the ports. We located far-field monitors in the limits of the desired frequency bands and also at the central frequency of each band, as already seen in section 3.2.

Remembering what we mentioned in section 3.2.2, the far-field patterns obtained from CST have to be plotted as E-fields, in linear scaling, using as reference distance 1m and without far-field approximation. Besides, the angle step width is recommended to be 5 degrees, in order to obtain a better accuracy when importing those files to MPA. Those recommendations will be followed for our two cases of study.

Hence, simulations for the usual 50 Ohms source impedance were performed firstly, to study the desired antenna characteristics.

Afterwards, the source impedance of all ports will be modified to study how this parameter influences on the total radiation efficiency, the correlation and finally the effective diversity gain, as already done in section 3.3, for the two parallel dipoles example.

To calculate the effective diversity gain between each pair of antennas, we used two different approaches. If the total radiation efficiency of both ports was quite similar, we used the mentioned equations (2.3), (2.4) in section 2.1.4.1, calculating the Effective Diversity Gain at 1% probability level. However, if the radiation efficiency

of the two antennas was quite different, we cannot apply the same equations as before. Instead, we implemented equation (2.5) from [12], to obtain a cumulative probability density function of the combined signal to plot it and so the effective diversity gain was obtained as in Figure 2.1.

All the result figures are included in Appendices A and B, at the end of this report. However, some examples are included in this section to clarify how all the simulation plots were performed.

It should be noticed that the first covered case was the 5-antenna model with a separation between the elements of 2.8 cm. Contrary to expect, this model gave us a low correlation and therefore we decreased the distance between the antennas, considering just three ports. The spacing between them was 1 cm and the obtained correlation was higher, showing a lower effective diversity gain.

6.1.1 Five-antenna case

6.1.1.1 50 Ohm Source Impedance

In order to achieve some simulation results from MPA for our model, as explained in section 3.2, a circuit layout has to be defined. In our case, as we are working with 5 ports, the circuit that will be used is seen in Figure 6.1:

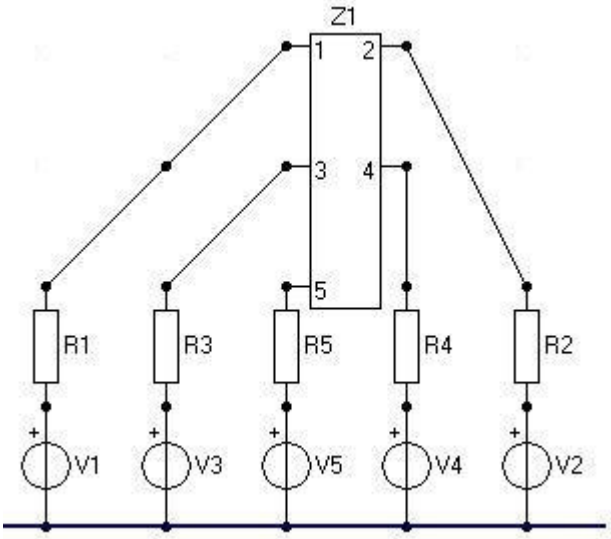

Figure 6.1: Five-port representation using CircSim

The efficiency for each port from CST is obtained directly when representing the far-field patterns. In the case of the efficiency obtained with MPA, for this first case, it was defined as efficiency per port, with source impedances of 50 Ω in the program. Therefore, in MPA, just the source voltage has to be defined. Besides, the sources in the CircSim circuit are chosen to be of 14.14 V to emulate the 1 W sources in CST, as in the dipoles example. The simulated results from CST and MPA can be seen on

Table 6.1. The radiation efficiency of our model obtained with 50 Ω source impedance using both programs is the same.

	Eff. Port1		Eff. Port2		Eff. Port3		Eff. Port4		Eff. Port5	
freq [GHz]	**CST**	**MPA**	**CST**	**MPA**	**CST**	**MPA**	**CST**	**MPA**	**CST**	**MPA**
1.92	0.6485	0.645	0.6545	0.6533	0.6248	0.6218	0.6274	0.624	0.5619	0.5603
1.95	**0.6603**	**0.6565**	**0.67**	**0.6688**	**0.6425**	**0.6399**	**0.6433**	**0.6403**	**0.5662**	**0.5637**
1.98	0.6694	0.6648	0.6928	0.6906	0.6666	0.663	0.6637	0.6601	0.5766	0.5714
2.11	0.6723	0.6707	0.6581	0.6554	0.6579	0.6542	0.6515	0.6493	0.5939	0.5909
2.14	**0.6774**	**0.6741**	**0.6795**	**0.6761**	**0.6891**	**0.6845**	**0.6767**	**0.6741**	**0.5989**	**0.5933**
2.17	0.6454	0.6402	0.6866	0.6827	0.6973	0.6927	0.6839	0.6827	0.585	0.5777
2.4	0.7731	0.7697	0.7974	0.7907	0.7574	0.7536	0.7817	0.7755	0.8046	0.7963
2.442	**0.7992**	**0.7968**	**0.7843**	**0.7752**	**0.7469**	**0.7427**	**0.7702**	**0.7611**	**0.7837**	**0.7753**
2.484	0.7509	0.747	0.7147	0.7039	0.6893	0.6845	0.7004	0.6888	0.7049	0.6961

Table 6.1: Simulated total radiation efficiency for the 5 ports using CST and MPA

In the following figure, Figure 6.2, a capture from the coupling obtained using CST between neighbouring antennas can be seen. In this figure we can see that there is an acceptable coupling between each pair of antennas.

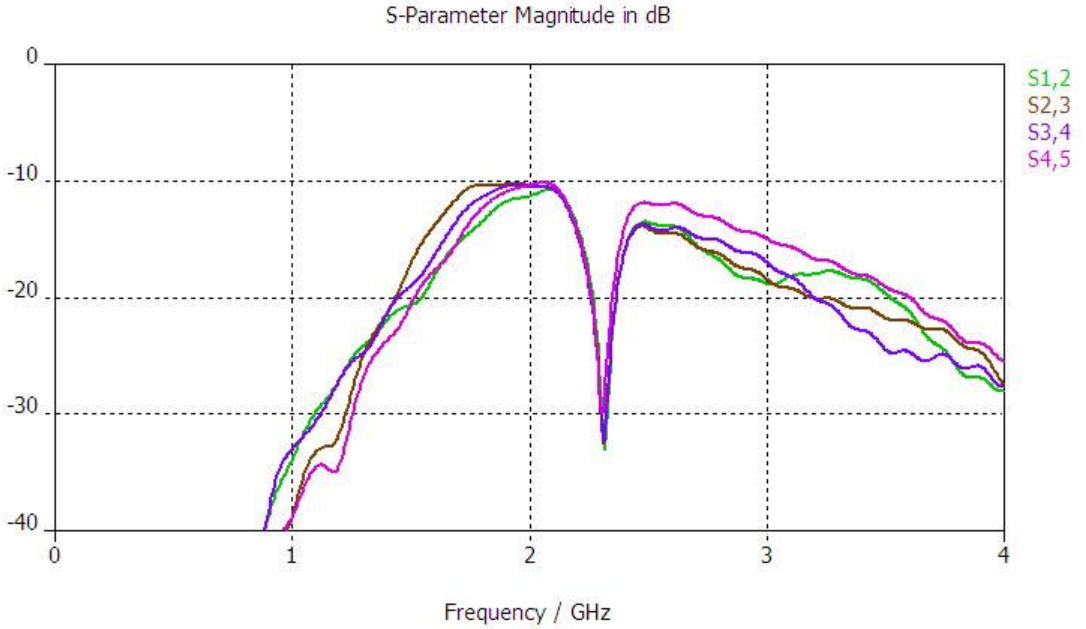

Figure 6.2: Coupling between the neighbour ports in 5-antenna case

Using MPA we can also obtain the correlation and the apparent diversity gain between each pair of ports. In the circuit design with CircSim just the two considered ports would be excited, leaving the rest of ports with zero volts. Besides, as we have to compute the ports two-by-two, just the central frequencies of our desired bands were included, to avoid a huge amount of results.

The effective diversity gain is obtained as explained in the introduction of this measurement results section, following two different approaches depending on the efficiencies of the ports. The two procedures will be clarified with two examples in section 6.1.1.2. Two tables are shown, each for the different frequency bands.

UMTS		Port 1-2	Port 1-3	Port 1-4	Port 1-5	Port 2-3	Port 2-4	Port 2-5	Port 3-4	Port 3-5	Port 4-5
UL (1.95 GHz)	Apparent Diversity Gain [dB]	9.95	9.90	9.93	9.98	9.99	9.93	9.85	9.99	9.76	9.91
	Effective Diversity Gain [dB]	8.09	7.92	7.95	8.45	8.01	7.95	8.45	8.01	7.78	8.45
	Correlation between the ports	0.16	0.21	0.18	0.09	0.07	0.18	0.26	0.05	0.33	0.20
DL (2.14 GHz)	Apparent Diversity Gain [dB]	9.97	9.89	9.92	9.94	9.99	9.95	9.89	9.99	9.85	9.96
	Effective Diversity Gain [dB]	8.17	8.09	8.12	8.45	8.19	8.15	8.45	8.19	8.45	8.45
	Correlation between the ports	0.11	0.22	0.19	0.17	0.058	0.16	0.22	0.05	0.26	0.13

Table 6.2: Correlation and Apparent and Effective Diversity Gain between each pair of ports for UMTS band

WLAN (2.442 GHz)	Port 1-2	Port 1-3	Port 1-4	Port 1-5	Port 2-3	Port 2-4	Port 2-5	Port 3-4	Port 3-5	Port 4-5
Apparent Diversity Gain [dB]	9.94	9.99	9.99	9.98	9.95	9.99	9.99	9.96	9.99	9.95
Effective Diversity Gain [dB]	8.81	9.54	8.86	8.85	8.82	8.86	8.86	8.83	8.86	8.82
Correlation between the ports	0.17	0.08	0.05	0.10	0.15	0.04	0.05	0.14	0.06	0.15

Table 6.3: Correlation and Apparent and Effective Diversity Gain between each pair of ports for WLAN band

The correlation obtained is not as high as we firstly expected and we obtained a high apparent diversity gain. Therefore, the only way that we can affect the effective diversity gain is by varying the radiation efficiency of the antennas.

6.1.1.2 Varying the Source Impedance

Changing the source impedance, the efficiency of each port plus the correlation and therefore the effective diversity gain can be influenced. Taking as example the published example for the dipoles, see [5], the source impedance can have also imaginary values. In our case, just positive imaginary part will be considered.

In this second case, the efficiency obtained with MPA was defined as total radiation efficiency per port but with source impedances obtained from an attached file as done in section 3.3. Again, the sources in the CircSim circuit are chosen to be of 14.14 V to emulate the 1 W sources in CST. In this case, to define the efficiency on MPA, we have to include the source voltage, the port current and the port current of each of the ports.

After obtaining the MPA results and using Matlab, we obtained several plots for each of the parameters and for all the frequency bands that can be seen in Appendix A. The study of each of the frequency bands is done manually and later on combined results can be seen.

As explained before, if the total radiation efficiency of both ports is more or less similar, we used the mentioned equations in section 2.1.4.1, calculating the effective diversity gain at 1% probability level.

To show this first procedure, we will take here the example of ports 2 and 3 for 1.95 GHz. The total radiation efficiencies plots for both ports are quite similar and can be seen in Figure 6.3:

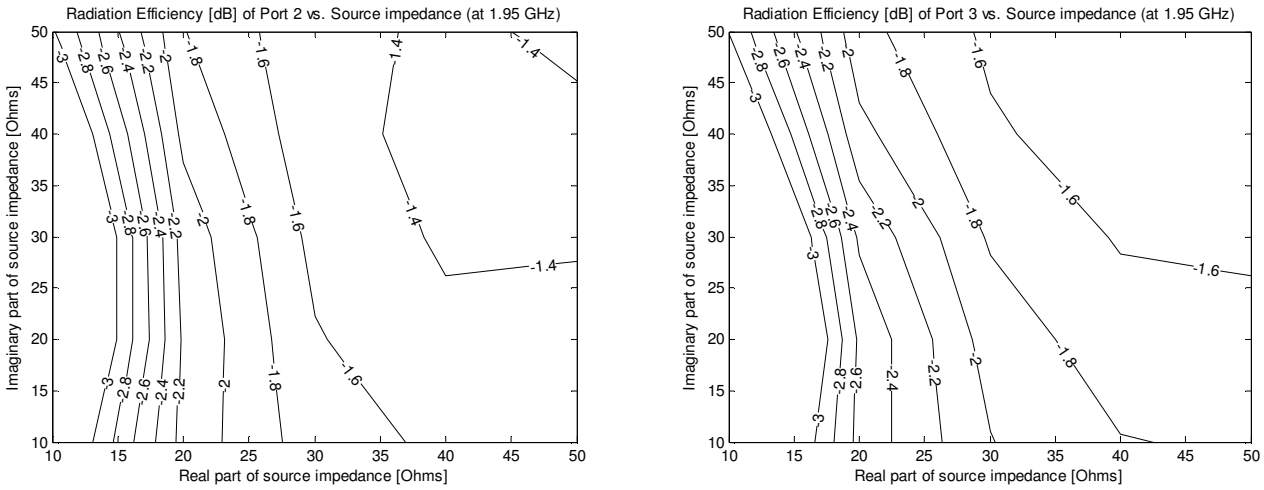

Figure 6.3: Total Radiation Efficiency for ports 2 (a) and 3 (b) at 1.95 GHz

The correlation between both ports calculated using MPA is represented using Matlab in Figure 6.4:

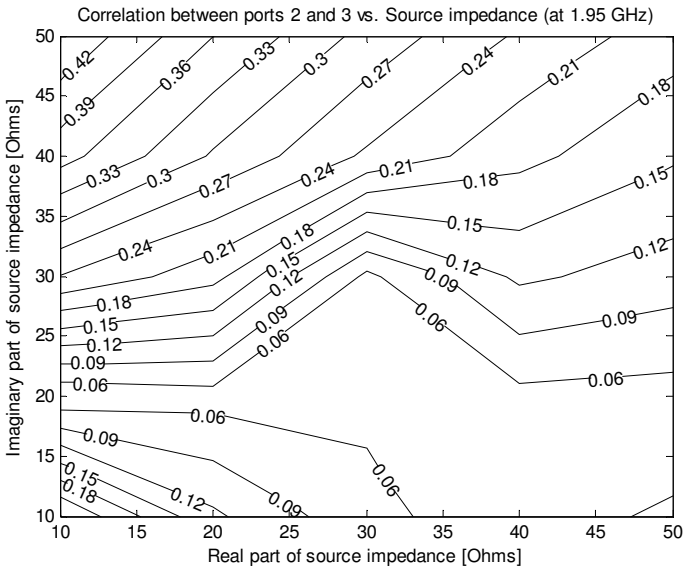

Figure 6.4: Correlation between ports 2 and 3 at 1.95 GHz

Therefore, just applying the equations (2.3) and (2.4), the calculated Effective Diversity Gain between port 2 and 3 can be represented in Matlab as a function of the different source impedances as in Figure 6.5:

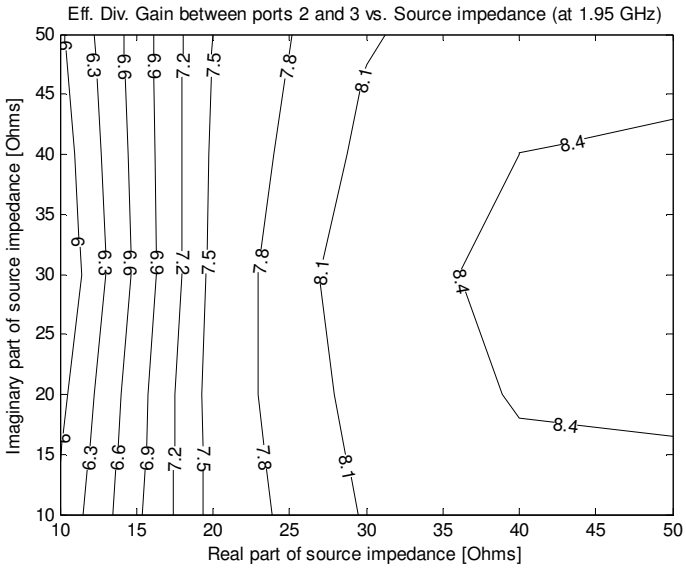

Figure 6.5: Effective Diversity Gain between ports 2 and 3 at 1.95 GHz

However, if the radiation efficiency of the two antennas is quite different, we implemented equation (2.5) to obtain the cumulative probability density function of the combined signal. This difference in the radiation efficiencies between two ports is mainly seen between the antennas on both ends of the laptop, ports 1 and 5. Thus, the difference in performance might be caused because those antenna ports have just one neighbour, whereas the rest of antennas have two, one on each side.

To show this second procedure, we will take here the example of ports 1 and 2 for 1.95 GHz. The total radiation efficiencies plots for both ports can be seen in Figure 6.6:

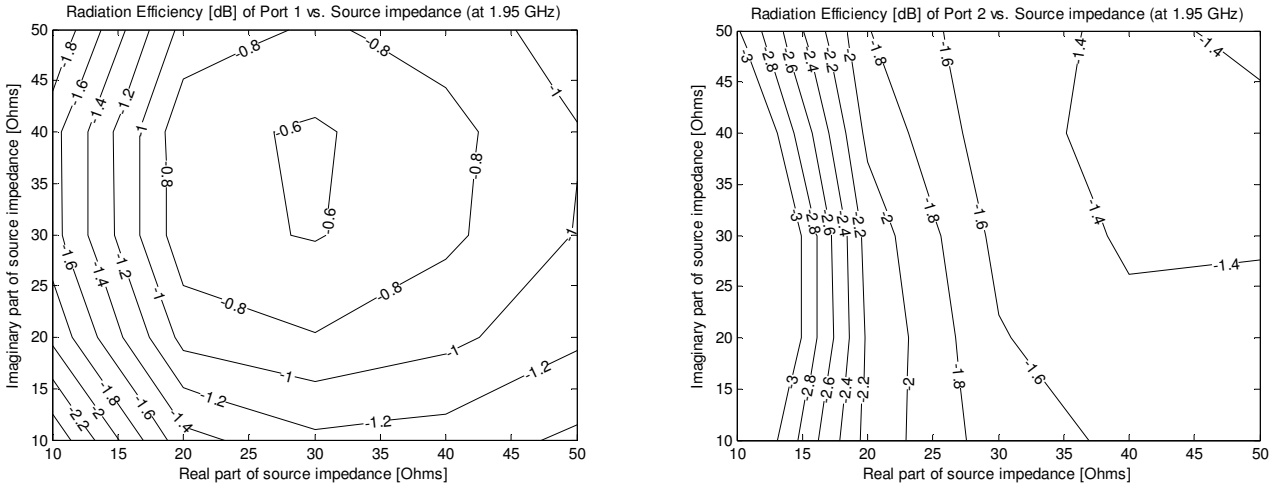

Figure 6.6: Total Radiation Efficiency for ports 1 (a) and 2 (b) at 1.95 GHz

The correlation between both ports calculated using MPA is represented in Figure 6.7 and applying equation (2.5) and computing the Effective Diversity Gain for each value of source impedance, the Matlab representation can be seen in Figure 6.8:

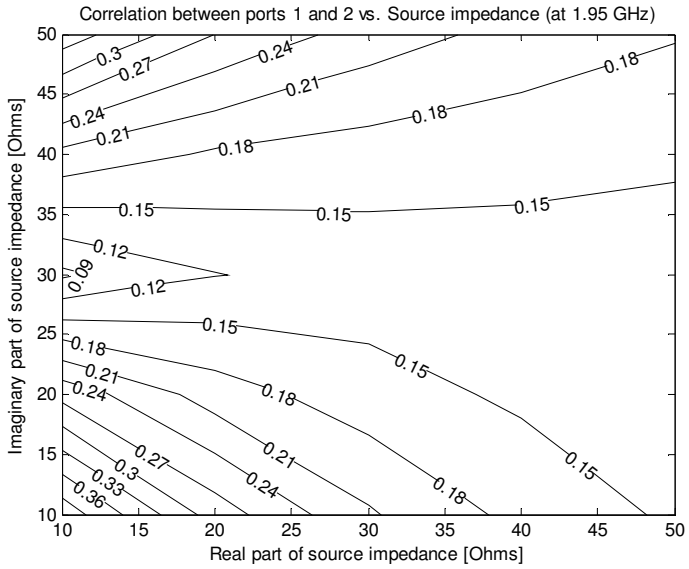

Figure 6.7: Correlation between ports 1 and 2 at 1.95 GHz

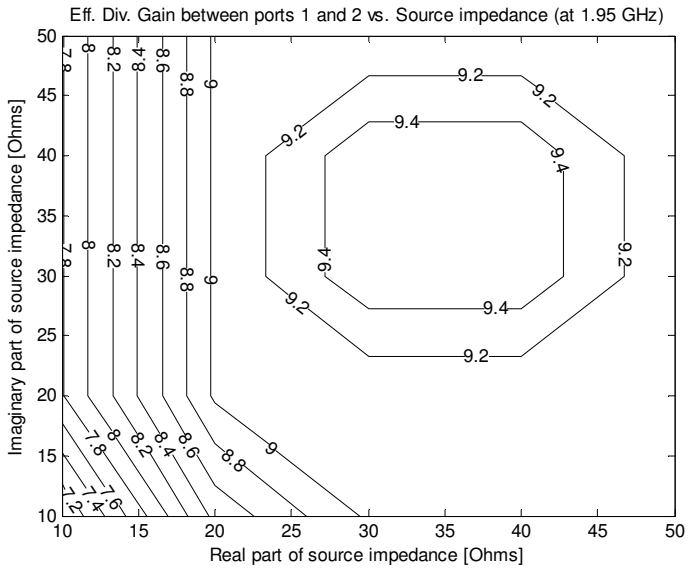

Figure 6.8: Effective Diversity Gain between ports 1 and 2 at 1.95 GHz

Analyzing manually the obtained plots for all ports, a combined representation of all the frequency requirements can be done. Those graphical results show the regions that when varying the source impedance, we can have an acceptable performance of our system. In Figure 6.9, we represented the source impedance intervals where the total radiation efficiency is better than –3 dB for each of the bands. And in Figure 6.10 we can see the source impedance intervals where the correlation is lower than 0.3. Each of the frequency intervals is represented with a different colour and a different pattern. Therefore, the common values for all the intervals can be clearly seen.

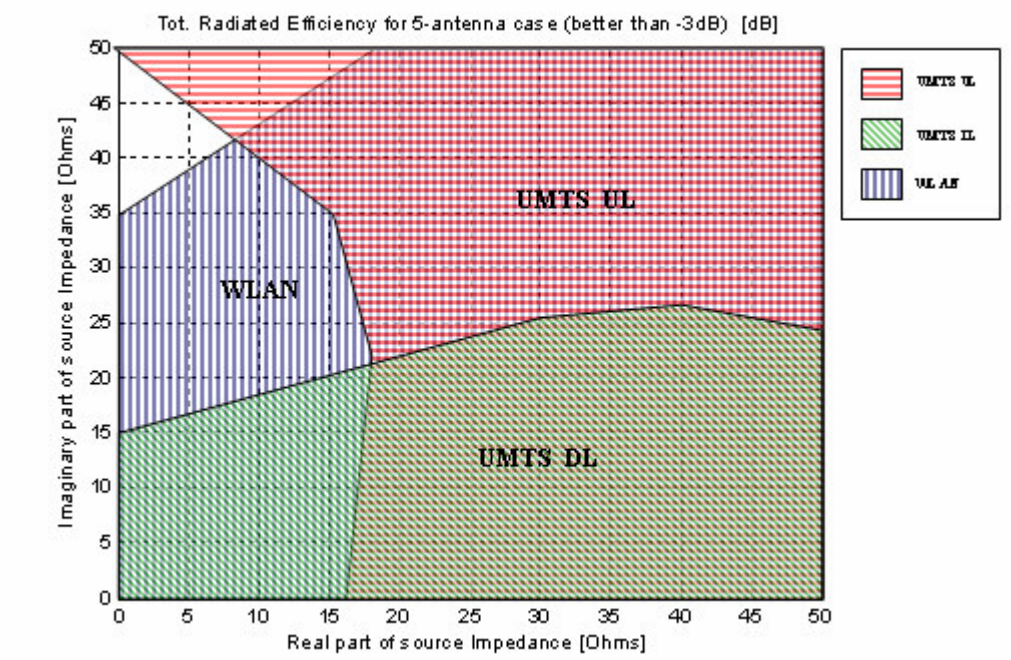

Figure 6.9: Representation of the Tot. Radiation Efficiency better than -3 dB for 5-antenna case

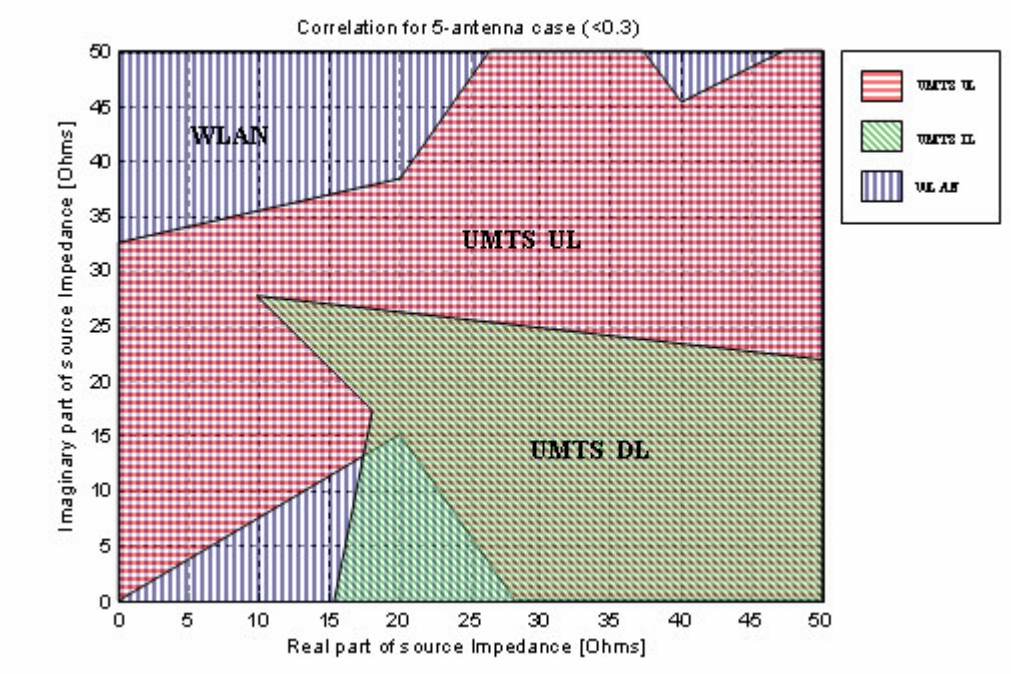

Figure 6.10: Representation of correlation better than 0.3 for 5-antenna case

Finally, in Figure 6.11, we can see a representation of the Effective Diversity Gain areas higher than 8 dB for each frequency band. Using again the same colour and pattern definition for the intervals, we can clearly see the common area.

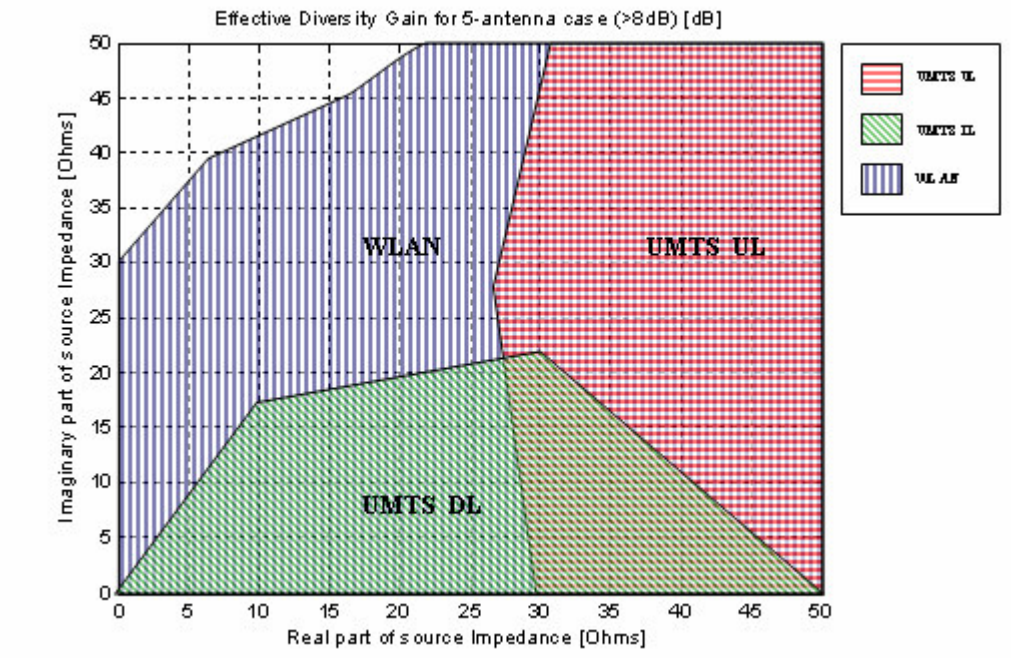

Figure 6.11: Representation of Effective Diversity Gain better than 8 dB for 5-antenna case

6.1.2 Three-antenna case

6.1.2.1 50 Ohm Source Impedance

As we have done in the previous example, to achieve some simulation results from MPA for our model, a circuit layout has to be defined. In this second case, we just need to define three ports (see Figure 6.12) as we have only three antenna elements.

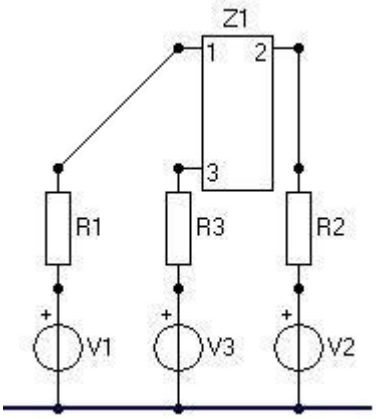

Figure 6.12: Three-port representation using CircSim

The efficiency for each port from CST is obtained once more directly when representing the far-field patterns. To define the efficiency in MPA, we defined it as efficiency per port, with source impedances of 50 Ω, proceeding as in section 6.1.1.1. Besides, the sources in the CircSim circuit are chosen again to be of 14.14 V to emulate the 1 W sources in CST.

In Figure 6.13, coupling obtained using CST between each pair of antenna ports can be seen. As opposed to the previous 5-antenna case, we have now a higher coupling between the 3-antenna ports that will influence the correlation and the effective diversity gain of the system.

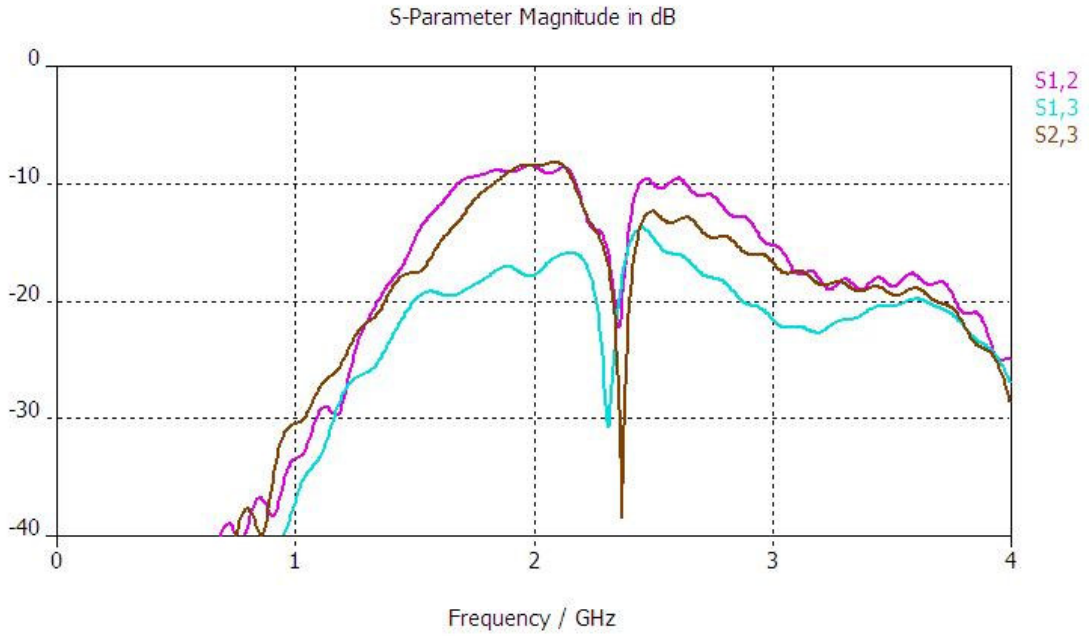

Figure 6.13: Coupling between the ports in 3-antenna case

The simulated radiation efficiency from CST and MPA can be seen on Table 6.4. The efficiency values obtained using both programs are almost the same.

	Eff. Port1		Eff. Port2		Eff. Port3	
freq [GHz]	**CST**	**MPA**	**CST**	**MPA**	**CST**	**MPA**
1.92	0.6636	0.661	0.6042	0.6038	0.6082	0.6038
1.95	0.6639	0.661	0.5954	0.5947	0.6218	0.6174
1.98	0.6657	0.6624	0.5899	0.5894	0.6400	0.6344
2.11	0.6316	0.6266	0.5787	0.5773	0.6334	0.6301
2.14	0.6301	0.6247	0.5879	0.5866	0.6578	0.6532
2.17	0.6348	0.6291	0.6187	0.6171	0.6700	0.6635
2.4	0.7240	0.7118	0.7849	0.7838	0.8185	0.8162
2.442	0.7203	0.7081	0.7454	0.7433	0.8219	0.8184
2.484	0.6778	0.6650	0.6873	0.6836	0.7572	0.7511

Table 6.4: Simulated total radiation efficiency for the 3 ports using CST and MPA

Using MPA for this second case, we can also obtain the correlation and the apparent diversity gain between each pair of ports. Just the far-field monitors in the central frequencies of our bands are studied. In the circuit design with CircSim, we just excite the two ports that are being studied, putting the rest of them to zero volts.

The effective diversity gain is computed as in previous part (see section 6.1.1) and two examples for the three-antenna case can be seen in section 6.1.2.2.

UMTS		Port 1-2	Port 1-3	Port 2-3
UL (1.95 GHz)	Apparent Diversity Gain [dB]	9.8196	9.6938	9.7531
	Effective Diversity Gain [dB]	8.4510	8.4510	7.2726
	Correlation between the ports	0.28518	0.3663	0.3311
DL (2.14 GHz)	Apparent Diversity Gain [dB]	9.6549	9.7778	9.7155
	Effective Diversity Gain [dB]	7.0583	7.5559	8.4510
	Correlation between the ports	0.38721	0.31501	0.35394

Table 6.5: Correlation and Apparent and Effective Diversity Gain between each pair of ports for UMTS band

WLAN (2.442 GHz)	Port 1-2	Port 1-3	Port 2-3
Apparent Diversity Gain [dB]	9.9312	9.98096	9.9937
Effective Diversity Gain [dB]	8.5931	9.0309	9.5424
Correlation between the ports	0.17833	0.29269	0.054267

Table 6.6: Correlation and Apparent and Effective Diversity Gain between each pair of ports for WLAN band

For the WLAN band, as the second antenna suffers more coupling caused by its two neighbour antennas, the correlation values obtained are higher. Besides, in all the frequency bands, we see that the effective diversity gain obtained is lower than in the 5-antenna case.

6.1.2.2 Varying the Source Impedance

Once more, we will study the influence of the source impedance in the radiation efficiency, the correlation and the diversity gain. Once we have obtained the simulated values from MPA for this second case, we will follow separate procedures if the radiation efficiency of each port is quite different from each other or not. Following the same procedure as explained before in the introduction of this chapter, we obtained effective diversity gain using two different approaches. Once more, the total radiation efficiency defined in MPA has to include the definition of the source voltages, the port voltages and the port currents, when using different source impedance values.

If the total radiation efficiency from both ports is similar, we will use again equations (2.3) and (2.4) from section 2.1.4.1.

In this second case of three antennas, we will take as example ports 1 and 3 for 1.95 GHz.

The total radiation efficiencies plots for both ports can be seen in Figure 6.14:

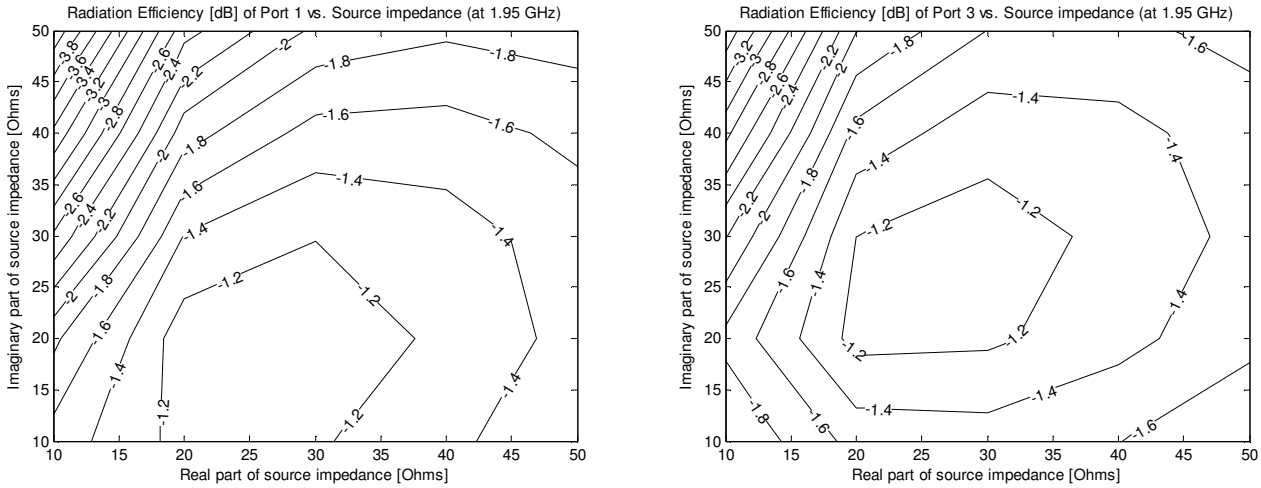

Figure 6.14: Total Radiation Efficiency for ports 1 (a) and 3 (b) at 1.95 GHz

The correlation between both ports calculated using MPA is represented using Matlab in Figure 6.15:

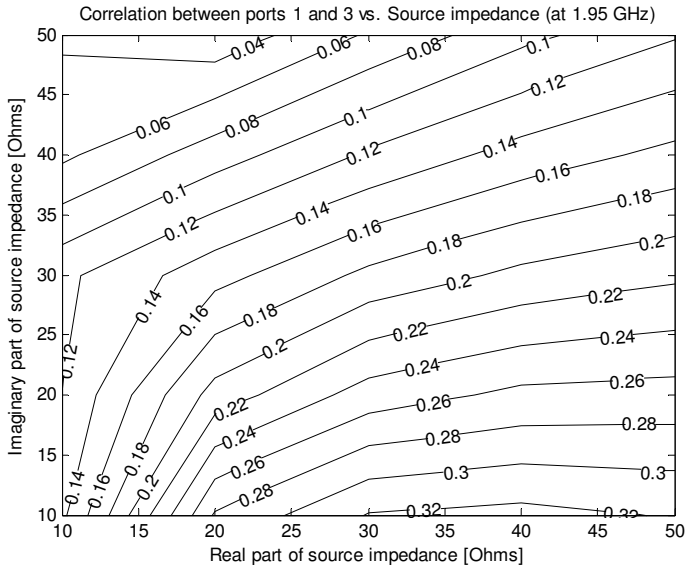

Figure 6.15: Correlation between ports 1 and 3 at 1.95 GHz

Finally, applying equations (2.3) and (2.4), the calculated effective diversity gain can be seen in Figure 6.16:

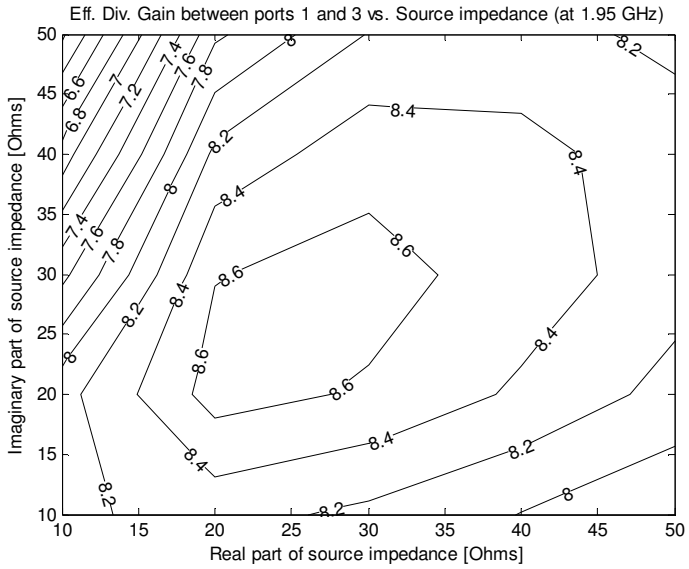

Figure 6.16: Effective Diversity Gain between ports 1 and 3 at 1.95 GHz

As we have done before, there are cases where the radiation efficiency of both ports is so different that we cannot simply apply the equations from section 2.1.4.1. Once more, the equation (2.5) will be used to obtain a combined signal and therefore, calculate the effective diversity gain. As it happened in the previous case, the difference in the radiation efficiencies between two ports is seen between the antennas on both ends of the laptop, ports 1 and 3 in this case. Thus, the difference in performance might be caused because those antenna ports have just one neighbour, whereas the central antenna, port 2, have as neighbours two antennas, ports 1 and 3.

Taking the example of ports 1 and 2 for 1.95 GHz, the radiation efficiency of each of them is shown in Figure 6.17:

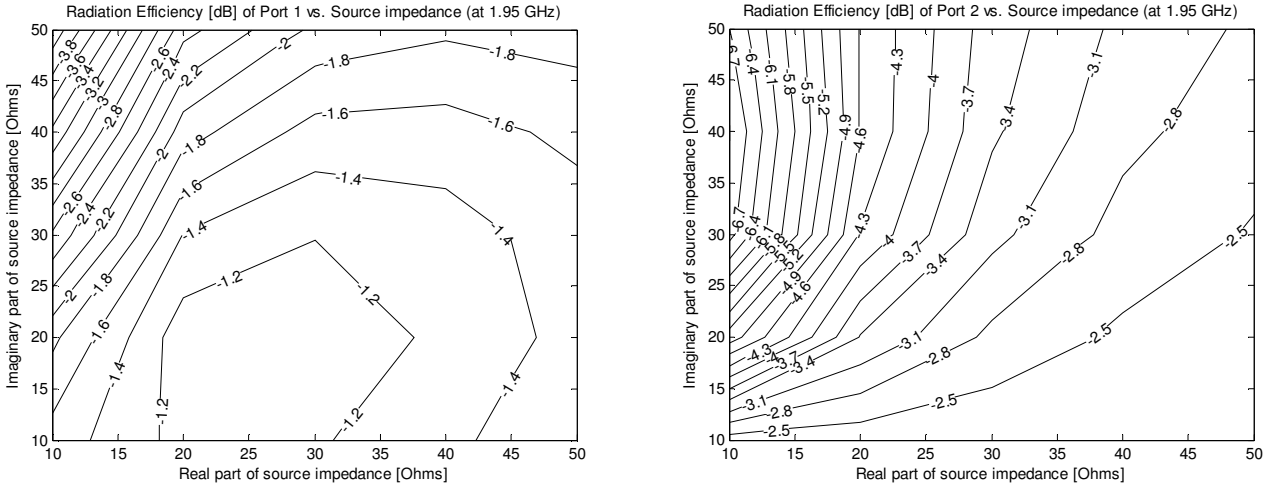

Figure 6.17: Total Radiation Efficiency for ports 1 (a) and 2 (b) at 1.95 GHz

The correlation between both ports calculated using MPA is represented in Figure 6.18:

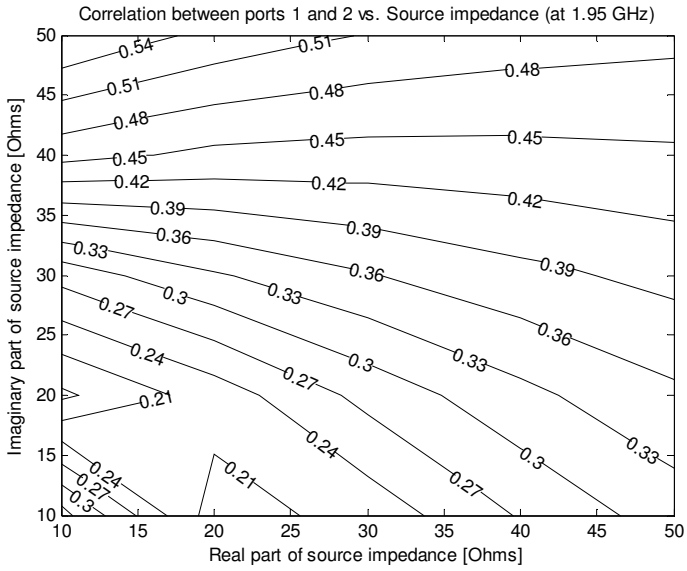

Figure 6.18: Correlation between ports 1 and 2 at 1.95 GHz

Finally, the calculated effective diversity gain using the combined signal obtained from equation (2.5) is represented in Figure 6.19:

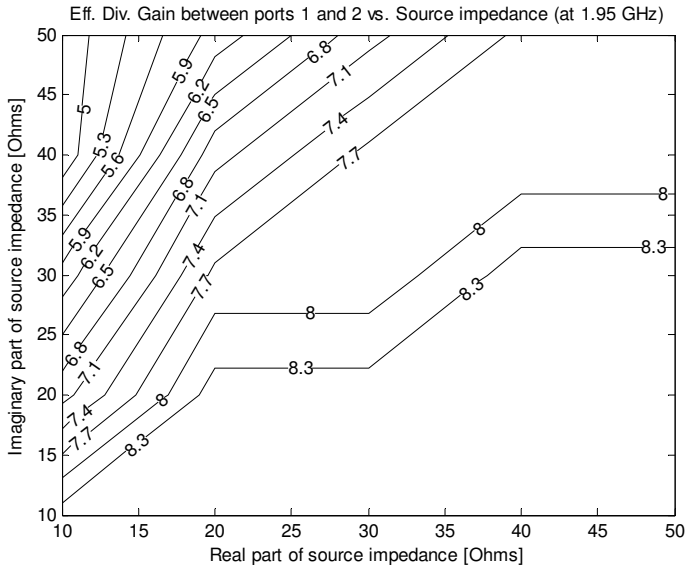

Figure 6.19: Effective Diversity Gain between ports 1 and 2 at 1.95 GHz

See the rest of the obtained simulations, for all the central frequency bands and for each pair of ports at the end of this thesis, in Appendix B, attached at the end of this report.

As we have done in the previous case, we can analyze manually the obtained plots for all ports. We can represent all the frequency band regions that fulfil each of the specifications in the same plot when varying the source impedance. In Figure 6.20, we represented the source impedance intervals where the total radiation efficiency is better than –3 dB for each of the bands. Each of the frequency intervals is represented with a different colour and a different pattern. Therefore, the common values for all the intervals can be clearly seen.

In Figure 6.21, the source impedance intervals where the correlation is lower than 0.3 can be seen. As there is no common region in this second case, we allowed a correlation lower than 0.4, as in Figure 6.22. Even though the correlation is higher in this case, we see that at least there is a common region between WLAN and the Up-Link band of UMTS. However, for the Down-Link band, the correlation is still higher than the allowed limit. In this second case, with 3-antennas placed closer, it is more difficult to find a common optimization value in terms of correlation.

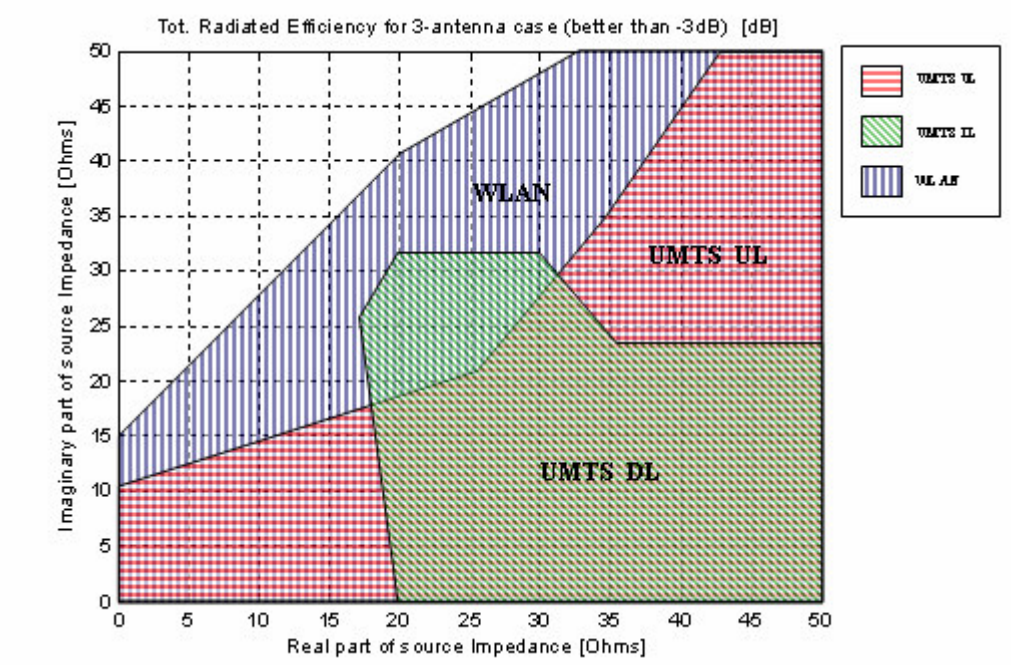

Figure 6.20: Representation of the Tot. Radiation Efficiency better than -3 dB for 3-antenna case

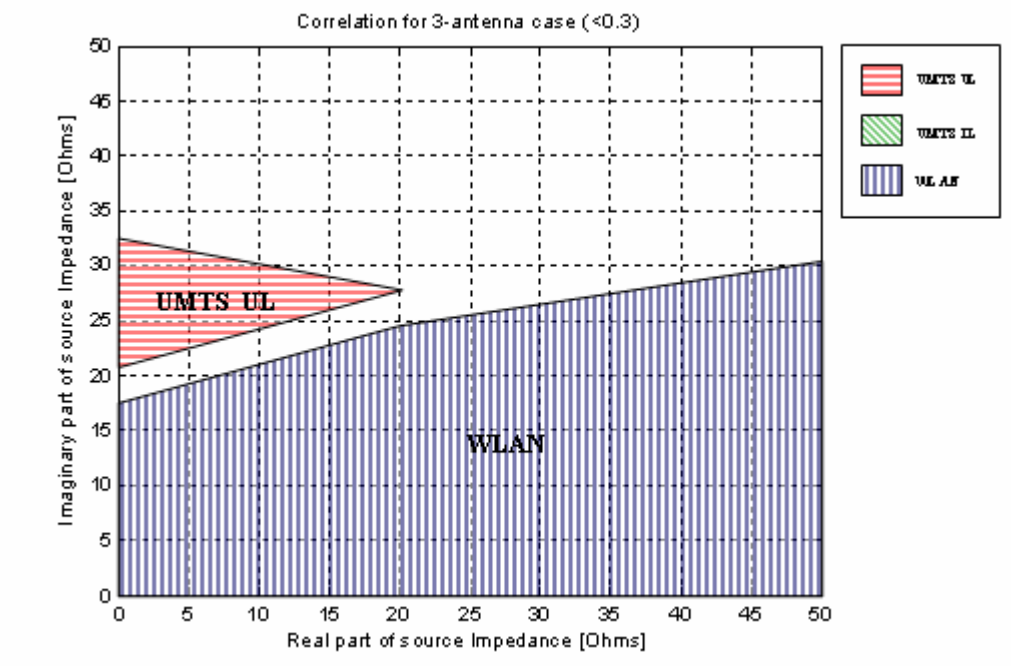

Figure 6.21: Representation of correlation better than 0.3 for 3-antenna case

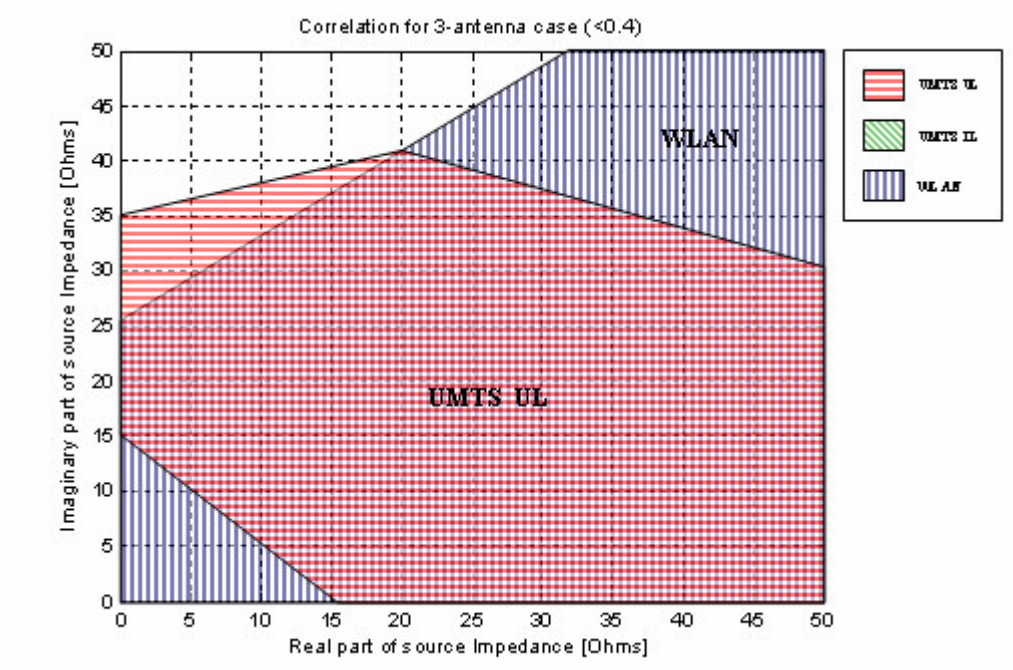

Figure 6.22: Representation of correlation better than 0.4 for 3-antenna case

Nevertheless, looking at Figure 6.23, we found that the variation of the source impedance allowed us to find a region where the effective diversity gain is better than 8 dB for all the frequency requirements.

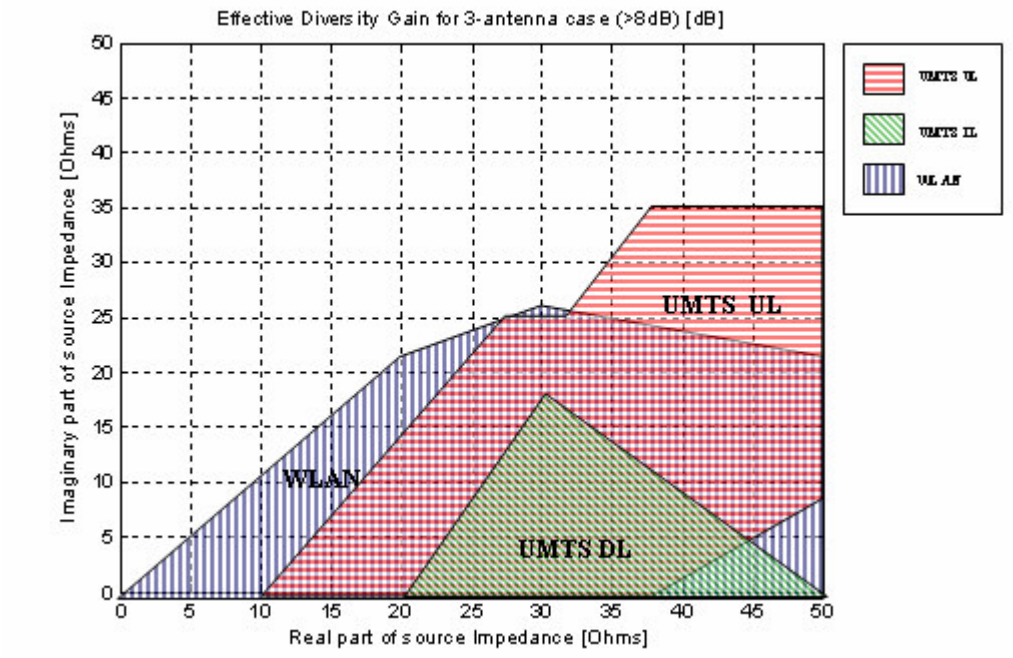

Figure 6.23: Representation of Effective Diversity Gain better than 8 dB for 3-antenna case

6.2 MEASUREMENT RESULTS

In this section, the measurement results from the real model will be included. It has to be mentioned that the measured results from the network analyzer were done tuning the antennas for the desired frequency bands specifications. Although, the exact dimensions from simulated antennas were taken, small variations on them were made in the real ones. Therefore, not a direct relationship between simulations and measurements can be done. The antennas will have small adjustments for fine-tuning, as real measurements most of the times differ from simulated and expected values.

The real model design corresponds to our 5-antenna port example.

6.2.1 Network Analyzer measurements

To start with the measurements using the network analyzer, firstly, it must be calibrated correctly. Then, the procedure that will be followed is to connect the two ports of the network analyzer to the different ports in our design. We will change them between each pair of ports to obtain the scattering parameters, and the rest of the ports in the antenna design will be terminated with 50 Ω impedances. The obtained results will be saved to represent them afterwards using Matlab. As can be seen in the figures below, the selected frequency range of our plots corresponds to the working range used for this Thesis. Thus, the important frequency values for the asked standards are included.

In the next figure (Figure 6.24), the input port voltage reflection coefficients for all the five ports are shown. As can be seen, for all our limit frequencies (1.92, 2.17, 2.4, 2.48 GHz) the reflection coeffients are below –6 dB.

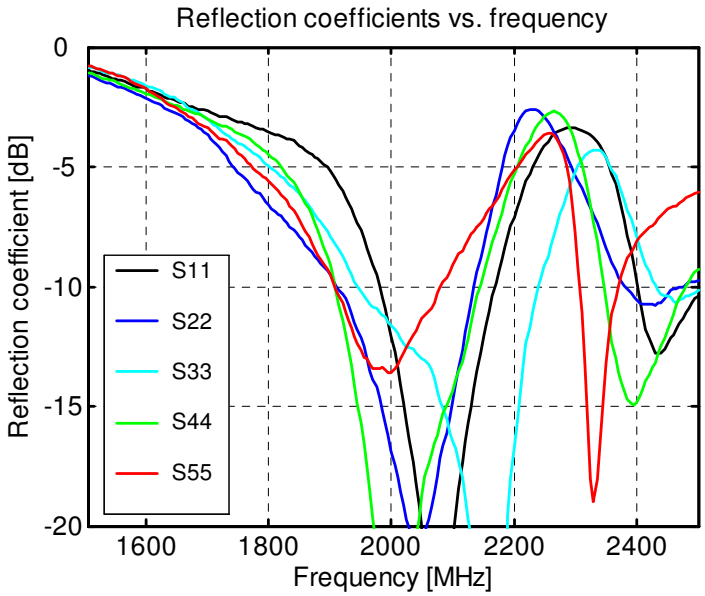

Figure 6.24: Measured reflection coefficient using network analyzer vs. frequency for 5-antenna case

In the following figures (Figures 6.25 to 6.29), the measured coupling between each of the ports and the rest of our antennas is shown. The coupling between each excited and the rest of the ports is shown following the notation "S_{ab}", where "b" represents the excited port and "a" the port that receives the coupled voltage from the excited port "b".

In Figure 6.25, we can see that the highest coupling when exciting port one is between port two, as it is the closest antenna. However, the coupling between those ports is lower than the specified limit for antenna design.

In Figure 6.26, when exciting port two, not only the coupling between this port and port one is important, but also the coupling with port three, the other neighbouring antenna. Once more, the coupling in this case is lower than expected and lower than the allowed limit.

When exciting port three, the coupling between this port and ports two and four will be the most significant as they are neighbours. Besides, as can be seen in Figure 6.27, the coupling with port five is also important. Nevertheless, none of the coupling plots are above our established limit of –10 dB.

For the last two cases, when exciting ports four and five, the coupling between them is out of the allowed bounds. Figures 6.28 and 6.29 show this behaviour. Moreover, when exciting port four, the coupling between this port and port three has to be also considered and therefore, varied using our mentioned approach in the simulated part. For real measurements, the source impedance variation should be done varying the matching network. Unfortunately, due to the reduced time, no results will be provided for this real case.

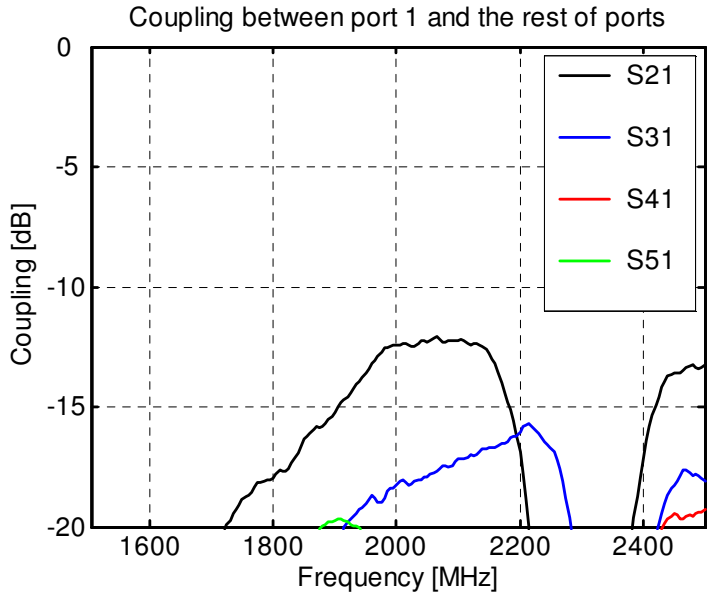

Figure 6.25: Measured coupling using network analyzer between port 1 and the rest of ports in the 5-antenna design

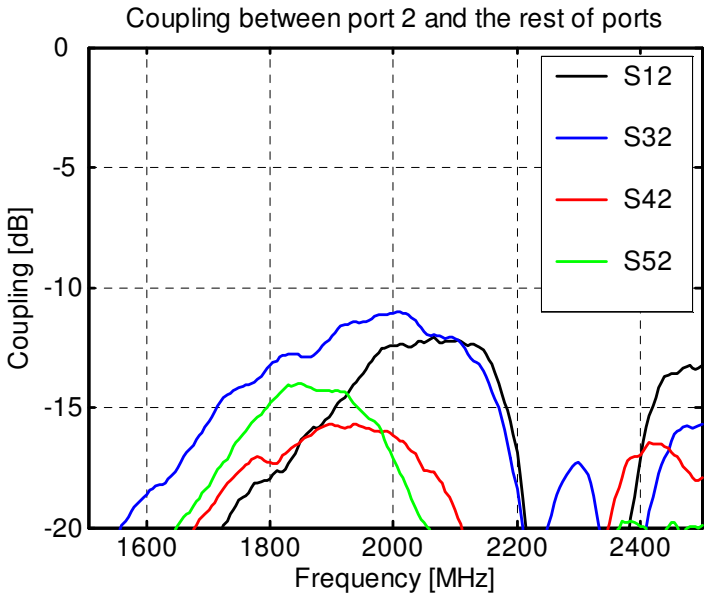

Figure 6.26: Measured coupling using network analyzer between port 2 and the rest of ports in the 5-antenna design

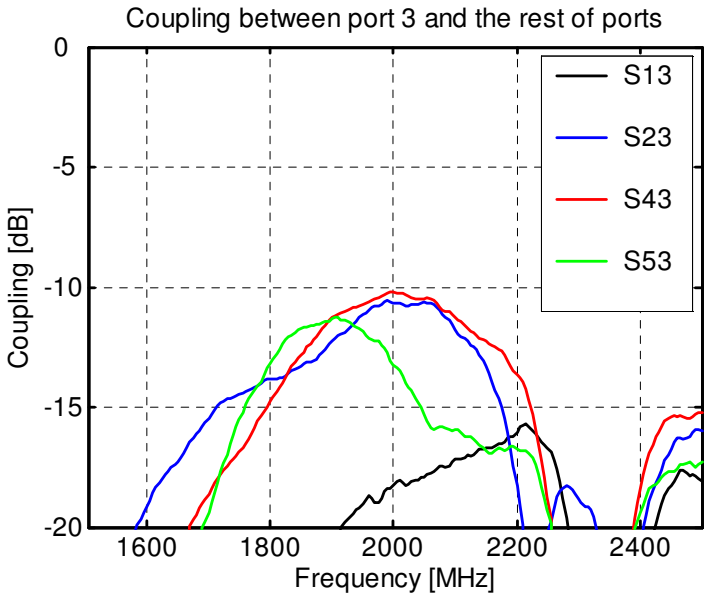

Figure 6.27: Measured coupling using network analyzer between port 3 and the rest of ports in the 5-antenna design

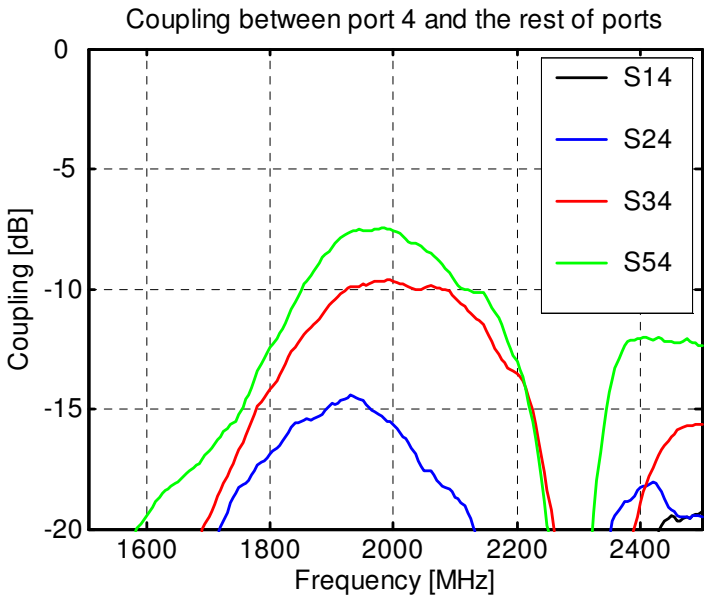

Figure 6.28: Measured coupling using network analyzer between port 4 and the rest of ports in the 5-antenna design

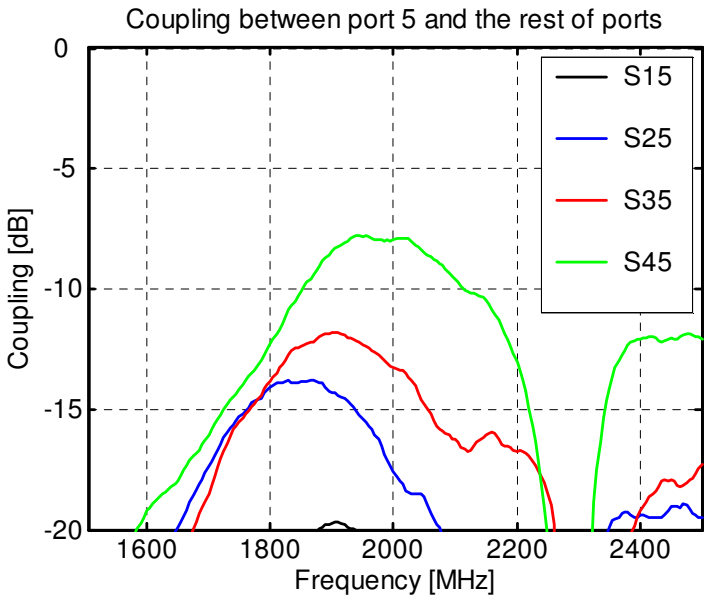

Figure 6.29: Measured coupling using network analyzer between port 5 and the rest of ports in the 5-antenna design

6.2.2 Reverberation chamber measurements

The measurements obtained will be passive since no electronics of the laptop will be used. Placing the laptop inside the chamber and also the reference dipole, for each of the frequency requirements, the measurements will be performed as explained in section 5.1. The obtained results can be seen in tables 6.7, 6.8 and 6.9.

		Port 1	Port 2	Port 3	Port 4	Port 5
Mean Radiation Efficiency [dB]	**UMTS**	-2.16	-2.38	-2.79	-3.08	-3.08
	WLAN	-2.52	-2.19	-2.72	-2.14	-2.5

Table 6.7: Measured mean radiation efficiency in dB for each port in both bands using the reverberation chamber

UMTS	**Port 1-2**	**Port 1-3**	**Port 1-4**	**Port 1-5**	**Port 2-3**	**Port 2-4**	**Port 2-5**	**Port 3-4**	**Port 3-5**	**Port 4-5**
Apparent Diversity Gain [dB]	10	10.4	10.6	9.98	9.95	9.81	10	9.93	9.64	9.34
Effective Diversity Gain [dB]	8.12	8.11	8.3	8.04	8.04	7.89	8.09	7.62	7.7	7.4
Correlation between the ports	0.07	0.047	0.028	0.026	0.02	0.059	0.026	0.019	0.094	0.15

Table 6.8: Measured apparent and effective diversity gain and correlation for each pair of ports in UMTS band using the reverberation chamber

WLAN	**Port 1-2**	**Port 1-3**	**Port 1-4**	**Port 1-5**	**Port 2-3**	**Port 2-4**	**Port 2-5**	**Port 3-4**	**Port 3-5**	**Port 4-5**
Apparent Diversity Gain [dB]	10.2	10.1	9.82	10.2	9.88	9.87	10.4	9.89	9.93	9.46
Effective Diversity Gain [dB]	8.53	8.62	8.95	8.49	8.37	9	8.45	9.02	8.43	8.59
Correlation between the ports	0.059	0.072	0.034	0.03	0.04	0.05	0.055	0.061	0.057	0.081

Table 6.9: Measured apparent and effective diversity gain and correlation for each pair of ports in WLAN band using the reverberation chamber

An example of the calculated diversity gain is shown below, in Figure 6.30. With the measurements obtained from the reverberation chamber, we can plot in Matlab all the cumulative density functions for each pair of ports and for the desired frequency band and thus, the effective diversity gain will be shown graphically. The rest of the result plots made with Matlab using the measured results of reverberation chamber are included in Appendix C at the end of this report.

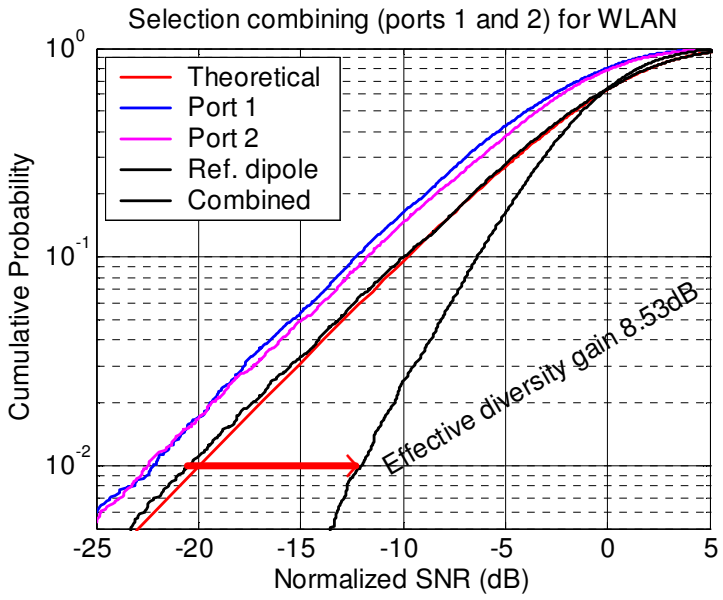

Figure 6.30: Eff. Diversity Gain for ports 1 and 2 at WLAN band obtained from measurements of the reverberation chamber

Even though some of the values for the apparent diversity gain are higher than the maximum theoretical limit, they are within the chamber error margin of ± 0.5 dB. The obtained correlation between each pair of ports is low, as it was expected due to the previously shown simulations. The simulated correlation corresponds to the amplitude of the complex correlation, whereas the reverberation chamber provided the power correlation. Both types were related in section 2.1.7.

It can be seen in Figure 6.30 that a small ripple appears when we have a lower probability, because the sampling rate for smaller probability levels is lower and therefore, the accuracy of the plots is a little bit degraded.

7. Comments and Conclusion

To begin with, I would like to comment that the antennas designed for this research have no commercial application, as they were mainly done for laboratory purposes. The objective was to develop a simulation method that can save a lot of time and that can be used in future designs too. Our proposed simulation method can help in the design and study of spatial diversity systems varying the source impedances. Besides, it can also be applied as a way to influence the correlation in MIMO systems if required.

One of the objectives of this thesis was to prove the correct performance of MPA using the CST far-field patterns. As it was seen using three different examples, the MPA works perfectly in terms of calculations of the radiation efficiency, the correlation and the effective diversity gain between pairs of ports. Firstly, a simple example of two parallel dipoles was performed and compared to previously publish results. Then, we used the software for our particular laptop model cases. However, we did not use the optimizer tool from MPA as it did not work perfectly for our particular cases. We followed instead our own method to influence the antennas, varying the source impedance.

A comparison between two different cases has been made. We saw that the spacing between the antennas affected the coupling and thus, the radiation efficiency, the correlation and the effective diversity gain.

For this particular case, we designed 5 identical dual-band antennas that showed good results compared to the measured ones. However, we have to mention that our antenna realization was not perfectly cut, the soldering to add the port can add some losses and some insertion losses can be inserted by the feeding coaxial cable too. Those small misadjustments can make the measured results differ from the simulated ones. Both the simulated and realized model showed a suitable location of the desired frequencies and a low correlation. However, the simulated model has a better effective diversity gain than the real model that can be due to the reasons mentioned above.

The obtained correlation for the 5-antenna case between all the ports was lower than expected and the antenna ports in this case did not show a high coupling (-10 dB). So in this 5-antenna case, the parameter that would affect the most the effective diversity gain was the radiation efficiency of the antennas. Taking as example, ports 1 and 5 at 1.95 GHz, see Figures A.1, A.2 in Appendix A, we can see that the correlation (Figure A.12) between them is really low. Looking at the effective diversity gain, in Figure A.13), we can see that it is mainly affected by the radiation efficiency of both ports, having the higher contour plot also following the higher contours for both efficiencies.

A different behaviour in both antenna ports at the edges was seen, in terms of efficiency. It can be due to the placement of this last antenna and due to the fact that it had just one neighbour. Also the measurements showed a higher coupling than the simulations in the edges antennas. Therefore, this difference in the radiation efficiency for the edge antenna varied the way of calculating the effective diversity gain, as we cannot apply the approximation at 1% cumulative probability level as seen in section 2.1.4.1. We implemented equation (2.5) instead.

Studying carefully the attached plots from Appendix A, we obtained some acceptable regions for the source impedance variation for each frequency band as seen in Figures 6.9, 6.10 and 6.11. Selecting any of the values included in the common region for all the frequency bands we can have an acceptable performance of our system. If desired, we can make a compromise between the specifications, by selecting just to optimize a desired antenna parameter.

In the measured results, we provided results from the network analyzer and the reverberation chamber. As simulations and measurements normally differ somehow, in our case, we have seen that in the measurements a coupling between some of the antenna ports appeared. The correlation is low in both results. In the case of measured radiation efficiency, the reverberation chamber gave us mean values for the whole frequency range, due to the followed approach to measure the model. However, in the simulated results, the values are individual for each of the frequencies. Thus, not a direct relationship between the values can be done.

Simulating our case with just three antennas located closely, separated by 1cm, we saw that the coupling was increased, having a value of –8 dB, and therefore, the correlation increased too, influencing the effective diversity gain. The correlation obtained in this case, was higher than required by the specifications.

If we study the coupling for this 3-antenna case, we saw that the coupling between ports 1 and 2 and between ports 2 and 3 was different, which might be due to the orientation of the antenna elements. Looking at Figure 3.2, we can see that the antenna elements are not symmetrical and oriented in the same direction. Hence, the performance of each of them is different.

After studying the plots for this 3-antenna case, attached in Appendix B, we also made a common representation of all the antenna specifications that can be seen in Figures 6.20, 6.21, 6.22 and 6.23. When selecting the correlation lower than 0.3, we were not able to find an optimum common region for all the frequency bands. In fact, the DL of the UMTS band had a high correlation and it was not included in the plot. Thus, we selected the correlation values that were below 0.4 and in this second case, a common region between the UMTS UL and BT bands can be found. Still, the UMTS DL band had a higher correlation.

Looking at the effective diversity gain in Figure 6.23, we found a common region for all the frequency requirements. In this case, the effective diversity gain of the three-port system can be higher than 8 dB for some source impedance values.

Therefore, the optimization of all the antenna characteristics for all the ports and all the desired frequency bands is more difficult for the 3-antenna case. In this case, it is better to make a compromise between the desired characteristics that want to be optimized and then choose the correct value within the common regions.

Thus, using the provided software, we develop a method to study the influence of the source impedance in our simulated results. We saw that a variation of the source impedance can affect the radiation efficiency of the antennas, the correlation and the effective diversity gain between them. If the antennas are too closely located, maybe it will be desirable to make a compromise between the desired specifications. However, we found that the limiting factor of the effective diversity gain is often the radiation efficiency.

Taking the example of the effective diversity gain, if the distance between the antenna elements is reduced, we can still have an acceptable gain if we vary the source impedance.

As explained, the maximum effective diversity gain appears in different areas of contour plots for the given frequency bands. In the case of UMTS, it might be useful to have separated transmitter and receiver to improve performance.

This research has mainly established a method that can be applied to many other examples to study the antenna performance of mobile terminals. Working with a 3D electromagnetic simulator such as CST, we can use the MPA to compute the main characteristics of the antennas in the design. This software saves a lot of time and computes efficiently important parameters such as radiation efficiency, correlation and diversity gain. In our case, we have made a study of the influence of the source impedance and manually, we found the common regions that gave us acceptable performance values. The simulated results can be compared with the measured ones obtained from the proved well-working reverberation chamber. For other particular examples, the same procedure can be followed and just the model has to be changed.

8. Final Discussion

As final discussion, some improvement possibilities are suggested for future work.

Firstly, some other frequency bands can be covered and some different distances too. We provided a method that using those two input parameters can find the optimum value of the source impedance in order to optimize the antenna characteristics. In this thesis, the optimum values for a given spacing can be found manually. However, it is desirable to be able to represent the results combined as d/λ and therefore, obtain easily the optimum source impedance value that will fulfill the radiation efficiency, the correlation and the efficiency diversity gain requirements within the desired frequency bands, for the minimum spacing between the antennas as possible. The code to obtain automatically the results could be programmed and it could be part of a future Master Thesis. Moreover, also negative values for the imaginary part of the source impedance can be added to see its influence in the antenna characteristics.

Besides, as the MPA will be improved soon, the optimizer tool that it provides can be used to add lumped components to optimize the high correlation obtained in the 3-antenna case. Besides, as a non-uniformly distributed propagation environment will not give the same signal correlation as a uniformly distributed environment, it could be a good idea to calculate the correlation in a non-uniformly distributed environment with the MPA.

Additionally, other correlation measurements can be done using a better reverberation chamber. Therefore, not only the amplitude of the complex correlation coefficient will be obtained but also the envelope correlation as well as the power correlation can be studied.

For the provided example, a practical implementation using matching networks can be done, to study the effect on the radiation efficiency, the correlation and the effective diversity gain as done in this research using just simulations.

There are currently some standards that use multiple antennas, such as WiMAX [21] and Wibro [22], so it is desirable to study those cases using our provided method too.

Besides, some other diversity techniques can be studied and the results can be compared to the ones obtained in this research for selection combining.

In the case of mobile phones, due to their reduced space, it is also desirable to be able to study its performance using the same procedure. The procedure to be followed will be the same, but in this other case, we will desire probably lower frequencies and moreover, the size restrictions will be higher. Maybe some polarization diversity should be included in this particular case of mobile phones.

As in our proposed method, if the requirements are not completely fulfilled, maybe we can include different antenna technologies and patterns. Even though the antennas will be different the same approach as in our thesis can be followed.

As mentioned in the MIMO chapter of this report, one of the most important characteristics is the capacity of the system. Therefore, it is desirable to be able to compute in the future the capacity of the design using the MPA and to compare the obtained results with the ones that can be given by the reverberation chamber. As mentioned in the Foschini experiment with BLAST [23], a study on the number of antennas that can be added to the model without worsening the capacity of the system can be done.

All the results provided for the studied diversity technique about the correlation between the antennas can be really useful for future studies on MIMO systems. Even though the principle of working of those two approaches is different, the correlation in both systems should be affected similarly between neighbouring antennas.

Therefore, there are many interesting reasons that could lead to continue with the started laptop project in the future as a new Master Thesis proposal.

References

[1] CST Studio Suite 2006, http://www.cst.com/

[2] Sveriges Tekniska Forskningsinstitut, http://www.sp.se/

[3] P-S. Kildal and K. Rosengren, "Electromagnetic analysis of effective and apparent diversity gain of two parallel dipoles", *IEEE Antennas and Wireless Propagation Letters, Vol. 2, No. 1, pp. 9-13, 2003*

[4] K. Karlsson, J. Carlsson, I. Belov, G. Nilsson and P-S. Kildal, "Optimization of antenna diversity gain by combining full-wave and circuit simulations", *EUCap 2007, Edinburgh, UK, Nov. 11-16, 2007*

[5] K. Rosengren, J. Carlsson and P-S. Kildal, "Maximizing the effective diversity gain of two parallel dipoles by optimizing the source impedances", *Microwave and Optical Technology Letters, Vol. 48, No. 3, March 2006*

[6] T. S. Rappaport, "Wireless Communications: Principle and practice", *Prentice Hall, 1996*

[7] P-S. Kildal and K. Rosengren, "Electromagnetic characterization of MIMO antennas including coupling using classical embedded element pattern and radiation efficiency", *IEEE AP-S Symposium, Monterey 2004*

[8] P-S. Kildal and K. Rosengren, "Correlation and capacity of MIMO systems and mutual coupling, radiation efficiency and diversity gain of their antennas: simulations and measurements in a reverberation chamber", *IEEE Communications Magazine, pp. 104-114, Vol. 42, No. 12, Dec 2004*

[9] D. Gesbert, M. Shafi, D-S. Shui, P. J. Smith and A. Naguib, "From theory to practice: An overview of MIMO space-time coded wireless Systems", *IEEE Journal on Selected Areas in Communications, Vol. 21, No. 3, April 2003*

[10] P-S. Kildal, K. Rosengren, J. Byun and J. Lee, "Definition of effective diversity gain and how to measure it in a reverberation chamber", *Microwave and Optical Technology Letters, Vol. 34, No. 1, pp. 56-59, July 2002*

[11] K. Rosengren and P-S. Kildal, "Radiation Efficiency, correlation, diversity gain and capacity of a six-monopole antenna array for a MIMO system: theory, simulation and measurement in reverberation chamber", *IEE Proceedings-Microwave, Antennas Propagation, Vol. 152, No. 1, Feb 2005*

[12] M. Schwartz, W. R. Bennett, S. Stein, "Communication Systems and Techniques", *IEEE Press, 1996*

[13] J. L. Volakis, "Antenna Engineering Handbook", *McGraw-Hill, 2007*

[14] J. S. Colburn, Y. Rahmat-Samii, M. A. Jensen and G. J. Pottie, "Evaluation of personal communications dual-antenna handset diversity performance", *IEEE Transactions on Vehicular Technology, Vol. 47, No. 3, August 1998*

[15] P-S. Kildal, "Foundations of Antennas. A unified approach", *Studentlitteratur, 2000*

[16] A. T. Gobien, "Investigation of Low Profile Antenna Designs for Use in Hand-Held Radios", *MSc. In Electrical Engineering, Virginia Polytechnic Institute and State University, Virginia 1997*

[17] K. Karlsson, J. Carlsson, P. Ankarson and Z. Ying, "Combination of full wave simulations and equivalent circuit models in predicting coupling between antenna element and nearby object in mobile phone", *International Workshop on Antenna Technology: Small and Smart Antennas, Metamaterials and Applications, IWAT '07, 21-23 March 2007, pp. 400-403*

[18] K. Rosengren, “Characterization of terminal antennas for diversity and MIMO systems by theory, simulations and measurements in reverberation chamber”, *Disertation Thesis, ISBN 91-7291-610-9, Ny serie nr. 2292, Chalmers University of Technology, Sweden 2005*

[19] Bluetest AB, http://www.bluetest.se/

[20] K. Rosengren, P-S. Kildal, C. Carlsson, J. Carlsson, “Characterization of antennas for mobile and wireless terminals using reverberation chambers: improved accuracy by Platform Stirring”, *IEEE International Symposium on Antennas and Propagation, Boston, July 2001*

[21] WiMAX Forum, http://www.wimaxforum.org/

[22] WiBro, http://www.wibro.or.kr/

[23] Bell-Labs, http://www.bell-labs.com/

Appendix A: Simulated results 5-antennas

Frequency = 1.95 GHz

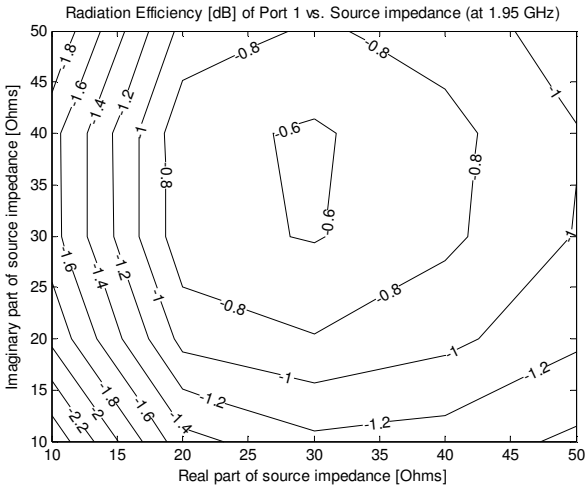

Figure A.1: Tot. Rad. Efficiency for port 1 at 1.95 GHz

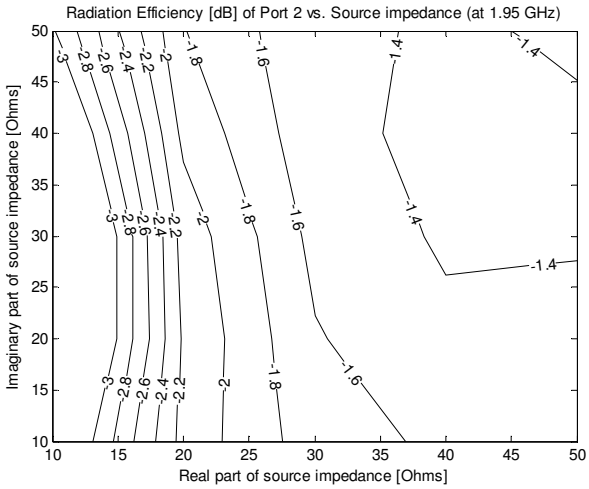

Figure A.2: Tot. Rad. Efficiency for port 2 at 1.95 GHz

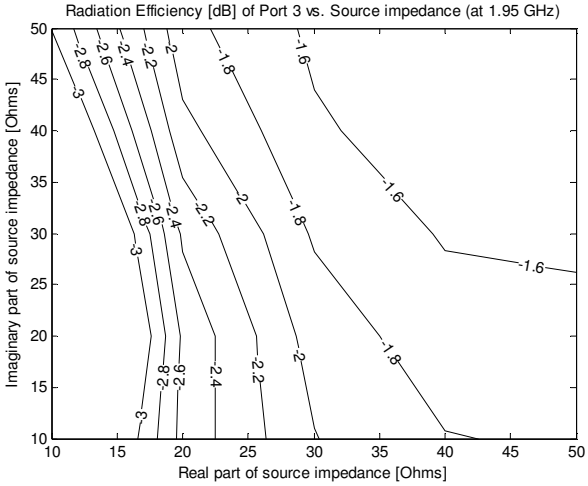

Figure A.3: Tot. Rad. Efficiency for port 3 at 1.95 GHz

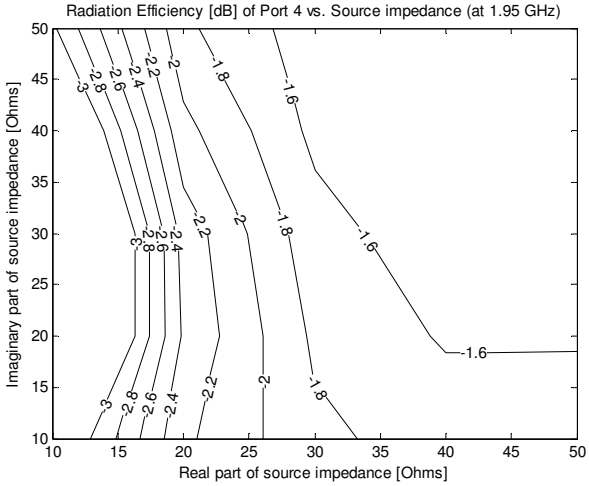

Figure A.4: Tot. Rad. Efficiency for port 4 at 1.95 GHz

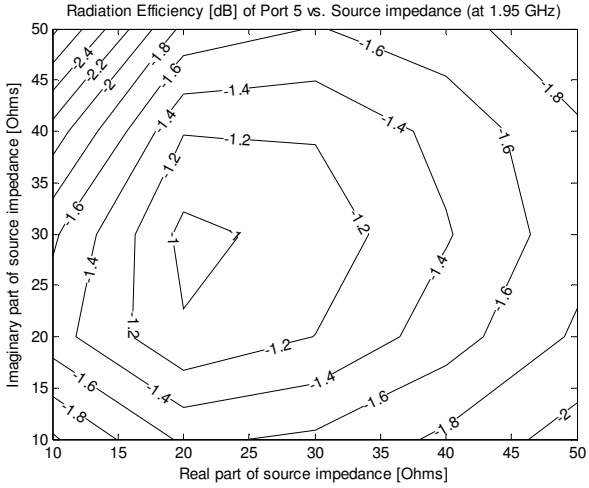

Figure A.5: Tot. Rad. Efficiency for port 5 at 1.95 GHz

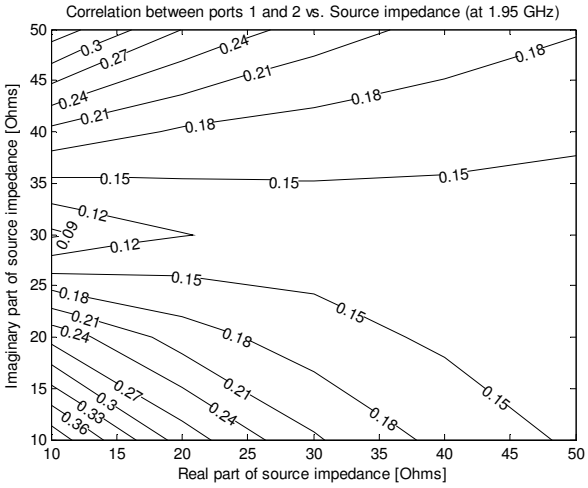

Figure A.6: Correlation between ports 1 and 2 at 1.95 GHz

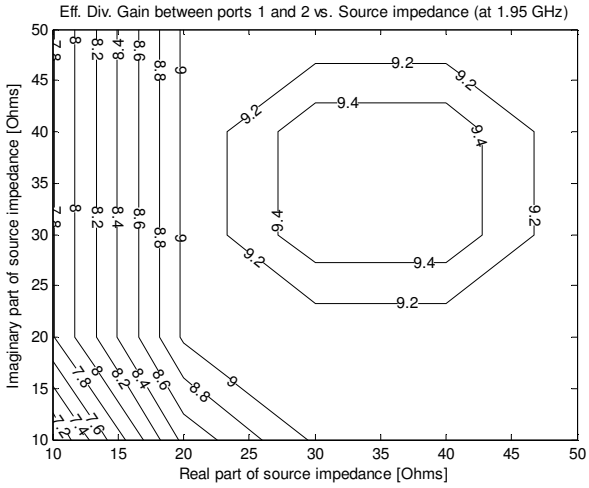

Figure A.7: Eff. Diversity Gain between ports 1 and 2 at 1.95 GHz

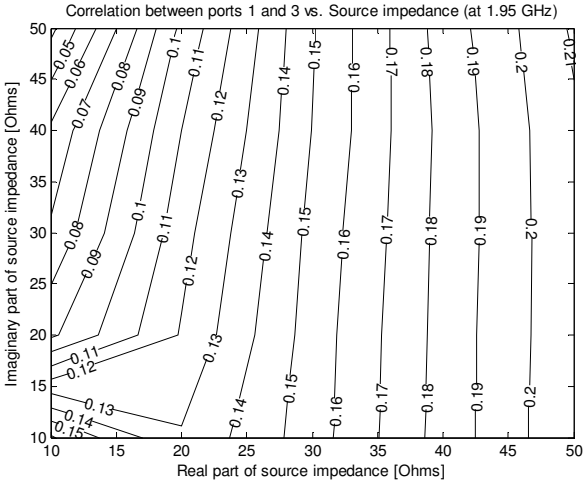

Figure A.8: Correlation between ports 1 and 3 at 1.95 GHz

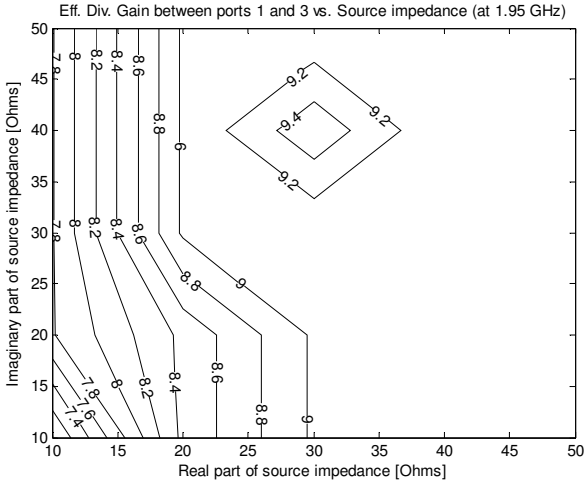

Figure A.9: Eff. Diversity Gain between ports 1 and 3 at 1.95 GHz

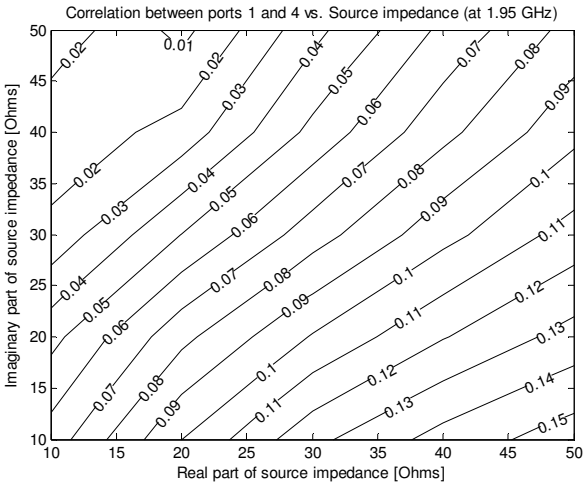

Figure A.10: Correlation between ports 1 and 4 at 1.95 GHz

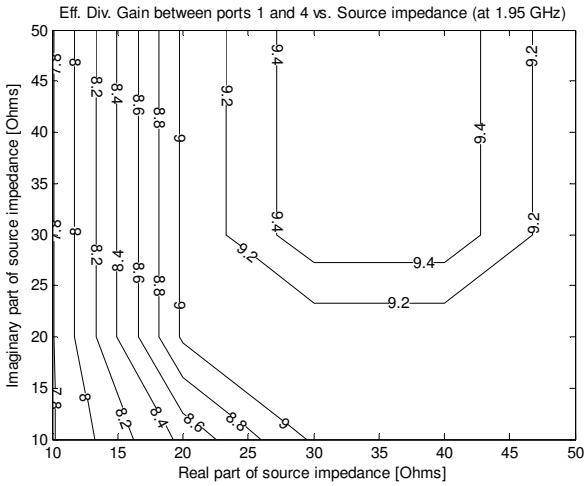

Figure A.11: Eff. Diversity Gain between ports 1 and 4 at 1.95 GHz

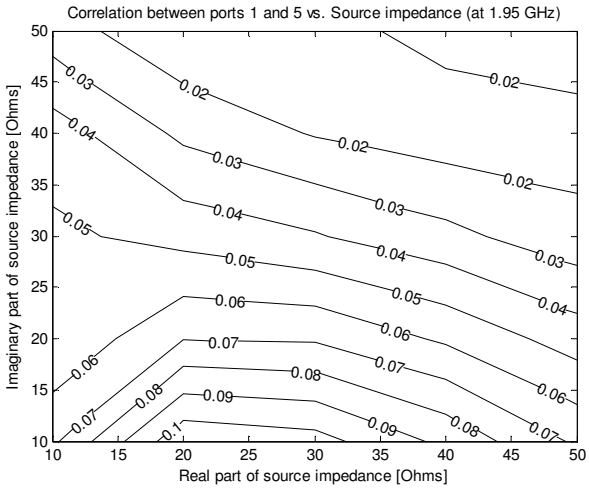

Figure A.12: Correlation between ports 1 and 5 at 1.95 GHz

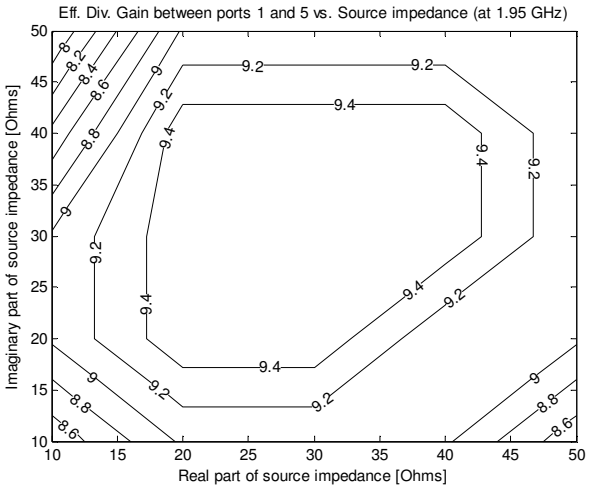

Figure A.13: Eff. Diversity Gain between ports 1 and 5 at 1.95 GHz

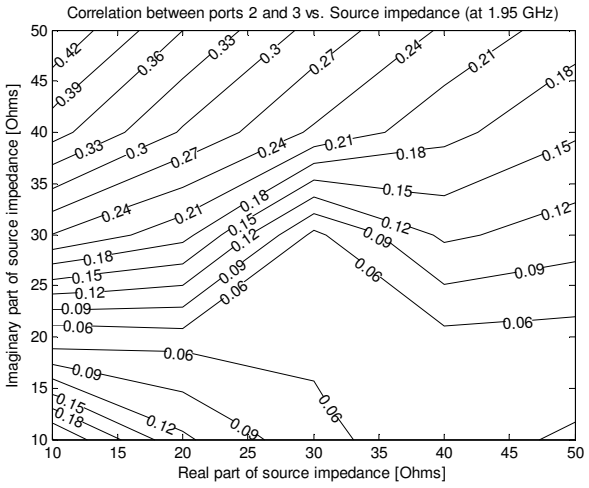

Figure A.14: Correlation between ports 2 and 3 at 1.95 GHz

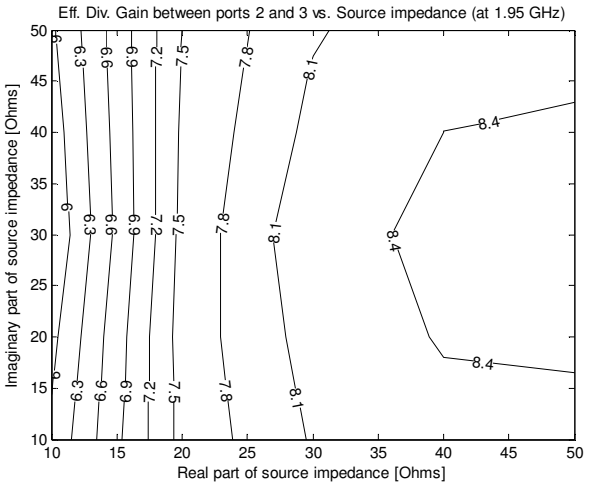

Figure A.15: Eff. Diversity Gain between ports 2 and 3 at 1.95 GHz

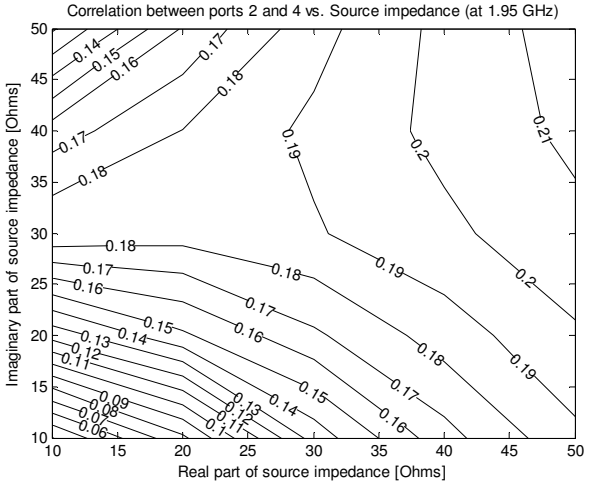

Figure A.16: Correlation between ports 2 and 4 at 1.95 GHz

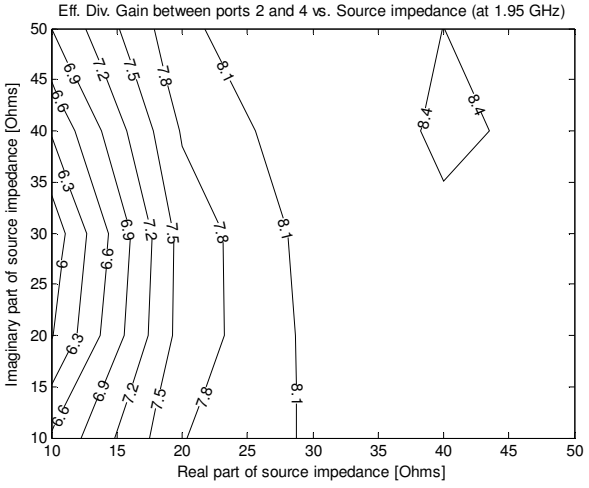

Figure A.17: Eff. Diversity Gain between ports 2 and 4 at 1.95 GHz

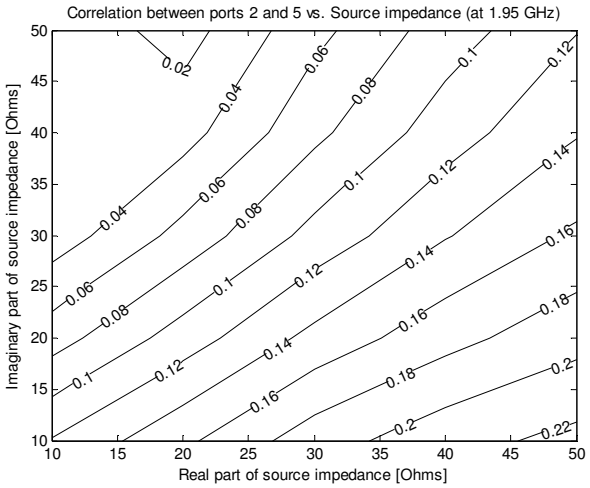

Figure A.18: Correlation between ports 2 and 5 at 1.95 GHz

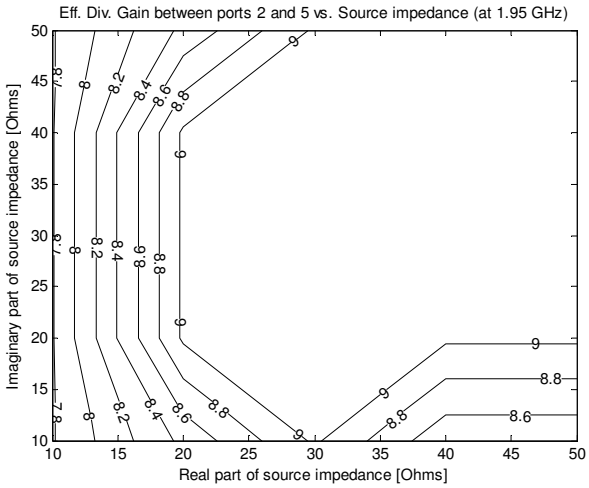

Figure A.19: Eff. Diversity Gain between ports 2 and 5 at 1.95 GHz

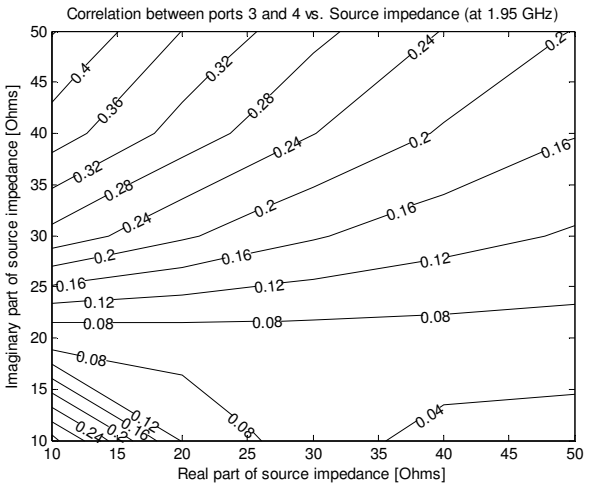

Figure A.20: Correlation between ports 3 and 4 at 1.95 GHz

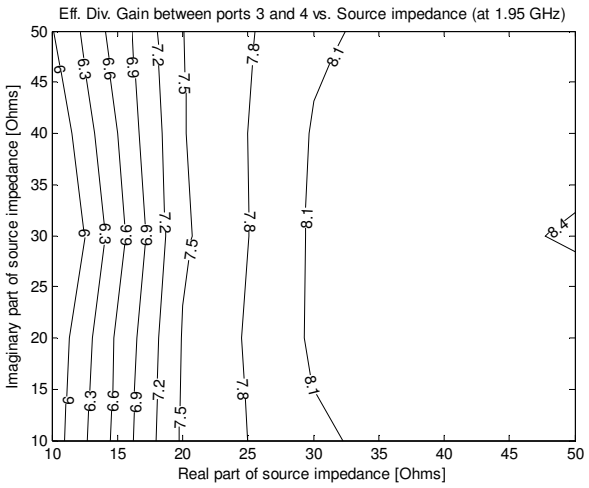

Figure A.21: Eff. Diversity Gain between ports 3 and 4 at 1.95 GHz

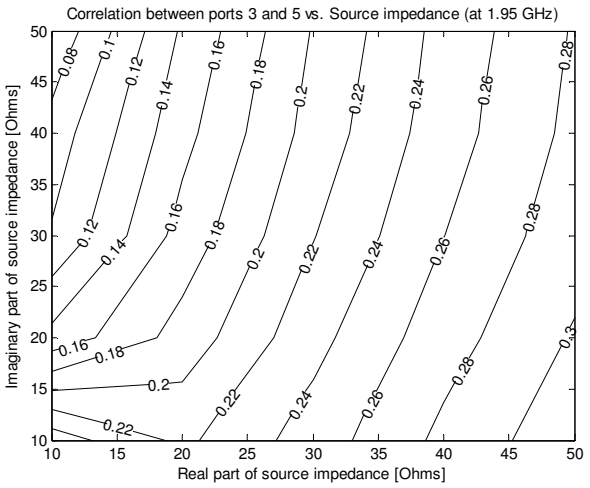

Figure A.22: Correlation between ports 3 and 5 at 1.95 GHz

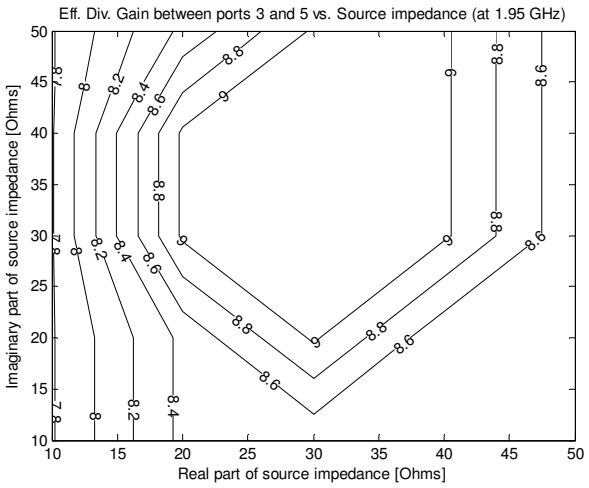

Figure A.23: Eff. Diversity Gain between ports 3 and 5 at 1.95 GHz

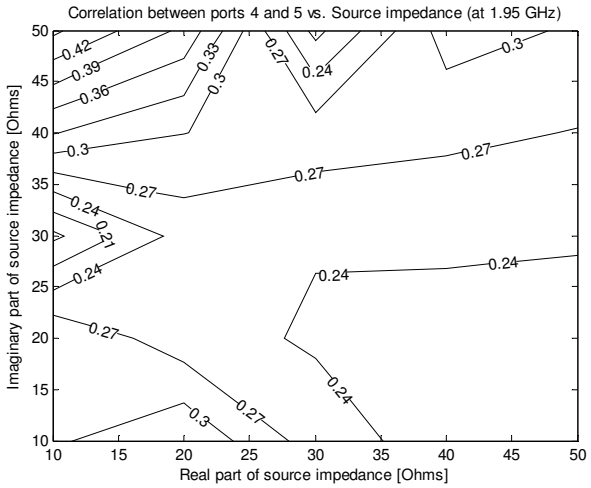

Figure A.24: Correlation between ports 4 and 5 at 1.95 GHz

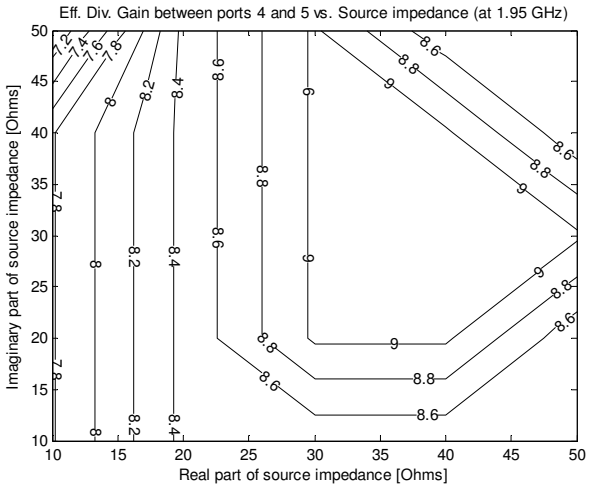

Figure A.25: Eff. Diversity Gain between ports 4 and 5 at 1.95 GHz

Frequency = 2.14 GHz

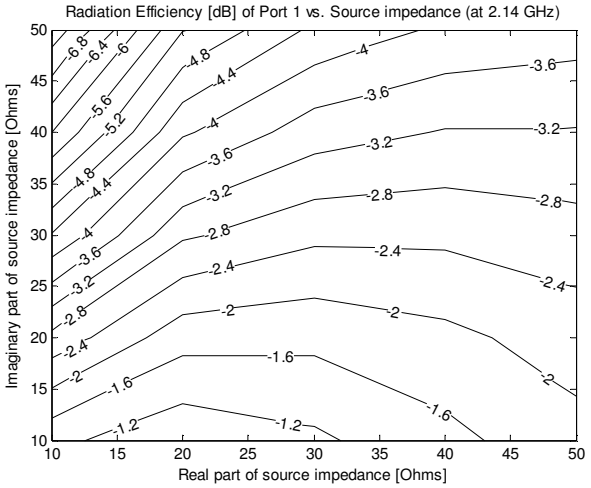

Figure A.26: Tot. Rad. Efficiency for port 1 at 2.14 GHz

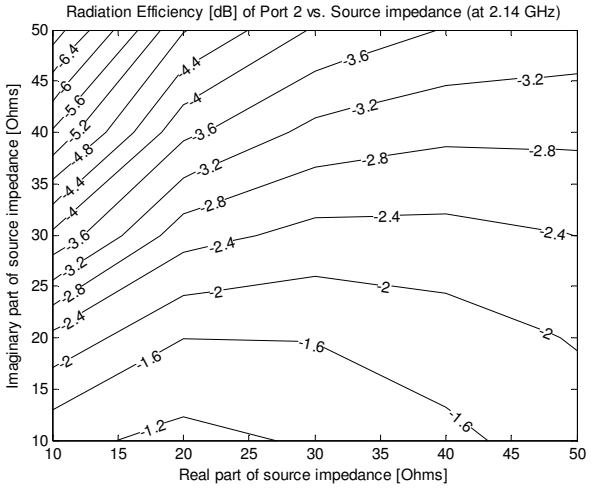

Figure A.27: Tot. Rad. Efficiency for port 2 at 2.14 GHz

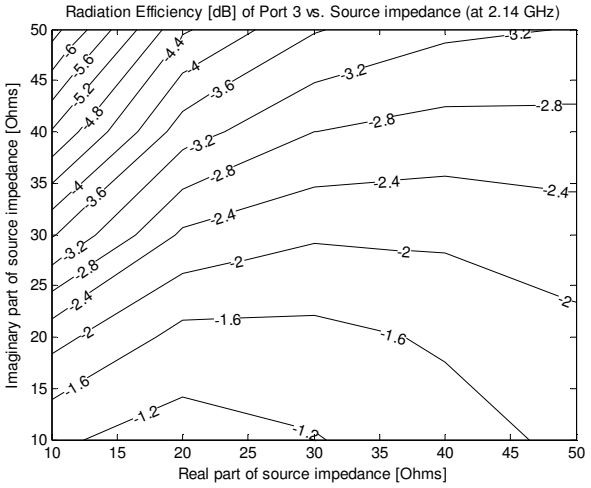

Figure A.28: Tot. Rad. Efficiency for port 3 at 2.14 GHz

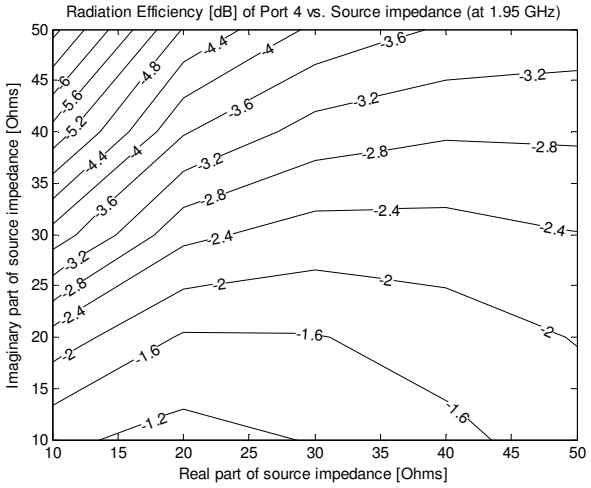

Figure A.29: Tot. Rad. Efficiency for port 4 at 2.14 GHz

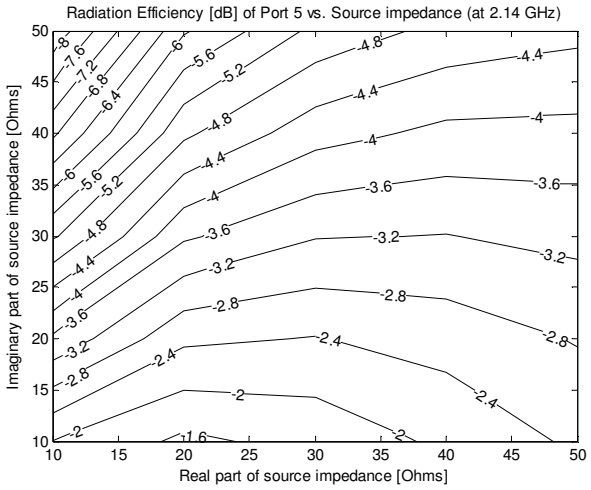

Figure A.30: Tot. Rad. Efficiency for port 5 at 2.14 GHz

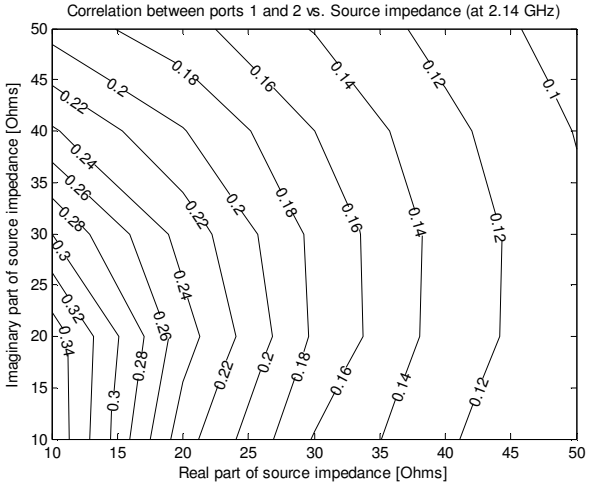

Figure A.31: Correlation between ports 1 and 2 at 2.14 GHz

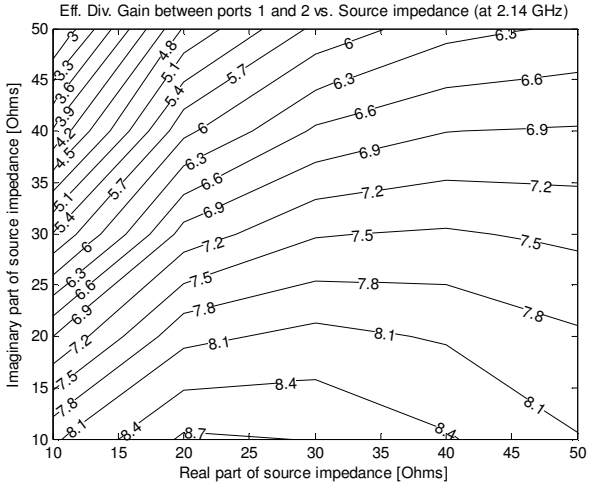

Figure A.32: Eff. Diversity Gain between ports 1 and 2 at 2.14 GHz

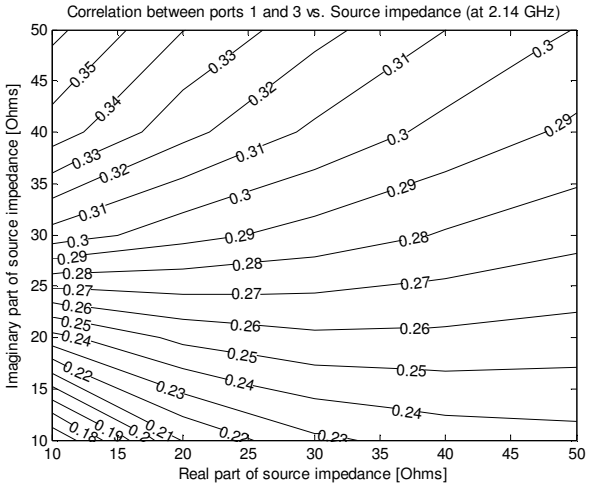

Figure A.33: Correlation between ports 1 and 3 at 2.14 GHz

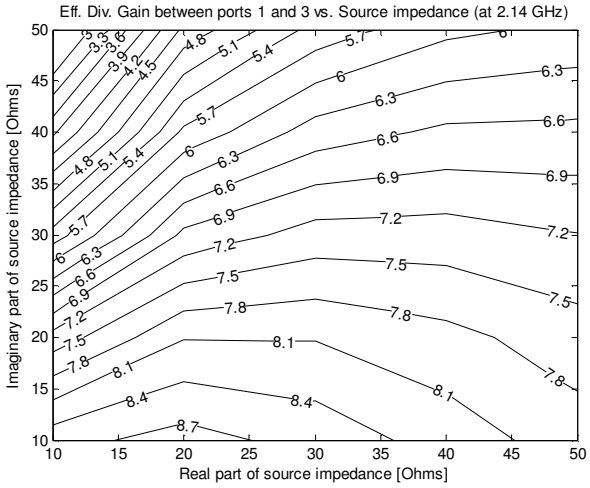

Figure A.34: Eff. Diversity Gain between ports 1 and 3 at 2.14 GHz

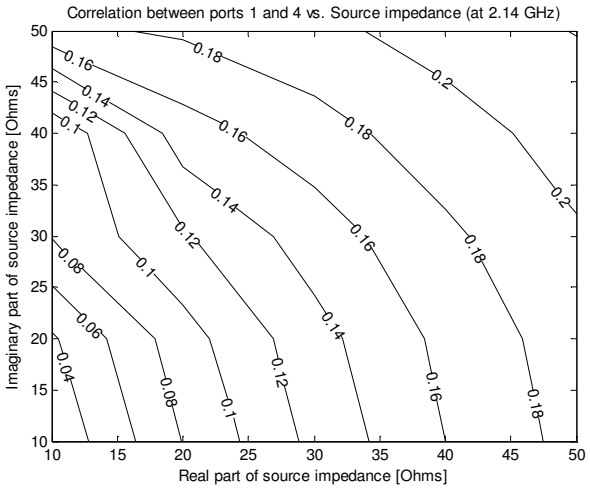

Figure A.35: Correlation between ports 1 and 4 at 2.14 GHz

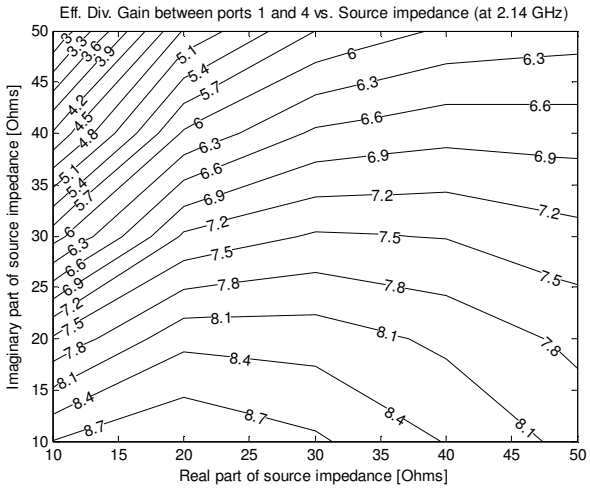

Figure A.36: Eff. Diversity Gain between ports 1 and 4 at 2.14 GHz

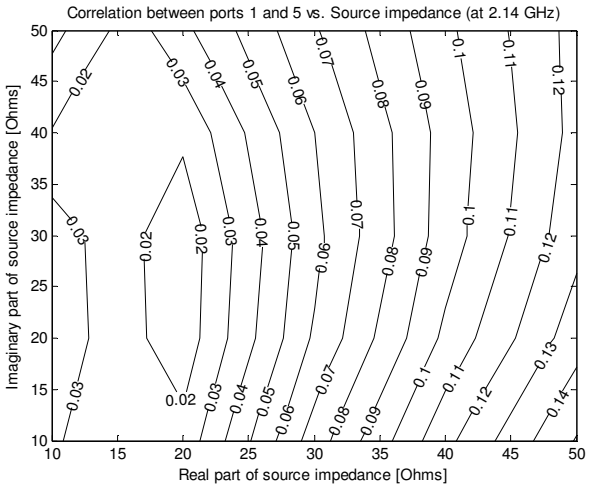

Figure A.37: Correlation between ports 1 and 5 at 2.14 GHz

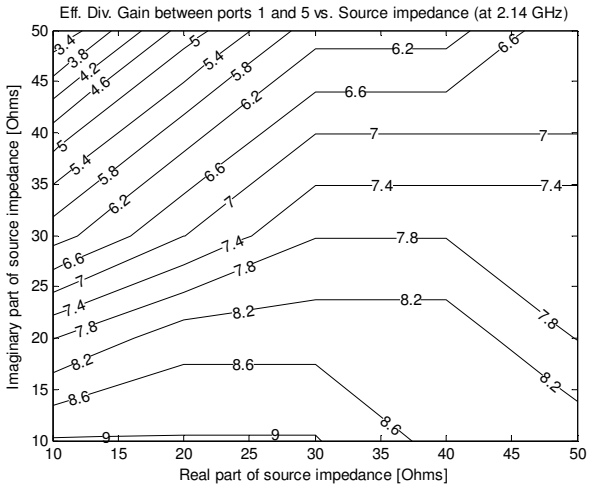

Figure A.38: Eff. Diversity Gain between ports 1 and 5 at 2.14 GHz

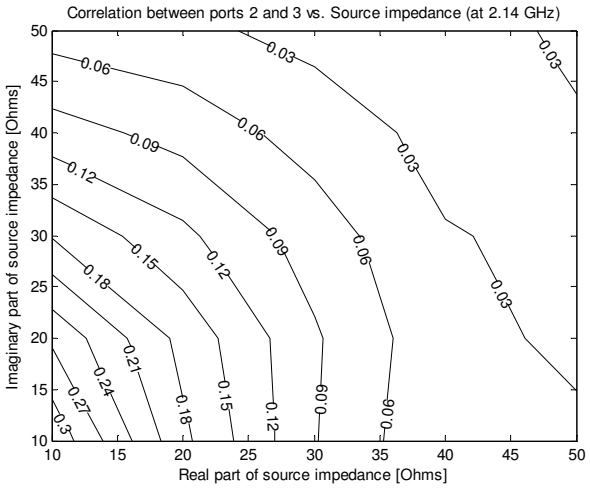

Figure A.39: Correlation between ports 2 and 3 at 2.14 GHz

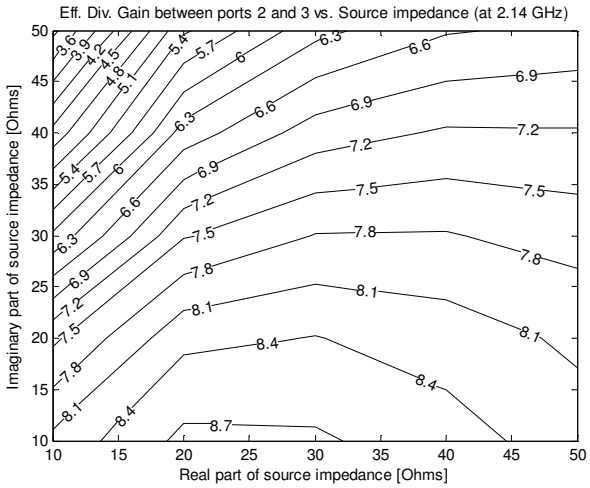

Figure A.40: Eff. Diversity Gain between ports 2 and 3 at 2.14 GHz

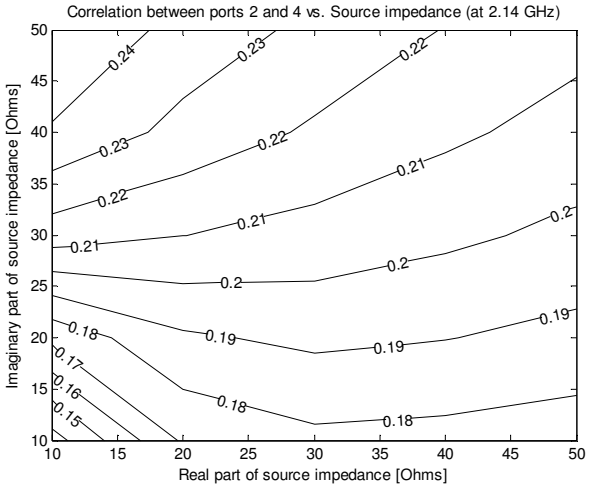

Figure A.41: Correlation between ports 2 and 4 at 2.14 GHz

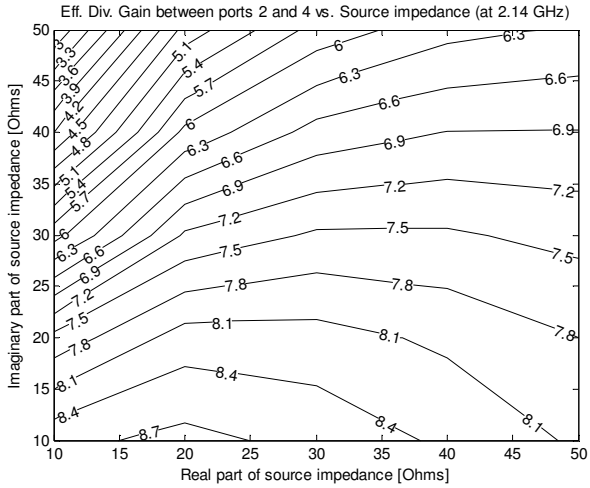

Figure A.42: Eff. Diversity Gain between ports 2 and 4 at 2.14 GHz

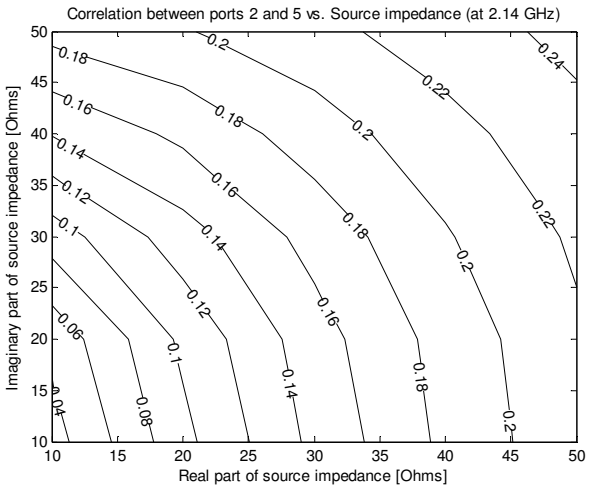

Figure A.43: Correlation between ports 2 and 5 at 2.14 GH**z**

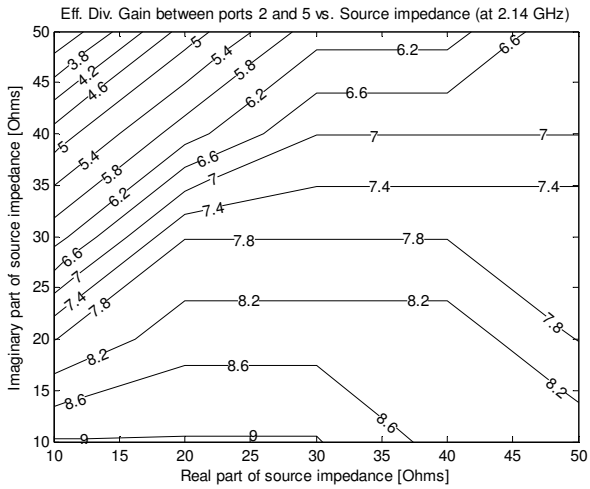

Figure A.44: Eff. Diversity Gain between ports 2 and 5 at 2.14 GHz

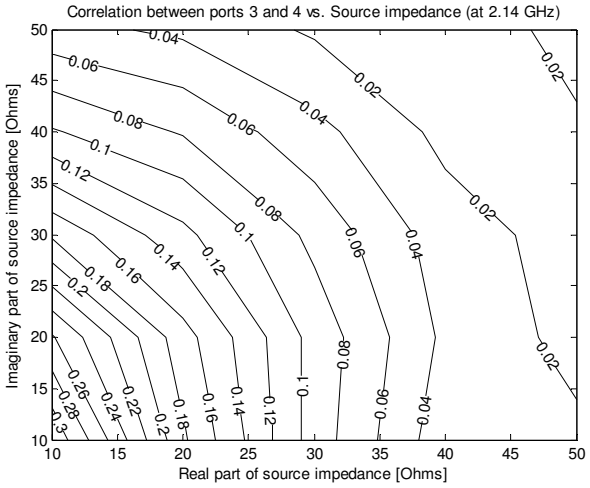

Figure A.45: Correlation between ports 3 and 4 at 2.14 GHz

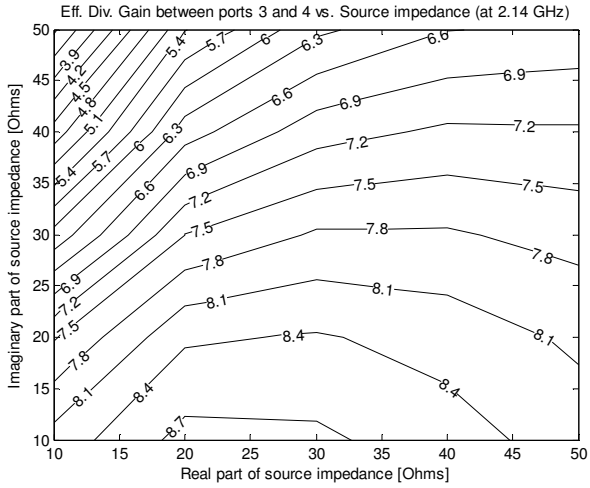

Figure A.46: Eff. Diversity Gain between ports 3 and 4 at 2.14 GHz

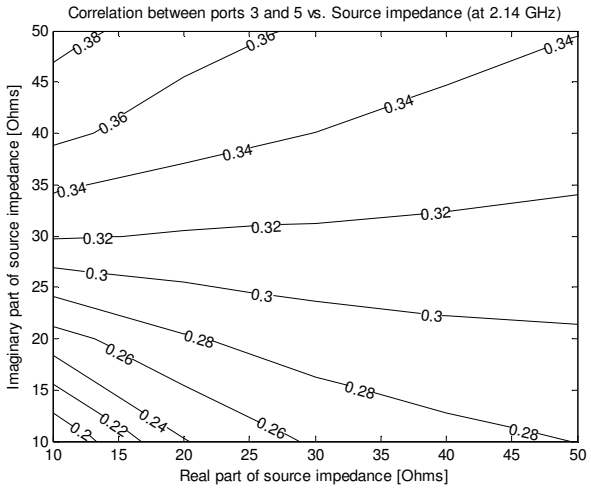

Figure A.47: Correlation between ports 3 and 5 at 2.14 GHz

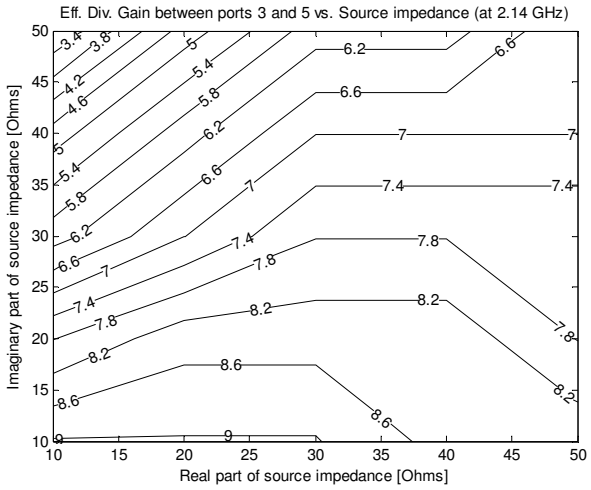

Figure A.48: Eff. Diversity Gain between ports 3 and 5 at 2.14 GHz

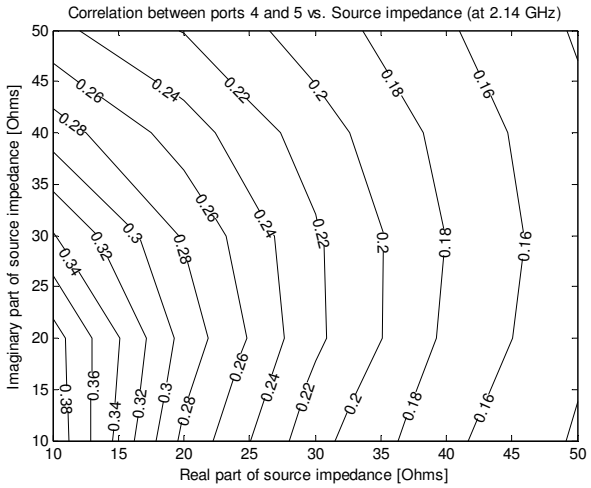

Figure A.49: Correlation between ports 4 and 5 at 2.14 GH**z**

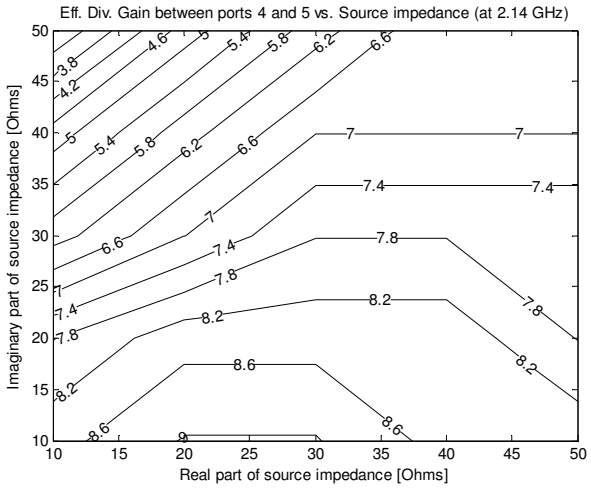

Figure A.50: Eff. Diversity Gain between ports 4 and 5 at 2.14 GHz

Frequency = 2.442 GHz

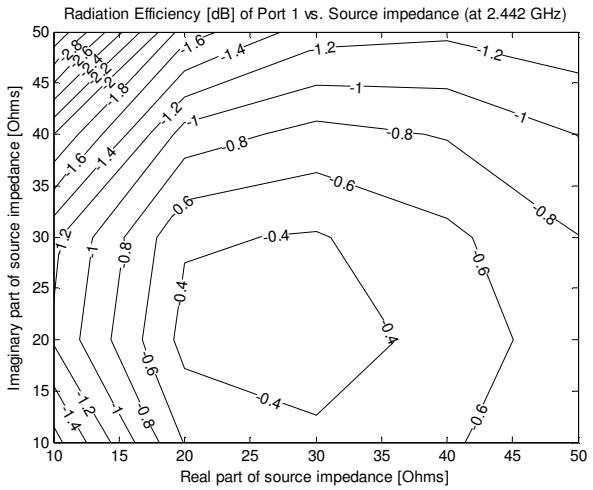

Figure A.51: Tot. Rad. Efficiency for port 1 at 2.442 GHz

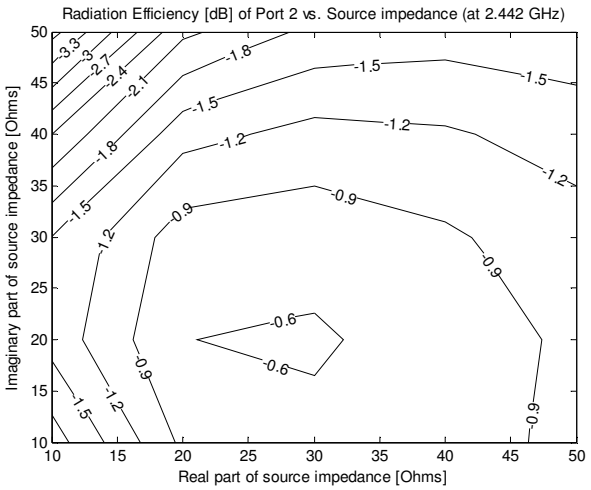

Figure A.52: Tot. Rad. Efficiency for port 2 at 2.442 GHz

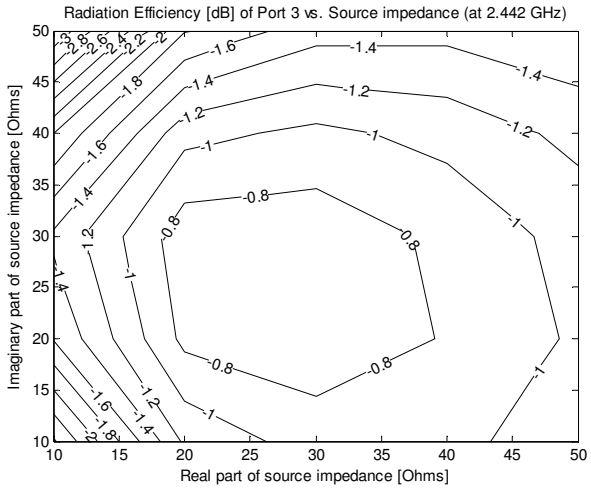

Figure A.53: Tot. Rad. Efficiency for port 3 at 2.442 GHz

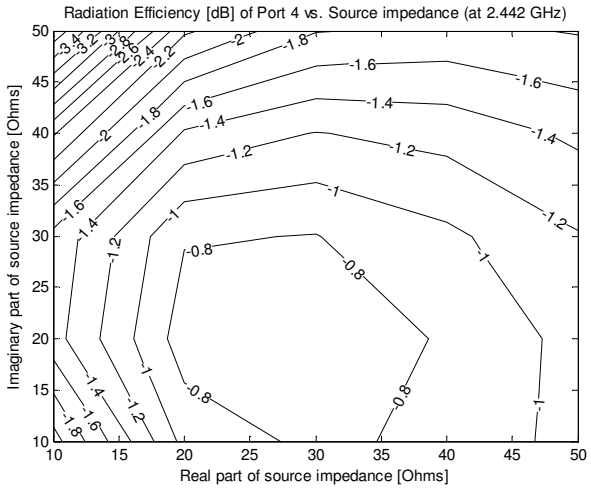

Figure A.54: Tot. Rad. Efficiency for port 4 at 2.442 GHz

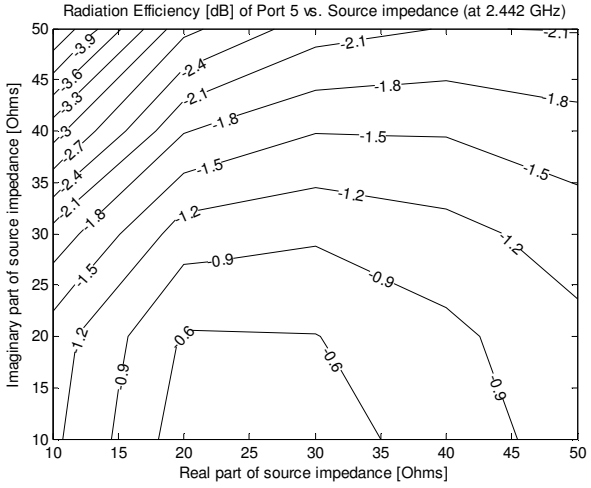

Figure A.55: Tot. Rad. Efficiency for port 5 at 2.442 GHz

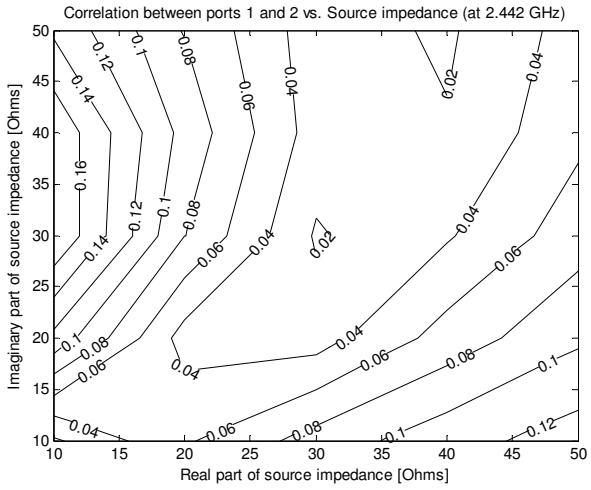

Figure A.56: Correlation between ports 1 and 2 at 2.442 GHz

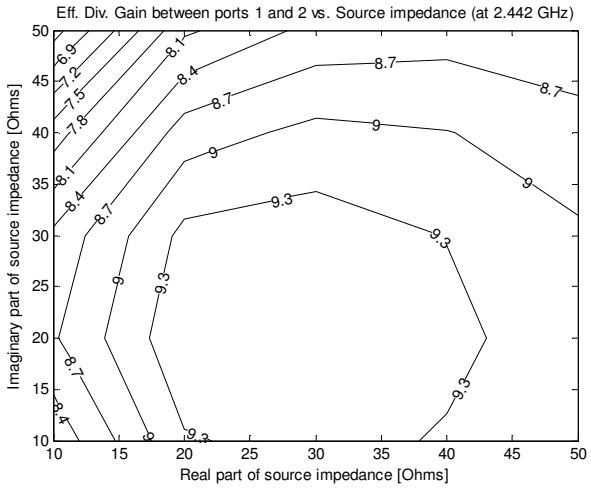

Figure A.57: Eff. Diversity Gain between ports 1 and 2 at 2.442 GHz

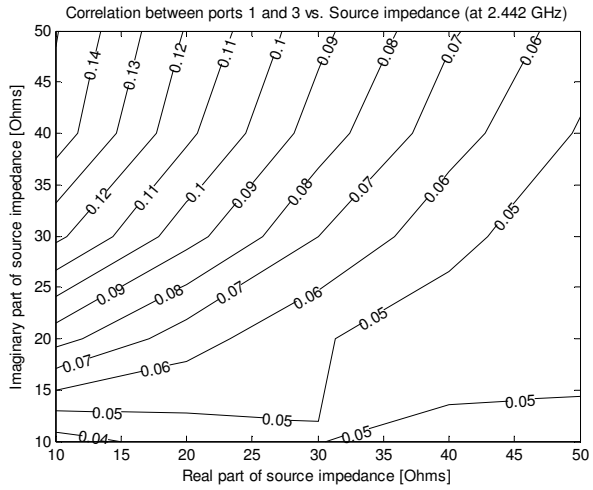

Figure A.58: Correlation between ports 1 and 3 at 2.442 GHz

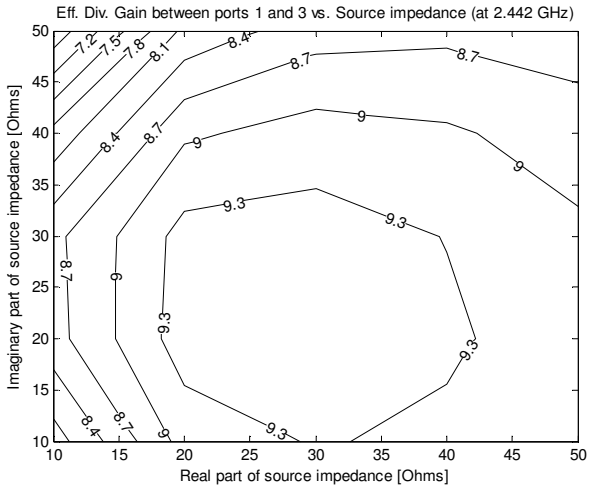

Figure A.59: Eff. Diversity Gain between ports 1 and 3 at 2.442 GHz

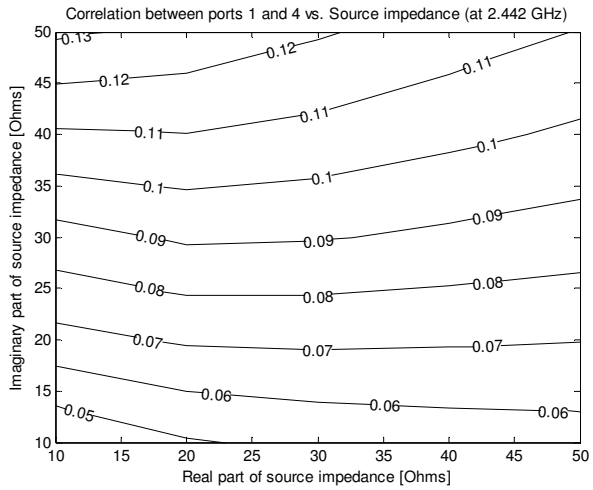

Figure A.60: Correlation between ports 1 and 4 at 2.442 GHz

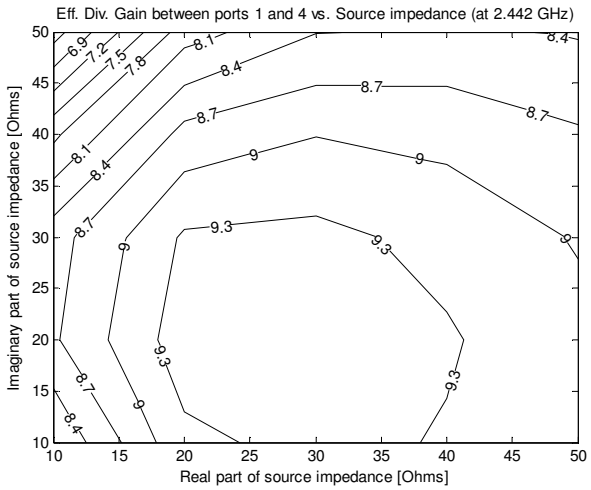

Figure A.61: Eff. Diversity Gain between ports 1 and 4 at 2.442 GHz

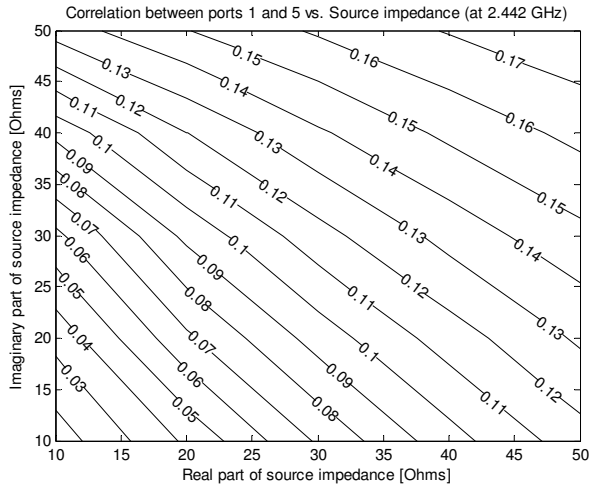

Figure A.62: Correlation between ports 1 and 5 at 2.442 GHz

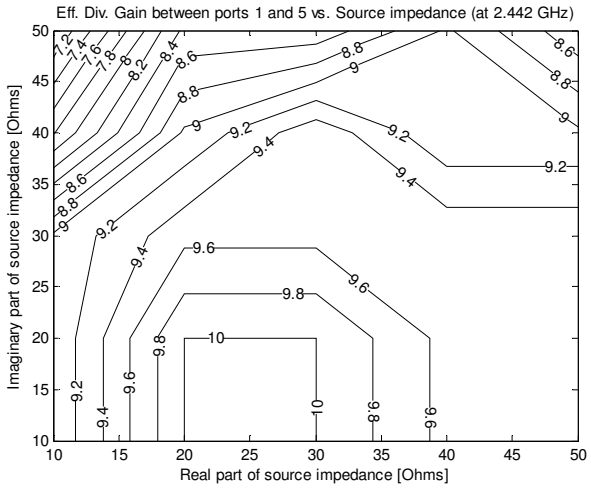

Figure A.63: Eff. Diversity Gain between ports 1 and 5 at 2.442 GHz

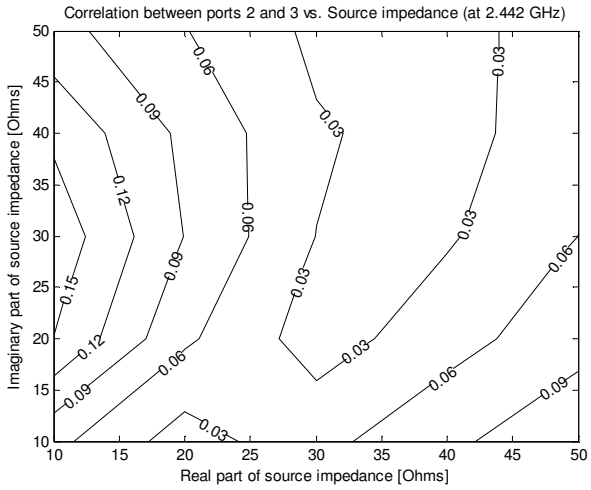

Figure A.64: Correlation between ports 2 and 3 at 2.442 GHz

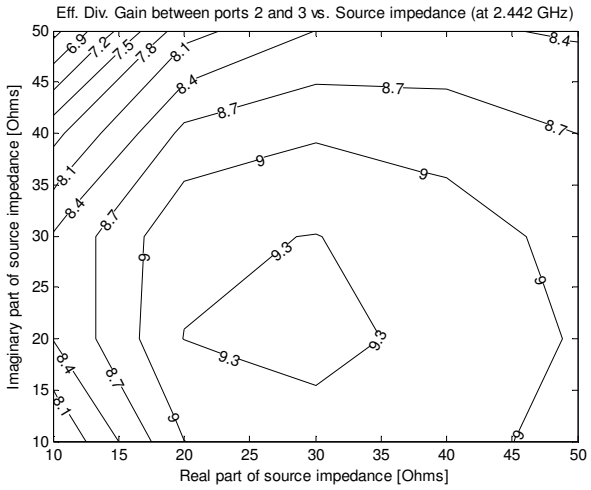

Figure A.65: Eff. Diversity Gain between ports 2 and 3 at 2.442 GHz

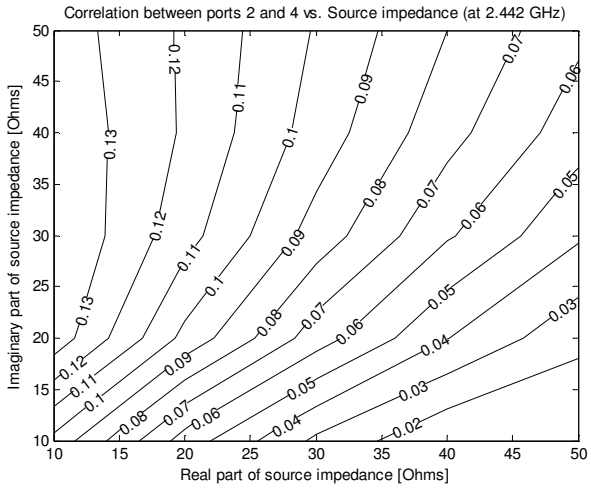

Figure A.66: Correlation between ports 2 and 4 at 2.442 GHz

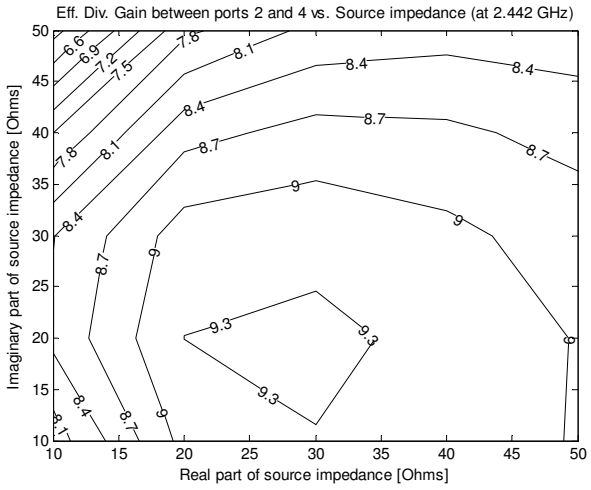

Figure A.67: Eff. Diversity Gain between ports 2 and 4 at 2.442 GHz

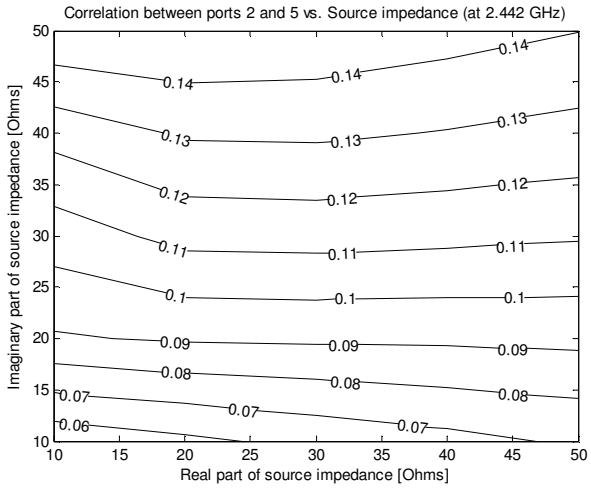

Figure A.68: Correlation between ports 2 and 5 at 2.442 GHz

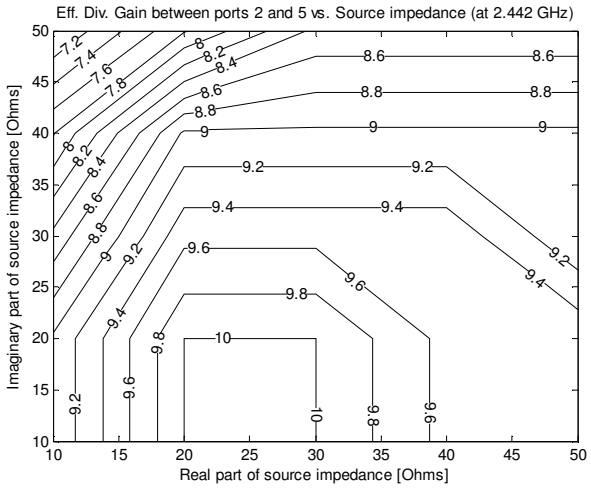

Figure A.69: Eff. Diversity Gain between ports 2 and 5 at 2.442 GHz

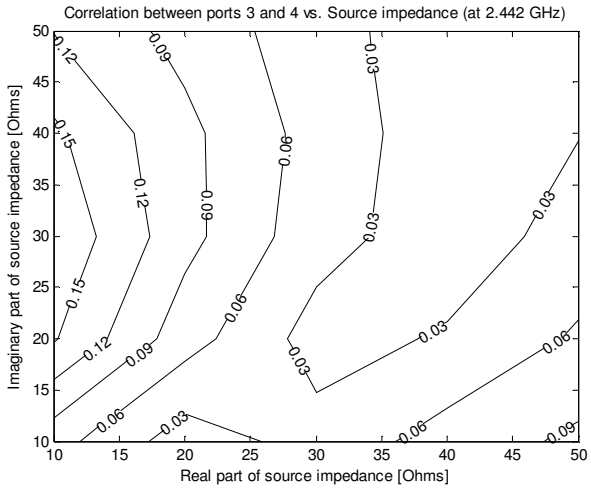

Figure A.70: Correlation between ports 3 and 4 at 2.442 GHz

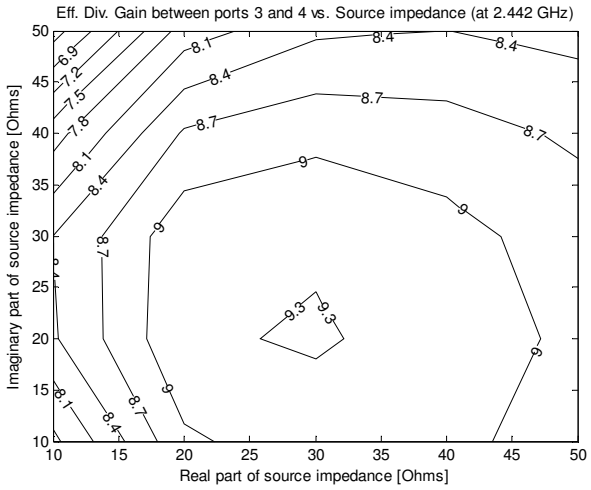

Figure A.71: Eff. Diversity Gain between ports 3 and 4 at 2.442 GHz

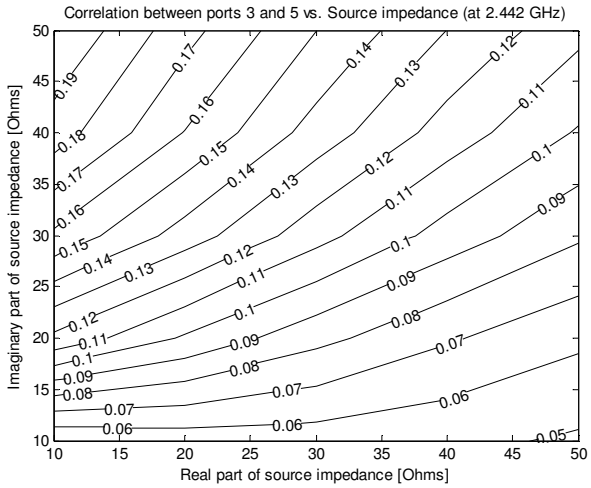

Figure A.72: Correlation between ports 3 and 5 at 2.442 GHz

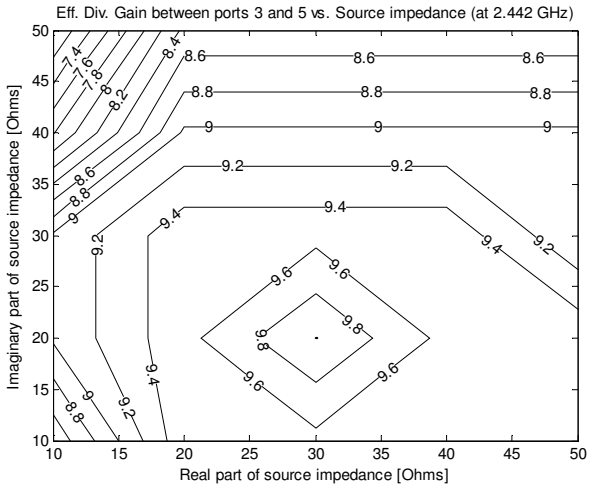

Figure A.73: Eff. Diversity Gain between ports 3 and 5 at 2.442 GHz

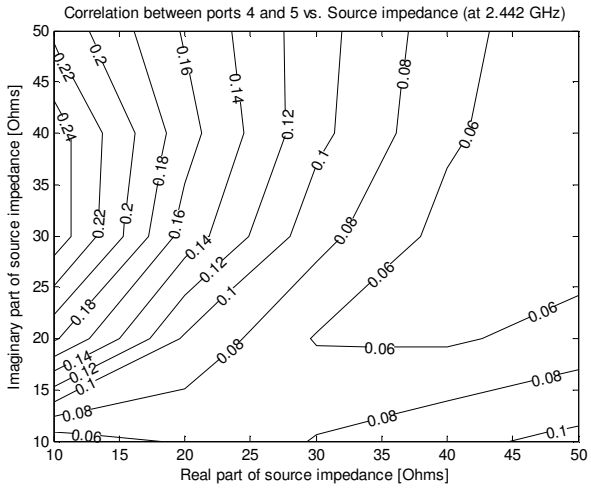

Figure A.74: Correlation between ports 4 and 5 at 2.442 GHz

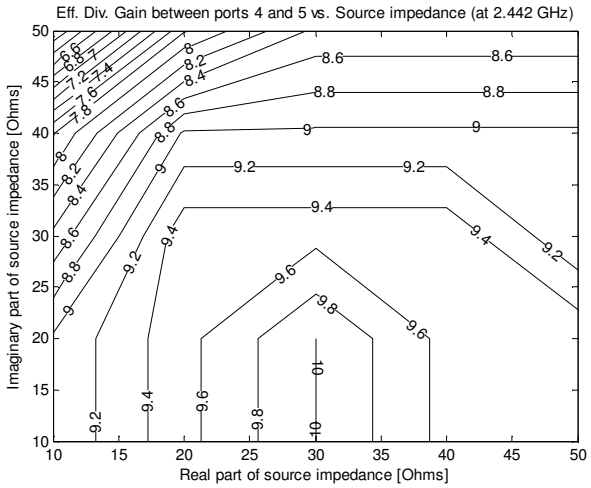

Figure A.75: Eff. Diversity Gain between ports 4 and 5 at 2.442 GHz

Appendix B: Simulated results 3-antennas

Frequency = 1.95 GHz

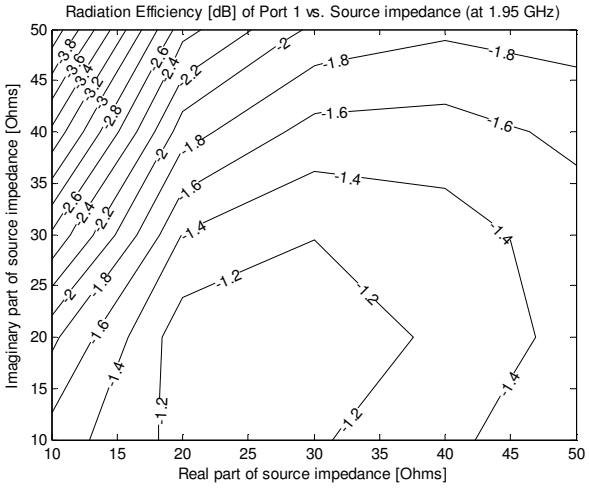

Figure B.1: Tot. Rad. Efficiency for port 1 at 1.95 GHz

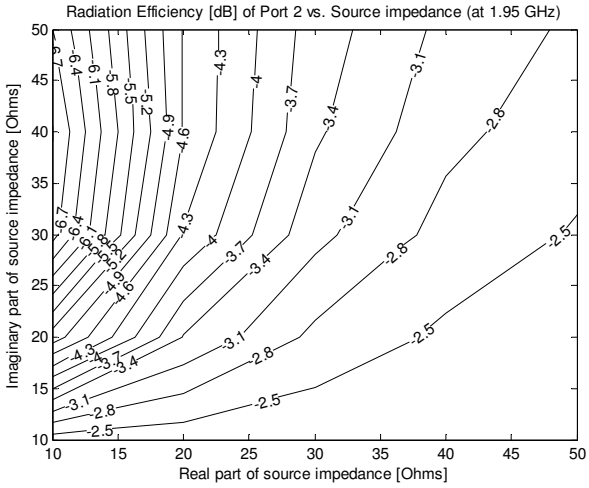

Figure B.2: Tot. Rad. Efficiency for port 2 at 1.95 GHz

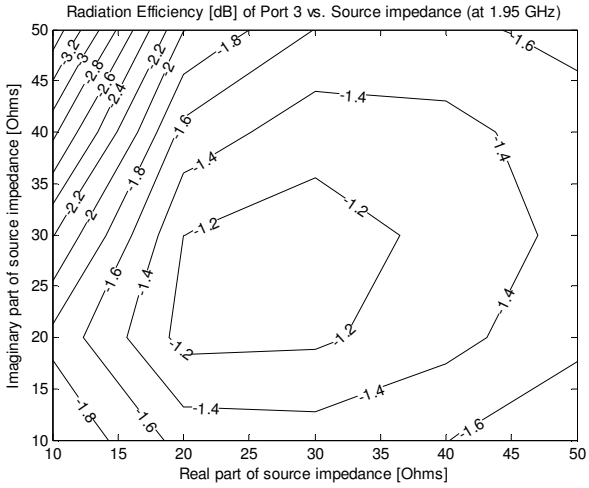

Figure B.3: Tot. Rad. Efficiency for port 3 at 1.95 GHz

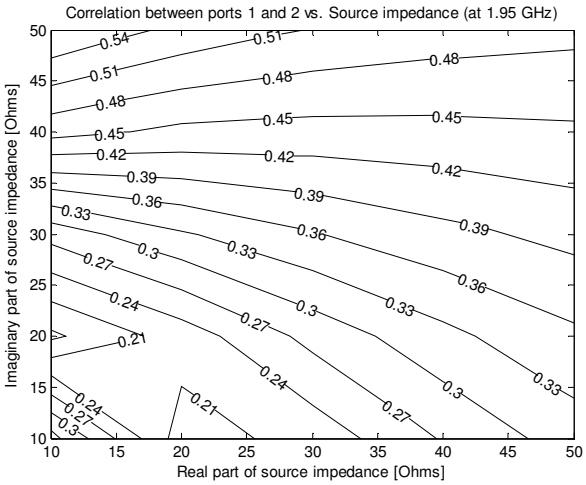

Figure B.4: Correlation between ports 1 and 2 at 1.95 GHz

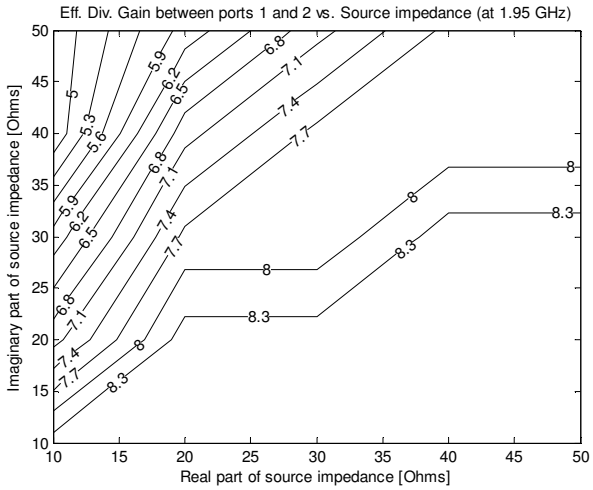

Figure B.5: Eff. Diversity Gain between ports 1 and 2 at 1.95 GHz

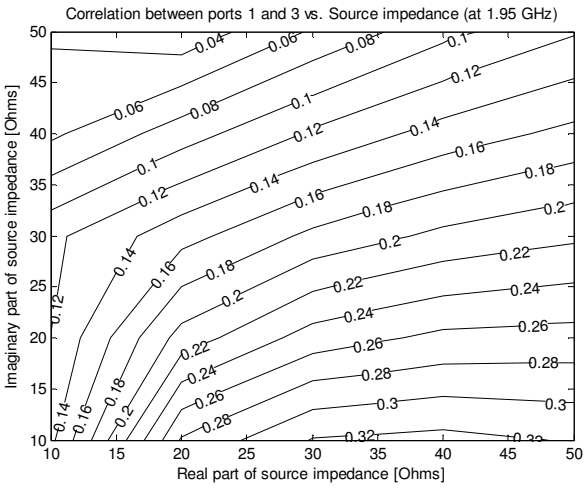

Figure B.6: Correlation between ports 1 and 3 at 1.95 GHz

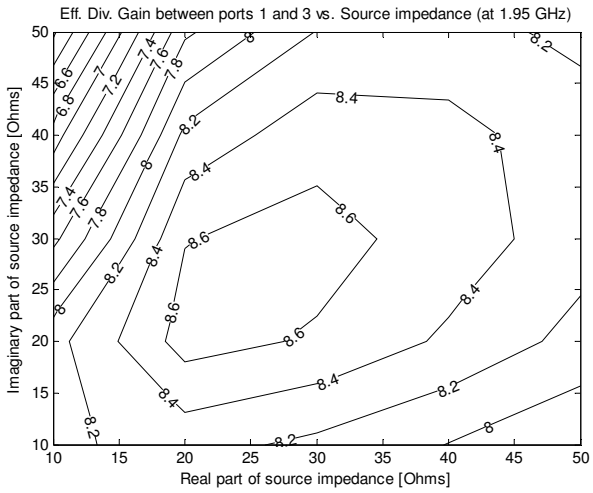

Figure B.7: Eff. Diversity Gain between ports 1 and 3 at 1.95 GHz

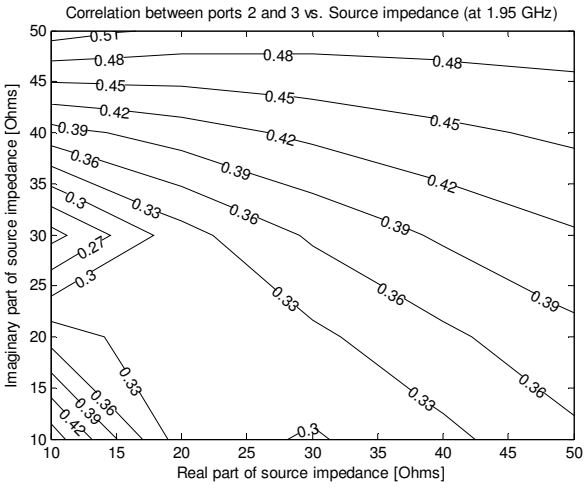

Figure B.8: Correlation between ports 2 and 3 at 1.95 GHz

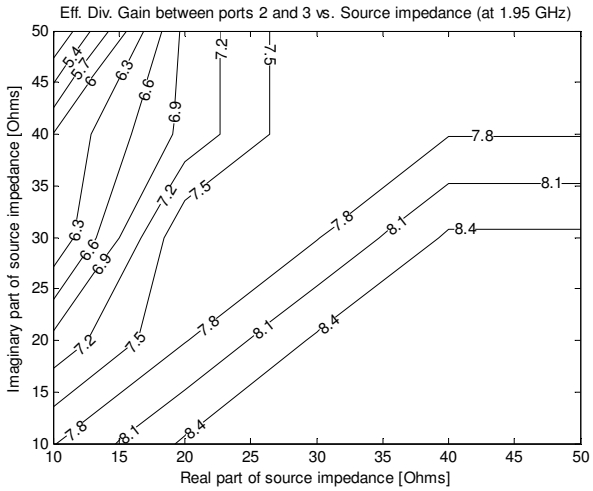

Figure B.9: Eff. Diversity Gain between ports 2 and 3 at 1.95 GHz

Frequency = 2.14 GHz

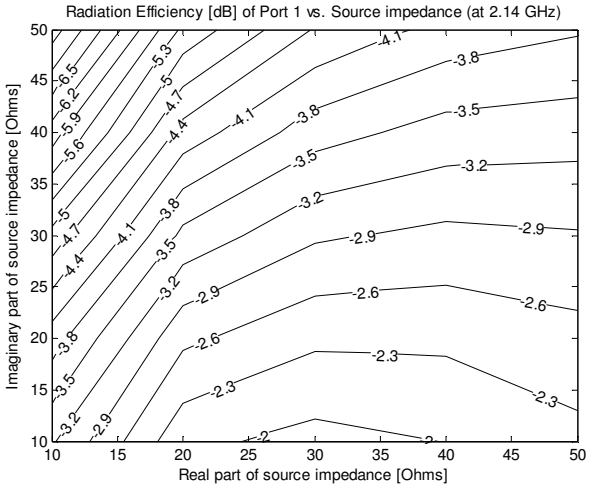

Figure B.10: Tot. Rad. Efficiency for port 1 at 2.14 GHz

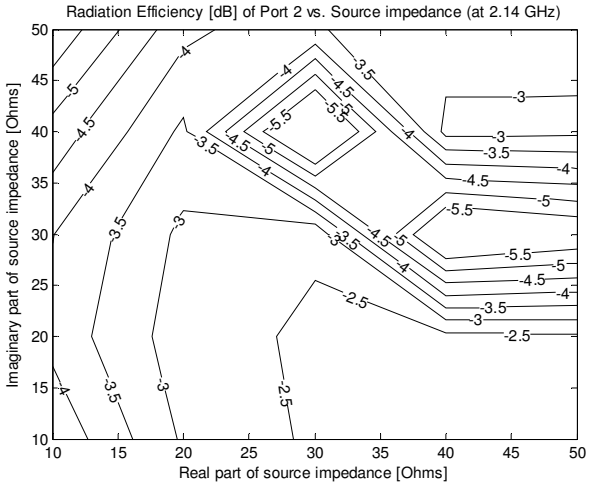

Figure B.11: Tot. Rad. Efficiency for port 2 at 2.14 GHz

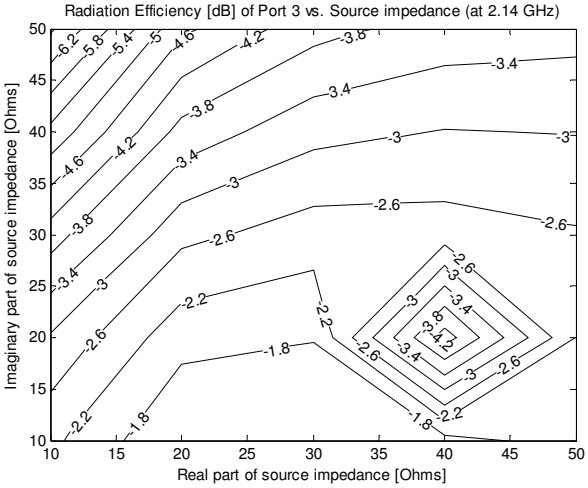

Figure B.12: Tot. Rad. Efficiency for port 3 at 2.14 GHz

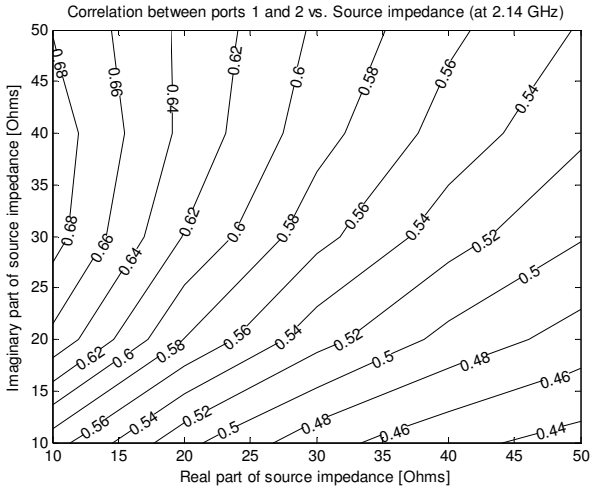

Figure B.13: Correlation between ports 1 and 2 at 2.14 GHz

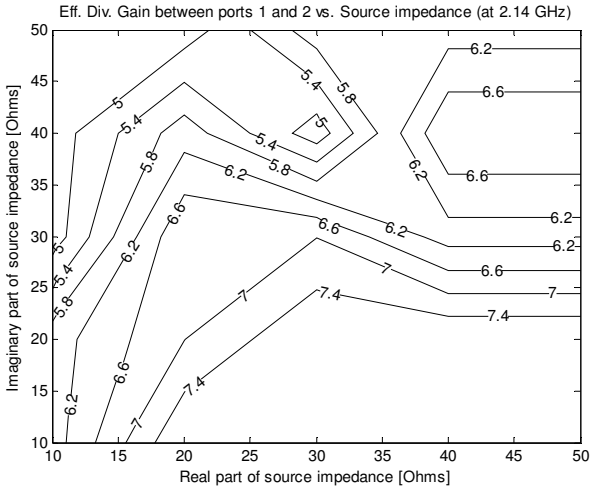

Figure B.14: Eff. Diversity Gain between ports 1 and 2 at 2.14 GHz

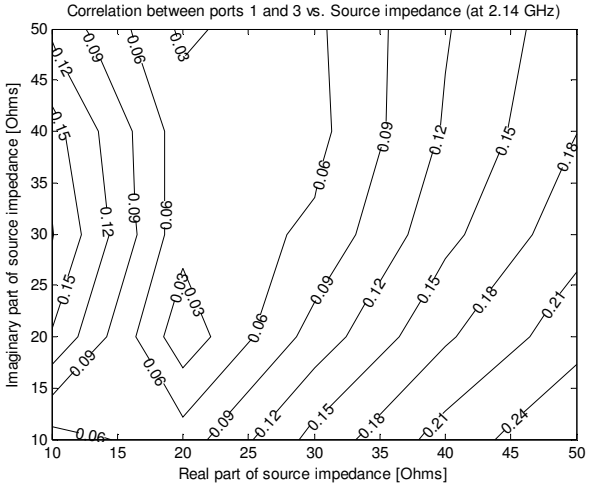

Figure B.15: Correlation between ports 1 and 3 at 2.14 GHz

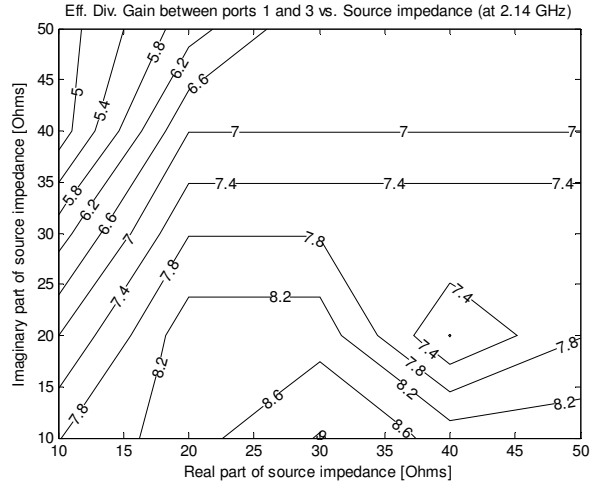

Figure B.16: Eff. Diversity Gain between ports 1 and 3 at 2.14 GHz

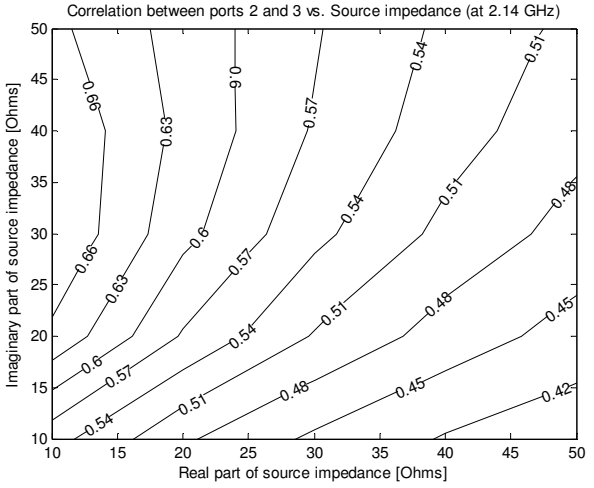

Figure B.17: Correlation between ports 2 and 3 at 2.14 GHz

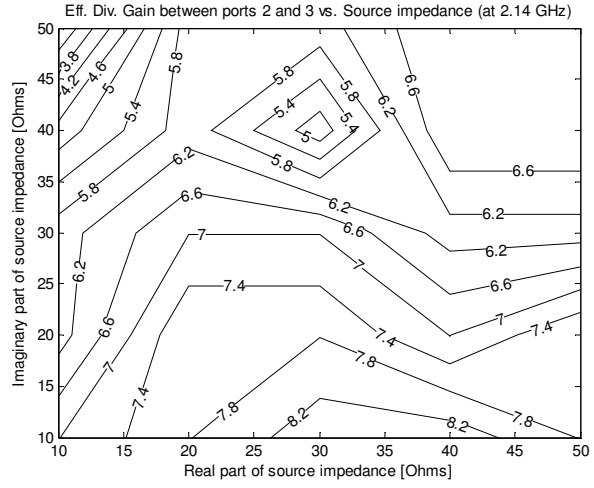

Figure B.18: Eff. Diversity Gain between ports 2 and 3 at 2.14 GHz

Frequency = 2.442 GHz

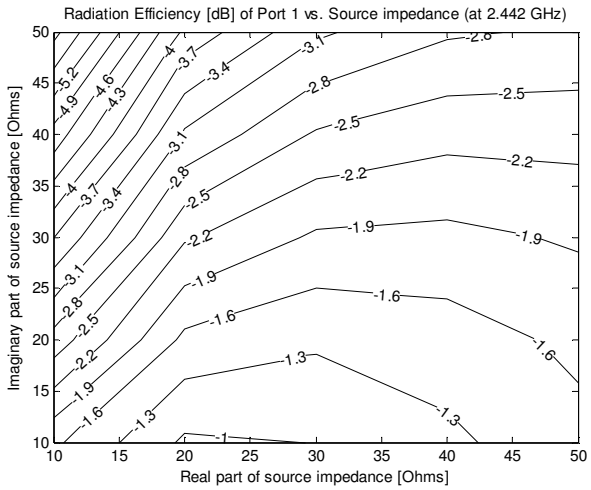

Figure B.19: Tot. Rad. Efficiency for port 1 at 2.442 GHz

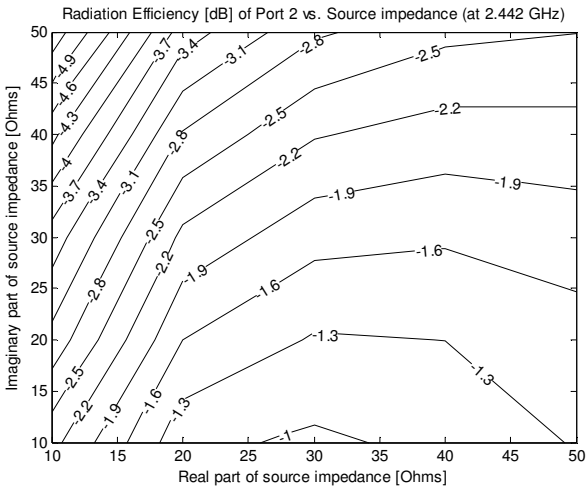

Figure B.20: Tot. Rad. Efficiency for port 2 at 2.442 GHz

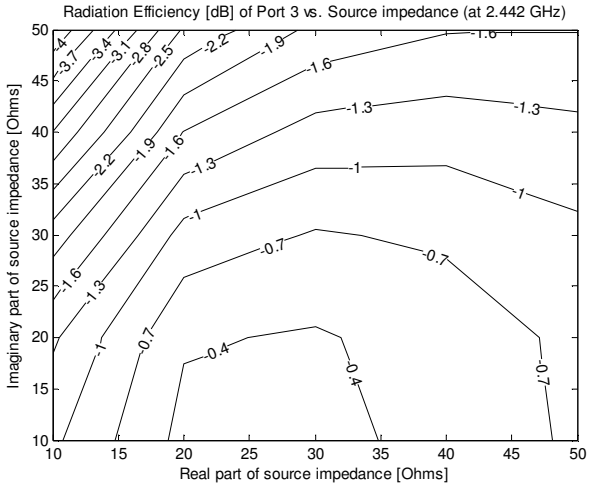

Figure B.21: Tot. Rad. Efficiency for port 3 at 2.442 GHz

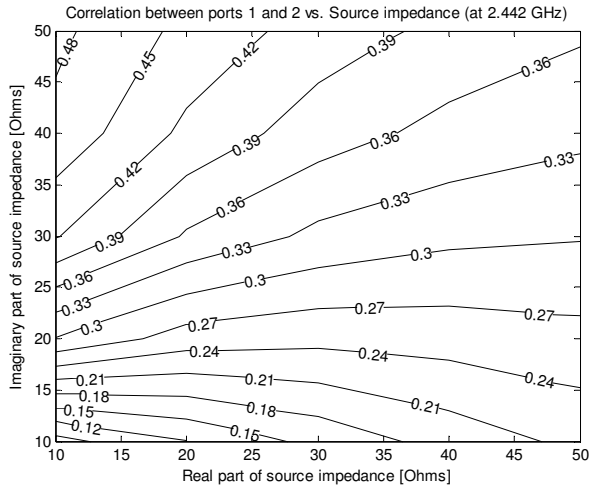

Figure B.22: Correlation between ports 1 and 2 at 2.442 GHz

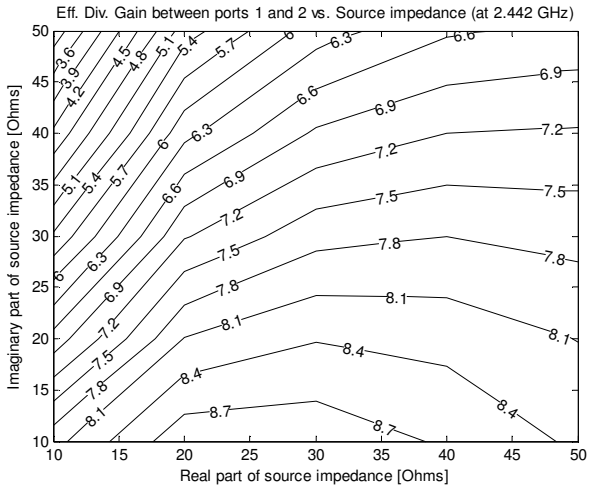

Figure B.23: Eff. Diversity Gain between ports 1 and 2 at 2.442 GHz

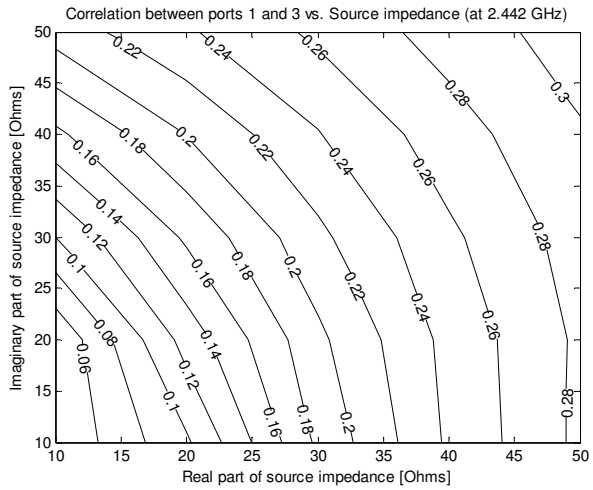

Figure B.24: Correlation between ports 1 and 3 at 2.442 GHz

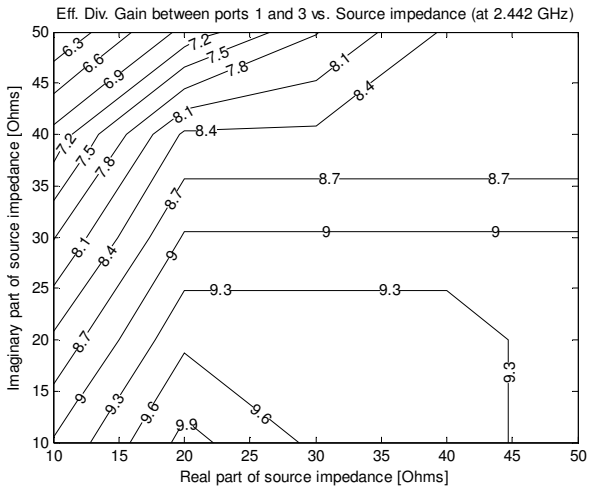

Figure B.25: Eff. Diversity Gain between ports 1 and 3 at 2.442 GHz

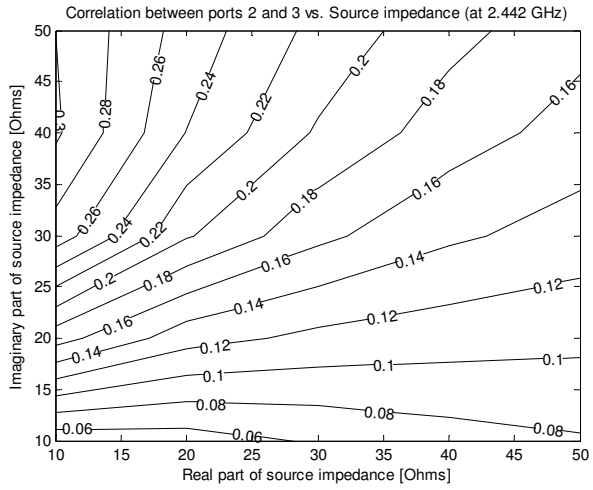

Figure B.26: Correlation between ports 2 and 3 at 2.442 GHz

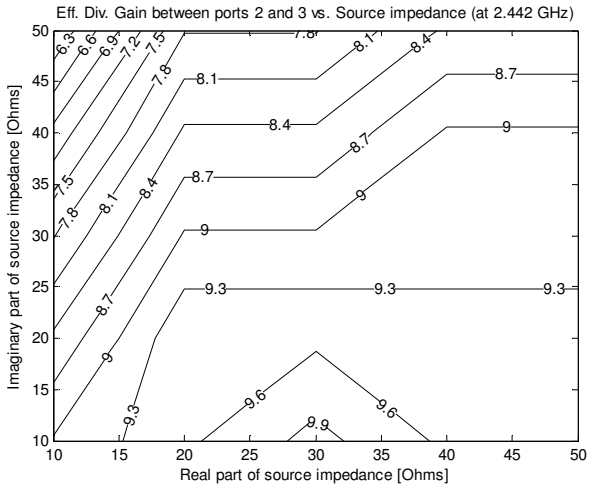

Figure B.27: Eff. Diversity Gain between ports 2 and 3 at 2.442 GHz

Appendix C: Measured results from reverberation chamber for 5-antenna case

W-CDMA band

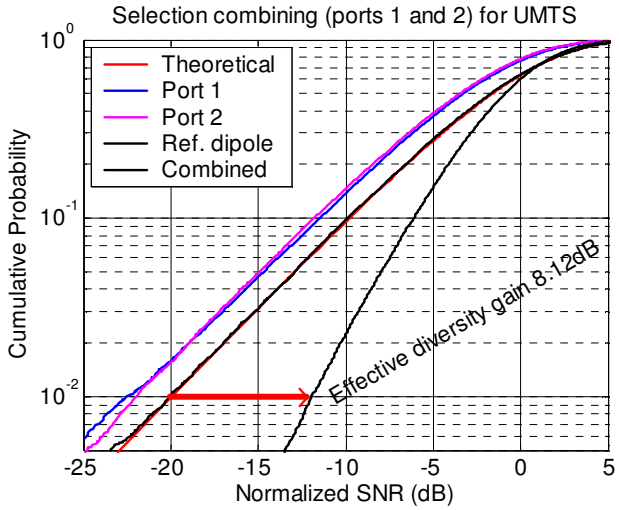

Figure C.1: Eff. Diversity Gain between ports 1 and 2 measured with Rev. Chamber for UMTS band

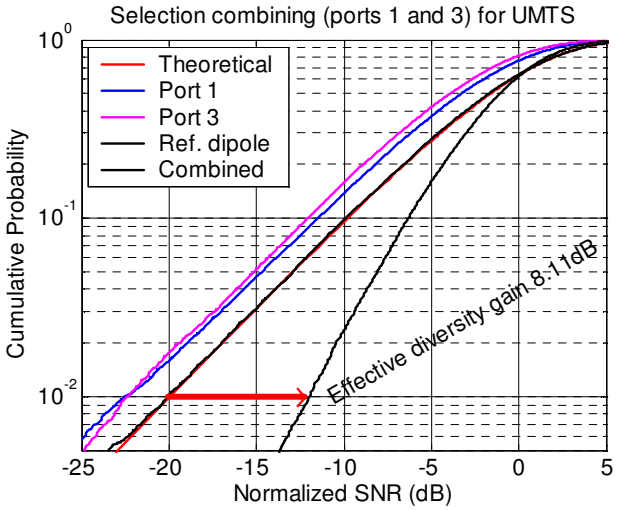

Figure C.2: Eff. Diversity Gain between ports 1 and 3 measured with Rev. Chamber for UMTS band

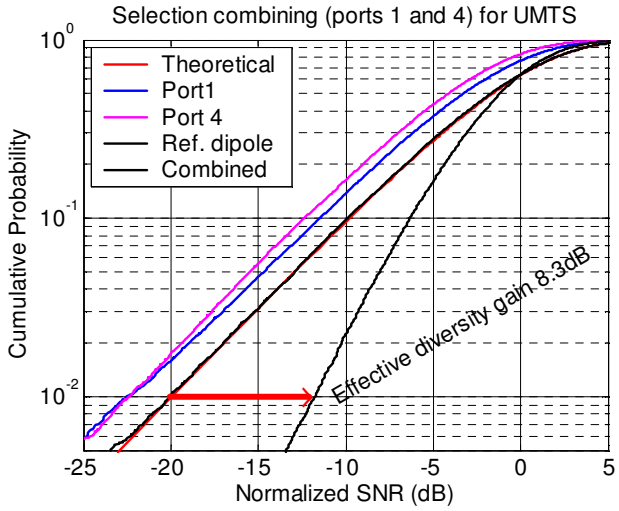

Figure C.3: Eff. Diversity Gain between ports 1 and 4 measured with Rev. Chamber for UMTS band

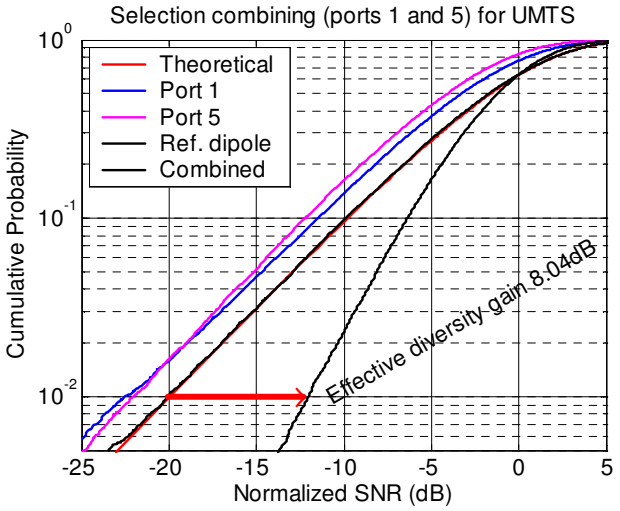

Figure C.4: Eff. Diversity Gain between ports 1 and 5 measured with Rev. Chamber for UMTS band

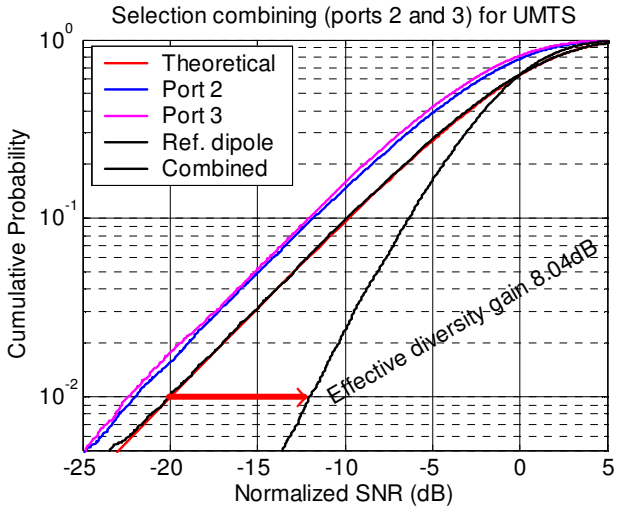

Figure C.5: Eff. Diversity Gain between ports 2 and 3 measured with Rev. Chamber for UMTS band

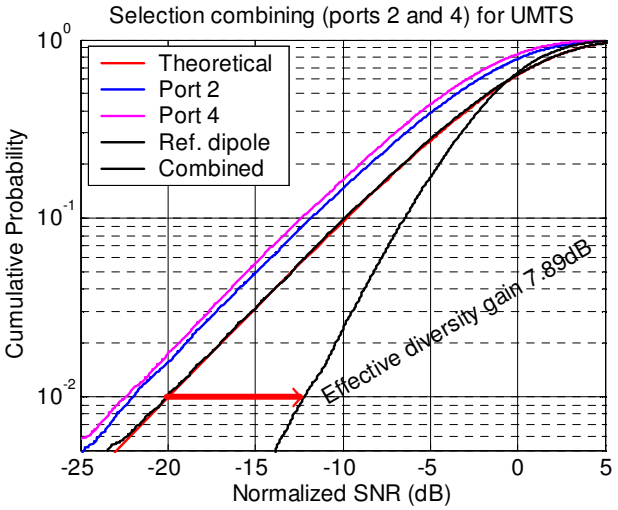

Figure C.6: Eff. Diversity Gain between ports 2 and 4 measured with Rev. Chamber for UMTS band

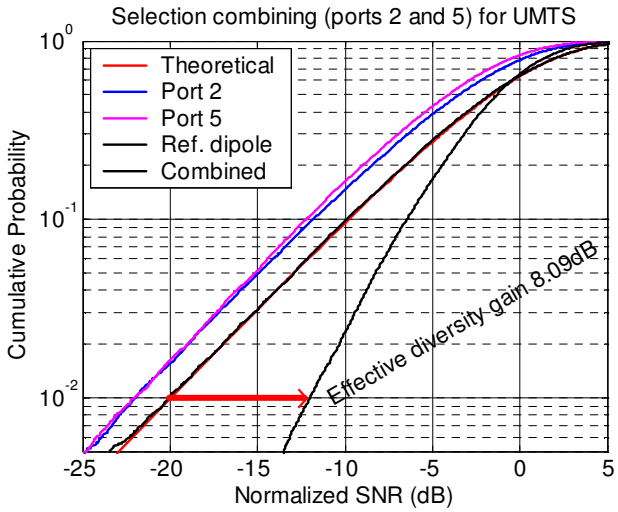

Figure C.7: Eff. Diversity Gain between ports 2 and 5 measured with Rev. Chamber for UMTS band

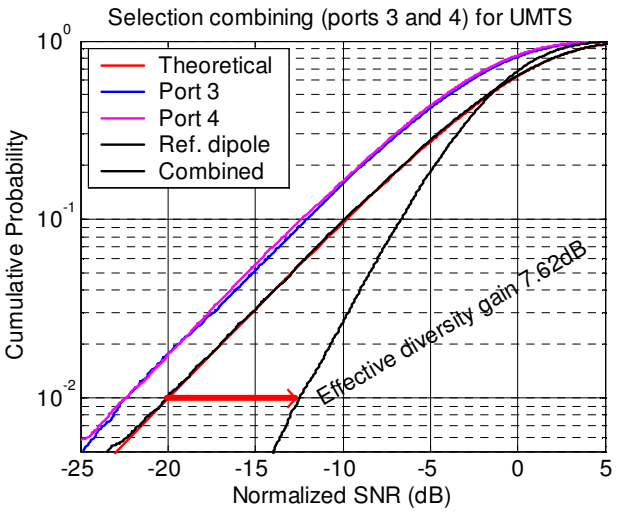

Figure C.8: Eff. Diversity Gain between ports 3 and 4 measured with Rev. Chamber for UMTS band

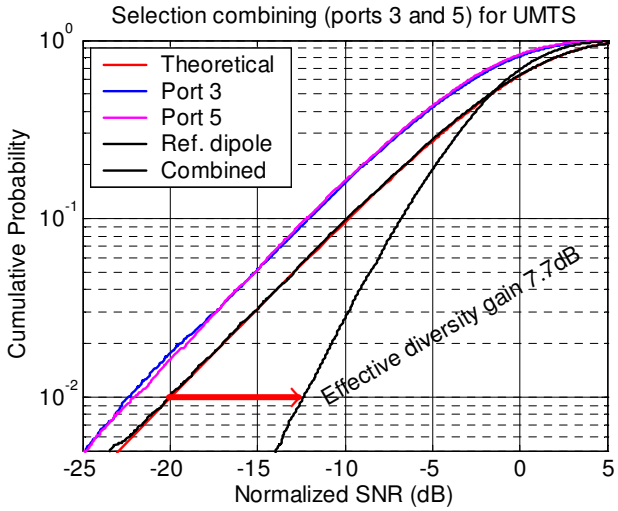

Figure C.9: Eff. Diversity Gain between ports 3 and 5 measured with Rev. Chamber for UMTS band

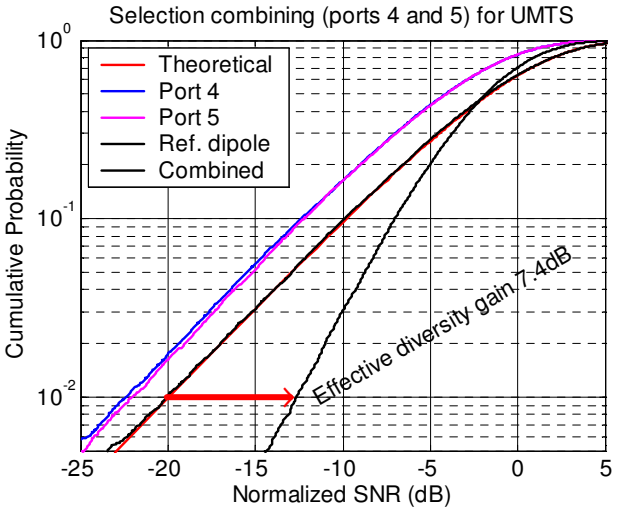

Figure C.10: Eff. Diversity Gain between ports 4 and 5 measured with Rev. Chamber for UMTS band

WLAN band

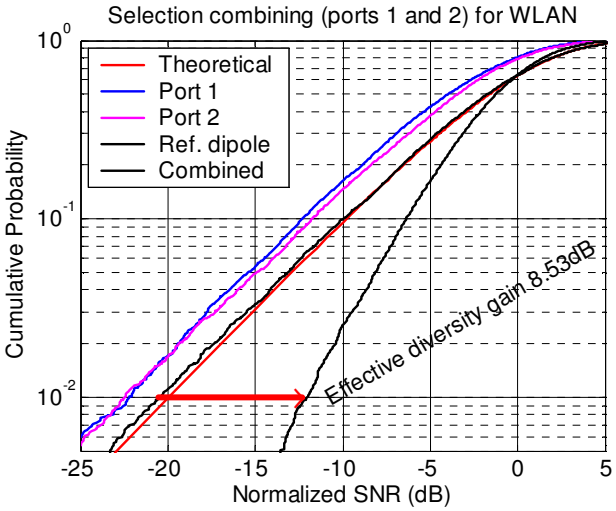

Figure C.11: Eff. Diversity Gain between ports 1 and 2 measured with Rev. Chamber for WLAN band

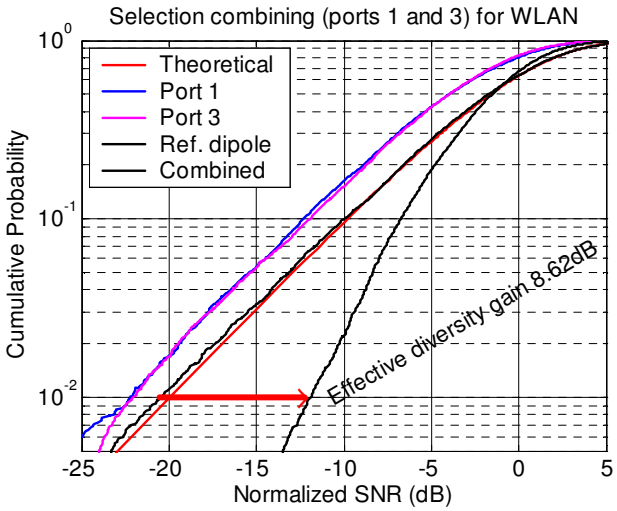

Figure C.12: Eff. Diversity Gain between ports 1 and 3 measured with Rev. Chamber for WLAN band

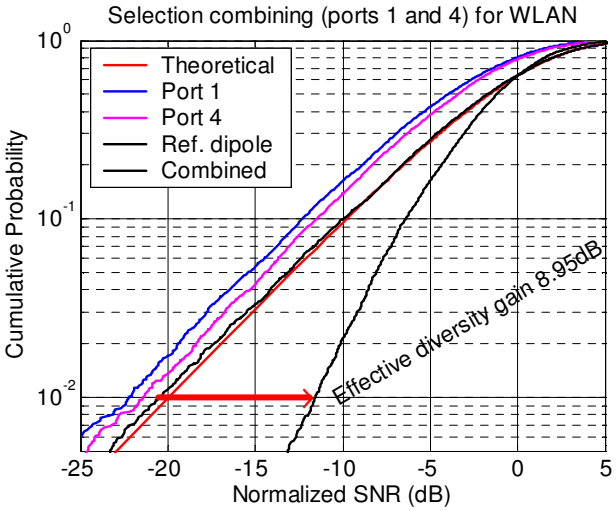

Figure C.13: Eff. Diversity Gain between ports 1 and 4 measured with Rev. Chamber for WLAN band

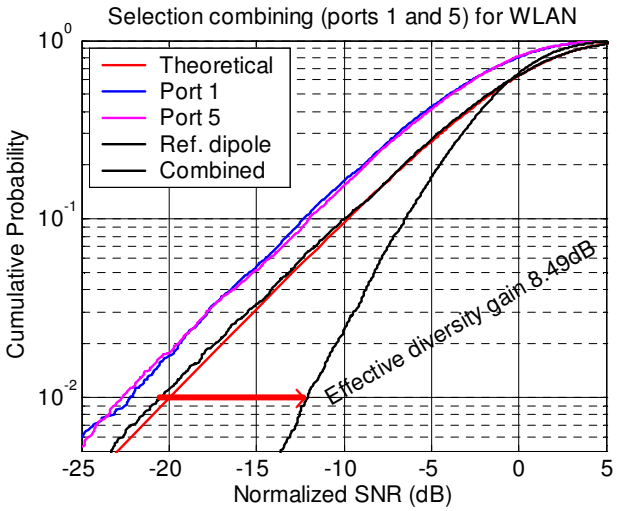

Figure C.14: Eff. Diversity Gain between ports 1 and 5 measured with Rev. Chamber for WLAN band

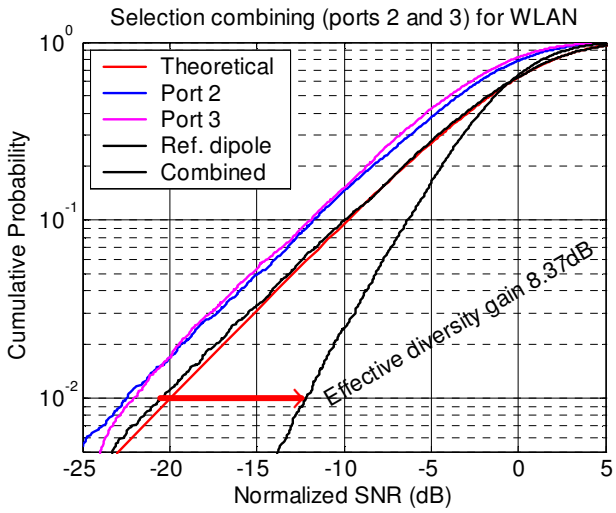

Figure C.15: Eff. Diversity Gain between ports 2 and 3 measured with Rev. Chamber for WLAN band

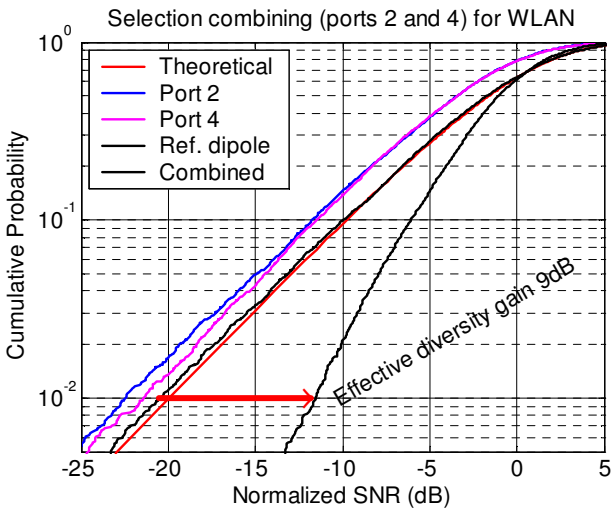

Figure C.16: Eff. Diversity Gain between ports 2 and 4 measured with Rev. Chamber for WLAN band

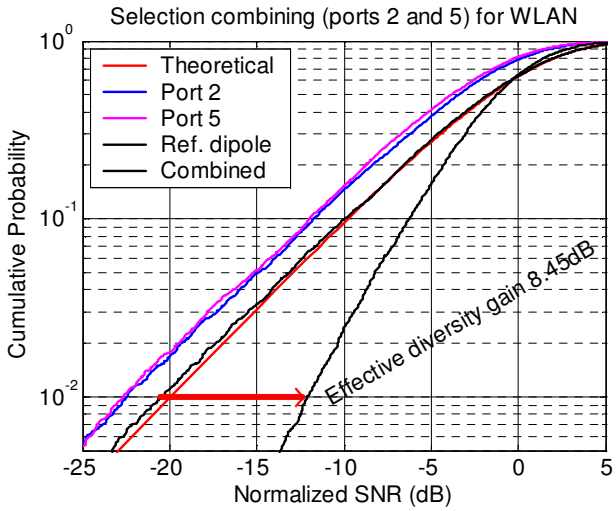

Figure C.17: Eff. Diversity Gain between ports 2 and 5 measured with Rev. Chamber for WLAN band

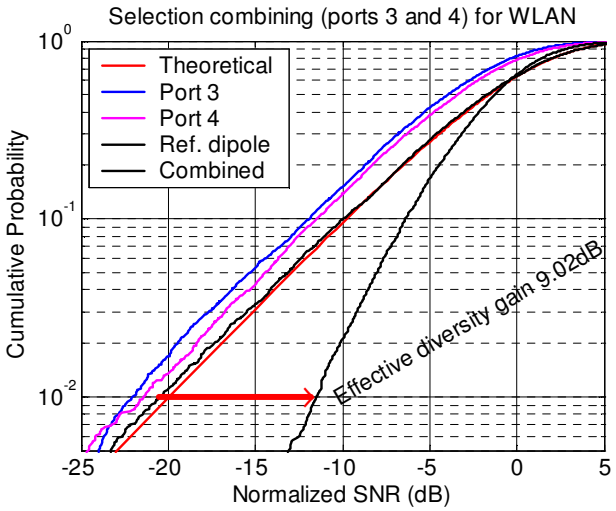

Figure C.18: Eff. Diversity Gain between ports 3 and 4 measured with Rev. Chamber for WLAN band

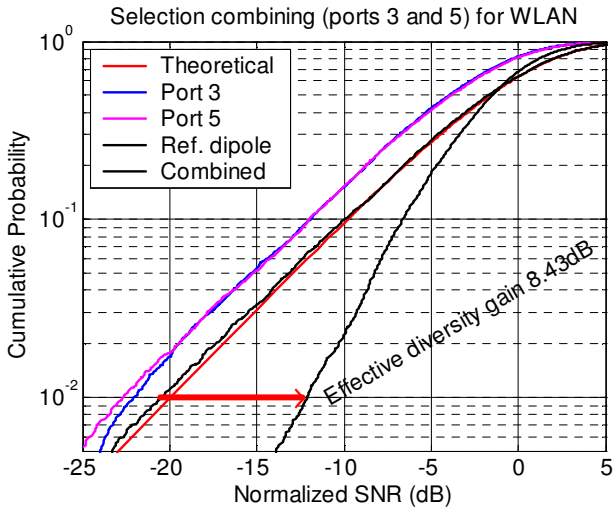

Figure C.19: Eff. Diversity Gain between ports 3 and 5 measured with Rev. Chamber for WLAN band

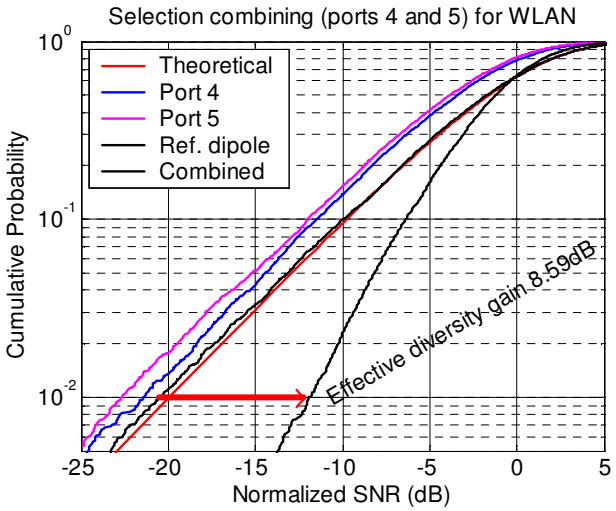

Figure C.20: Eff. Diversity Gain between ports 4 and 5 measured with Rev. Chamber for WLAN band

Appendix D: Spanish Summary

Resumen

En los últimos años, la demanda de altas tasa de transmisión de datos para video, imágenes y otras comunicaciones ha crecido de forma considerable. Muchas investigaciones se han centrado en mejorar el radio enlace entre las estaciones móviles y la estación base. Los sistemas "Multiple Input and Multiple Output" (MIMO) se han introducido recientemente usando la correlación de las señales de todo el entorno multipath. En dichos sistemas, la capacidad del enlace de comunicación depende de la relación señal a ruido y de la correlación de las señales cuando varias antenas reciben la señal que fue transmitida. La correlación también juega un papel importante en los esquemas de diversidad pero la eficiencia de radiación es normalmente un factor limitante de gran importancia en la ganancia efectiva obtenida por diversidad de muestras.

El objetivo de este proyecto es estudiar la influencia de la eficiencia de radiación y la correlación en la ganancia efectiva obtenida por diversidad de muestras entre varias antenas, variando la impedancia de entrada.

Se han llevado a cabo diversas simulaciones para estudiar el comportamiento de la ganancia efectiva obtenida por diversidad de muestras usando los programas CST Microwave Studio y un software llamado "Multi-Port Antenna evaluator" (MPA) que se está desarrollando en "Chalmers Antenna Systems Excellence centre" (CHASE).

A lo largo de este proyecto se han tratado varios ejemplos, comenzando con dos dipolos paralelos, para comprobar el correcto funcionamiento del MPA. Posteriormente, configuraciones de 5 y 3 antenas sobre un ordenador portátil, separadas 2.8 y 1 cm respectivamente, serán consideradas y se realizarán simulaciones de su comportamiento empleando los programas mencionados anteriormente. En el caso de las antenas incluidas en el ordenador portátil, se diseñarán para cubrir las especificaciones de frecuencia de las bandas W-CDMA y WLAN.

Por último, el modelo con 5 antenas se construirá en el laboratorio de modo que éstas puedan ser incluidas en un ordenador portátil real y posteriormente medidas con el analizador de redes y en una cámara de reverberación.

Por tanto, se provee un método para mejorar la ganancia efectiva obtenida por diversidad de muestras variando la impedancia de entrada de las antenas. El método puede ser perfectamente aplicable en el caso de sistemas MIMO ya que la eficiencia de radiación y la correlación también son parámetros de diseño importantes en dichos sistemas.

Agradecimientos

Quiero aprovechar esta oportunidad para agradecer a todas las personas que de un modo u otro han hecho posible este proyecto, porque todas ellas son parte de mí y por tanto, parte de él también.

En primer lugar, quisiera agradecer a Per-Simon Kildal la motivación que su clase de antenas me infundió y por permitirme participar en este proyecto. Deseo agradecer el tiempo, el apoyo y los consejos de mi supervisor y tutor Kent Rosengren. Ha sido una gran ayuda, paciente e increíblemente entusiasta, ofreciéndome siempre grandes recomendaciones y sugerencias. Tack så mycket! Y por supuesto, a mi coordinador en Madrid, Daniel Segovia Vargas que me ayudó durante toda mi estancia.

Gracias a todos mis compañeros de Ethertronics (y Flextronics) por el buen ambiente en la empresa. Me dieron su tiempo y sus conocimientos cuando así lo necesité. Gracias especialmente a Carmen, más que una simple compañera de trabajo. Por su amistad sincera, su energía y su ayuda altruista en todo. Mis agradecimientos a Kristian Karlsson y Jan Carlsson por ayudarme con MPA y CircSim. Y también a Laurent Desclos por su tiempo y sus valiosos comentarios que tanto me han ayudado. Gracias a mis compañeros de Endesa por apoyarme en la última etapa de mi carrera.

Gracias a todos mis compañeros de la Universidad Carlos III que me ayudaron durante los años más difíciles de mi carrera en Madrid y también cuando vine a Suecia. Transformaron nuestro estrés en días de risas y alegría. Especialmente a Patri, David, Myris, María, Vicky y Blanca por sus ánimos y su apoyo y por todos nuestros buenos momentos.

Mil gracias a todos mis amigos de Chalmers que compartieron conmigo la increíble experiencia Erasmus. ¡No fue sólo un año más! Gracias a Laura y a Natalia por su apoyo, por escucharme tantas veces y por la amistad que me han dado. Gracias a toda la "Högsbo family", especialmente a Guzmán, Miguel y Dominik por su alegría. Y a Fabien por los momentos, por la amistad.

Quisiera agradecer a todos mis amig@s cada momento que hemos compartido. ¡Sois geniales! Especialmente a Lucía, que siempre ha estado a mi lado desde que nos conocimos en el "kinder", por su compañía todos estos años y su amistad. Y a Mamen por sus palabras, su amistad y ser tan buena siempre.

Debo dar gracias a David por su paciencia, su comprensión, su cariño y motivación. Siempre creyó en mí y me apoyó a lo largo de este camino. Conocerle fue un regalo.

Por último, mi más sincero agradecimiento a mis padres, Piedad y Manuel, ¡porque me lo han enseñado todo! Admiro su forma de ser y son un verdadero ejemplo a seguir. Gracias por quererme tanto, por protegerme y apoyarme siempre. Me lo han dado todo y no tengo palabras para expresar mi gratitud. Gracias a mi maravilloso hermanito Víctor, siempre tan generoso, sincero y de tan buen corazón. Y en general a toda mi familia, por su cariño y su constante apoyo, y especialmente a mis abuelos.

… Porque no podría haberlo hecho sin todos vosotros y tampoco sería quien soy… ¡Gracias de corazón a todos!

D.1. Especificaciones

Los terminales móviles inalámbricos, como teléfonos y ordenadores, están evolucionando continuamente para ofrecer más servicios y mayores tasas de datos. Esta creciente demanda debe implicar un mantenimiento del canal inalámbrico, considerando el desvanecimiento de la señal, la interferencia entre símbolos (ISI) y la interferencia entre canales consecutivos. El uso de múltiples antenas permitirá incrementar la tasa de datos pero también debe reforzar el canal frente a las interferencias y el desvanecimiento comentados.

La tendencia actual en el diseño de terminales móviles conlleva construir antenas con el menor volumen posible y con una eficiencia de radiación y un ancho de banda optimizado para conseguir las especificaciones requeridas.

Las bandas de frecuencias estudiadas en este proyecto son W-CDMA (1920-2170 MHz) y WLAN (2.4 GHz). Las especificaciones de las antenas simuladas e implementadas en este proyecto se recogen en la tabla 2.1.

		TCH	**[MHz]**	**Return Loss RL (S_{11}) [dB]**	**Efficiency η [%]**	**Correlation ρ**
UMTS band 1 1.92-2.17 GHz	**Tx**	9750	1950.0	>6	>50	0.05
	Rx	10700	2140.0	>6	>50	0.05
WLAN 2.4 GHz			2400.0	>6	>50	0.05
			2483.0	>6	>50	0.05

Tabla 2.1: Especificaciones de las antenas

En este proyecto, se ha desarrollado un método que permite variar la ganancia efectiva obtenida por diversidad de muestras. Además, la correlación entre los diferentes puertos de las antenas situadas en la parte superior de un ordenador portátil también puede ser minimizada. Sin embargo, se comprobará que la eficiencia de radiación será el factor limitante de la ganancia efectiva obtenida por diversidad de muestras. El método propuesto consiste en una variación de la impedancia de entrada de las antenas que influenciará todos los parámetros mencionados.

D.2. Resultados

D.2.1. Simulaciones

Para las simulaciones se ha construido un modelo de real de un ordenador portátil empleando CST Microwave Studio (ver sección 3). En la parte superior de la pantalla de dicho ordenador se han colocado diversas antenas que se utilizarán para realizar las simulaciones. Para extraer resultados, se han empleado los parámetros S y los diagramas de radiación de cada una de las antenas extraídos de CST e importados en MPA, siguiendo las recomendaciones mencionadas en la sección 3 de esta memoria. En MPA, se han empleado circuitos compuestos por una fuente y una impedancia de entrada, que inicialmente estaba a 50 Ω y que variaba de 0 a 50 + 50 Ω. Se han extraído los valores de eficiencia de radiación, correlación y ganancia aparente obtenida por diversidad de muestras. Mediante las ecuaciones mencionadas en la sección 2, se puede calcular la ganancia eficiente de diversidad para todos los valores de impedancias y representar gráficamente en Matlab las curvas de nivel obtenidas para cada uno de los parámetros de las antenas.

D.2.1.1. Caso 5 antenas:

En este primer caso, las 5 antenas están separadas entre ellas 2.8 cm. Para impedancias de entrada de 50 Ω se puede ver en la sección 6.1.1.1 que la correlación obtenida no es tan alta como inicialmente habíamos supuesto y que la ganancia aparente obtenida por diversidad de muestras es alta. Por tanto, el único modo de modificar la ganancia efectiva obtenida por diversidad de muestras, es variando la eficiencia de radiación de las antenas.

Variando la impedancia de entrada de los puertos, obtenemos los valores de eficiencia de radiación, correlación y ganancia aparente obtenida por diversidad de muestras mediante MPA y los representaremos empleando curvas de nivel.

Como se explica en esta memoria, si la eficiencia de radiación de los dos puertos considerados es más o menos similar, usaremos las ecuaciones de la sección 2.1.4.1, calculando la ganancia efectiva obtenida por diversidad de muestras al 1% de probabilidad de error.

Para mostrar este primer procedimiento, tomaremos el ejemplo de los puertos 2 y 3 a 1.95 GHz, cuyos gráficos de eficiencia son similares:

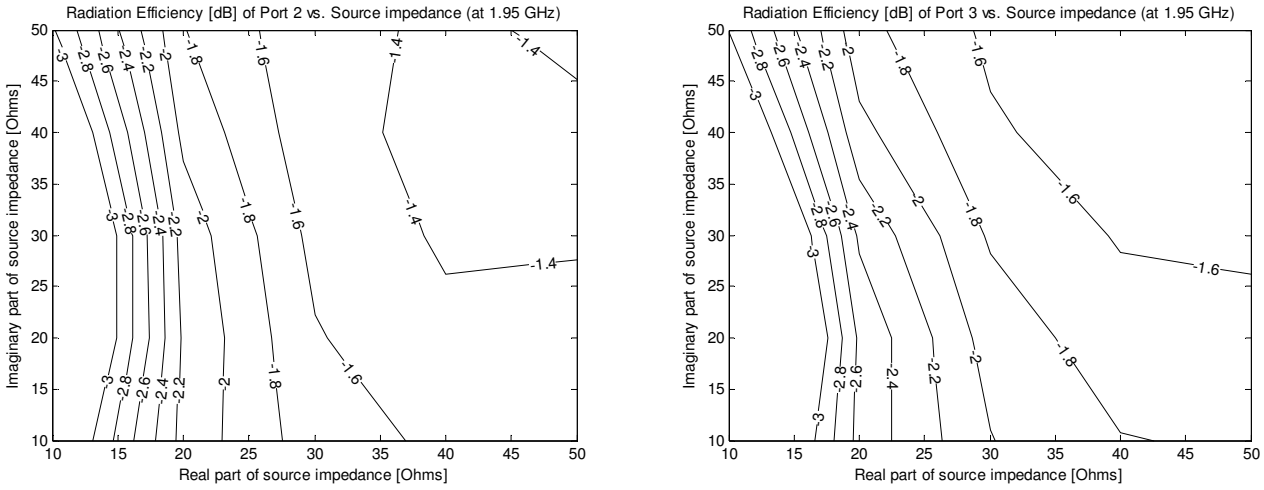

Figura 6.3: Eficiencia de radiación para los puertos 2 (a) y 3 (b) a 1.95 GHz

Y la correlación entre ellos es:

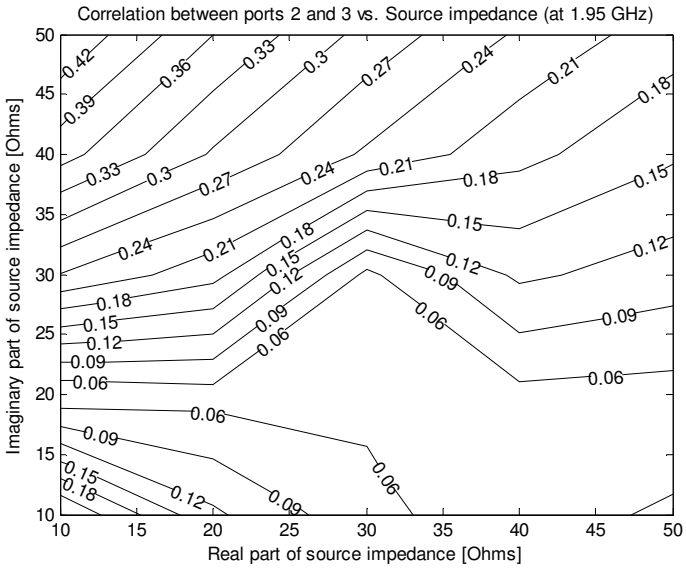

Figura 6.4: Correlación entre los puertos 2 y 3 a 1.95 GHz

Y por tanto, si aplicamos las ecuaciones (2.3) y (2.4), se puede calcular la ganancia efectiva obtenida por diversidad de muestras entre los puertos 2 y 3, que representada en Matlab como una función de las diferentes impedancias de entrada queda como se ve la Figura 6.5:

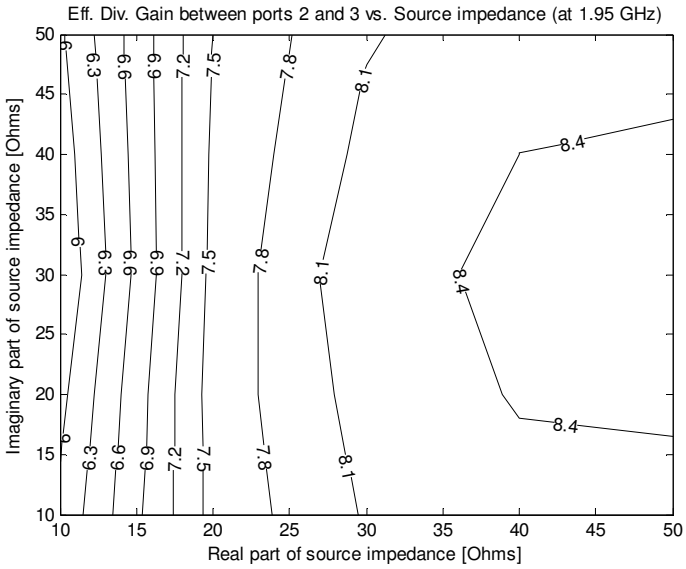

Figura 6.5: Ganancia efectiva obtenida por diversidad de muestras entre los puertos 2 y 3 a 1.95 GHz

Sin embargo, si la eficiencia de radiación de las dos antenas es muy distinta, se debe implementar la ecuación (2.5) para obtener la función de densidad de probabilidad acumulada de la señal combinada. La mayor diferencia entre las eficiencias de radiación de las antenas puede apreciarse entre los puertos situados en los extremos del ordenador portátil, los puertos 1 y 5. Por tanto, dicha diferencia puede deberse a la existencia de un sólo vecino mientras que el resto de puertos tienen dos vecinos, uno a cada lado.

Para mostrar este segundo procedimiento, cogeremos el ejemplo de los puertos 1 y 2, para 1.95 GHz. Así, las representaciones de la eficiencia de radiación y la correlación pueden verse en las Figuras 6.6 y 6.7.

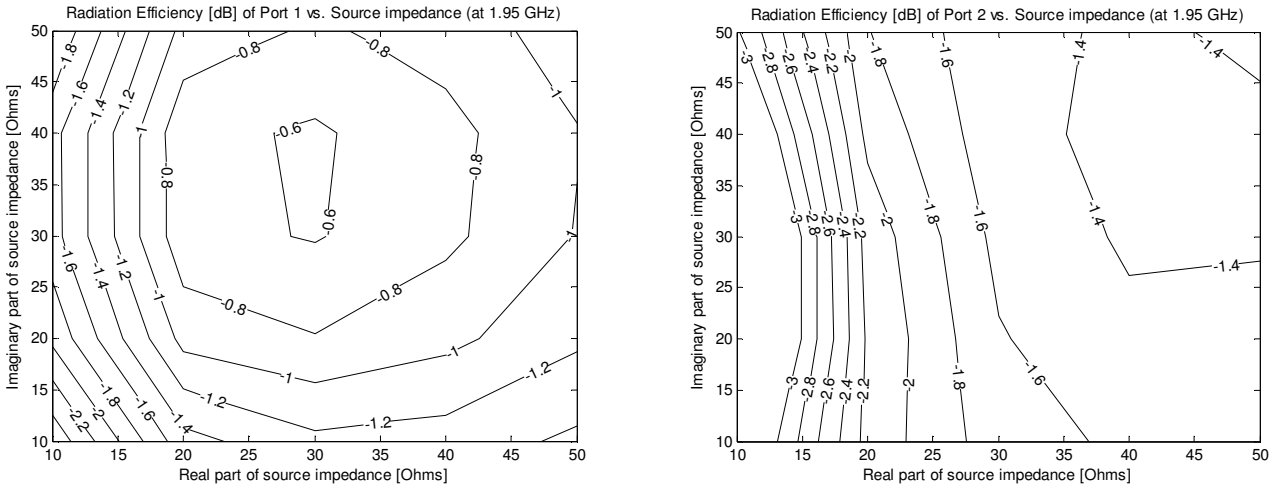

Figura 6.6: Eficiencia de radiación de los puertos 1 (a) y 2 (b) a 1.95 GHz

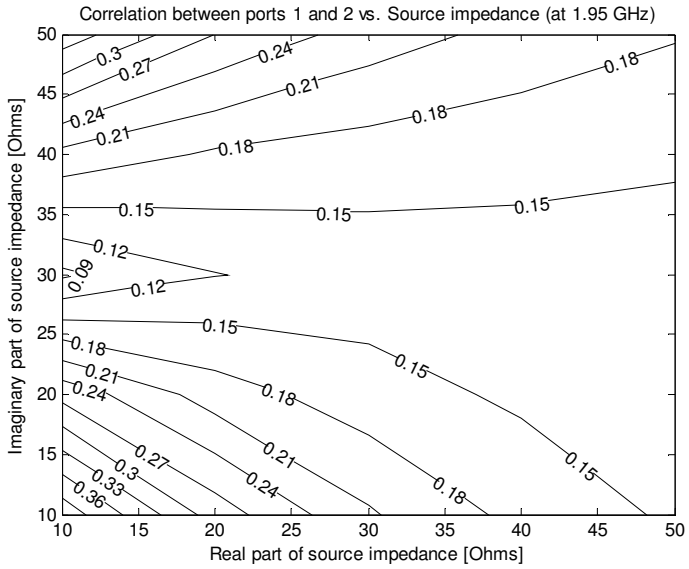

Figura 6.7: Correlación entre los puertos 1 y 2 a 1.95 GHz

Y aplicando la ecuación (2.5), puede calcularse la ganancia efectiva obtenida por diversidad de muestras para cada valor de impedancia de entrada que se representa en la Figura 6.8:

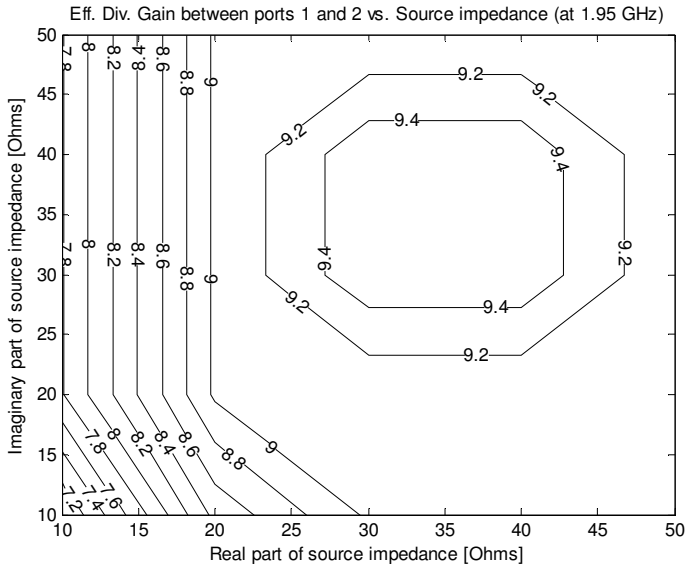

Figura 6.8: Ganancia efectiva obtenida por diversidad de muestras entre los puertos 1 y 2 a 1.95 GHz

Analizando manualmente los gráficos obtenidos para todos los puertos, puede hacerse una representación combinada de todos los requerimientos de frecuencia para mostrar las regiones donde el sistema presenta un funcionamiento adecuado. Así, en la Figura 6.9 se representan los intervalos de impedancia para cada una de las bandas de frecuencia donde la eficiencia de radiación es mejor que -3 dB. En la Figura 6.10 puede verse la representación de los intervalos donde se obtiene una correlación menor que 0.3 y por último, en la Figura 6.11 se representan los intervalos donde la ganancia efectiva obtenida por diversidad de muestras es mayor que 8 dB.

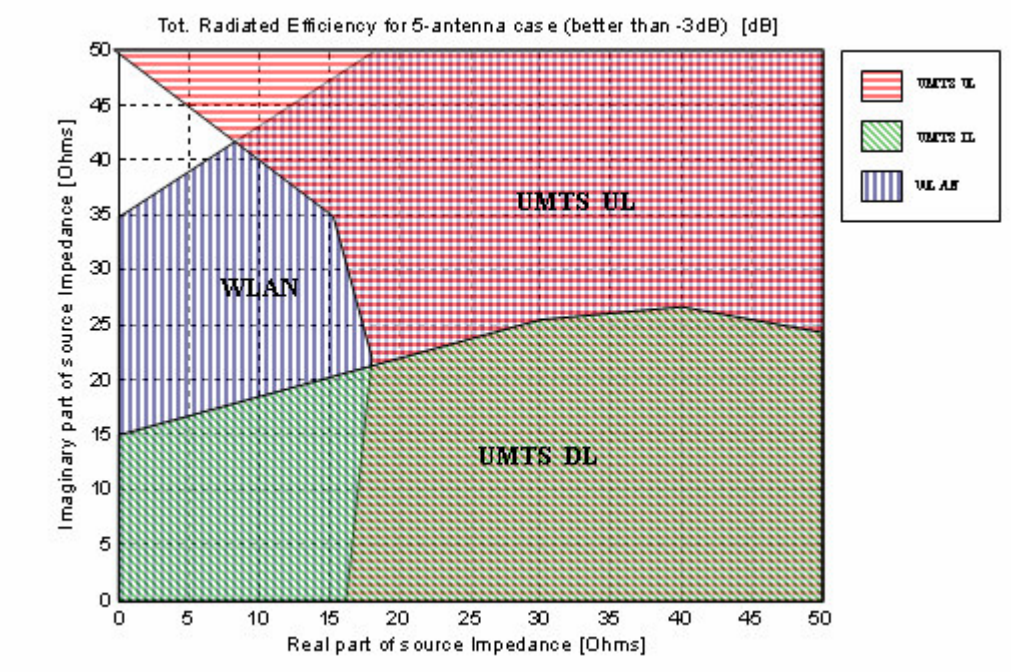

Figura 6.9: Representación de la eficiencia de radiación total mejor que -3 dB para el caso con 5 antenas

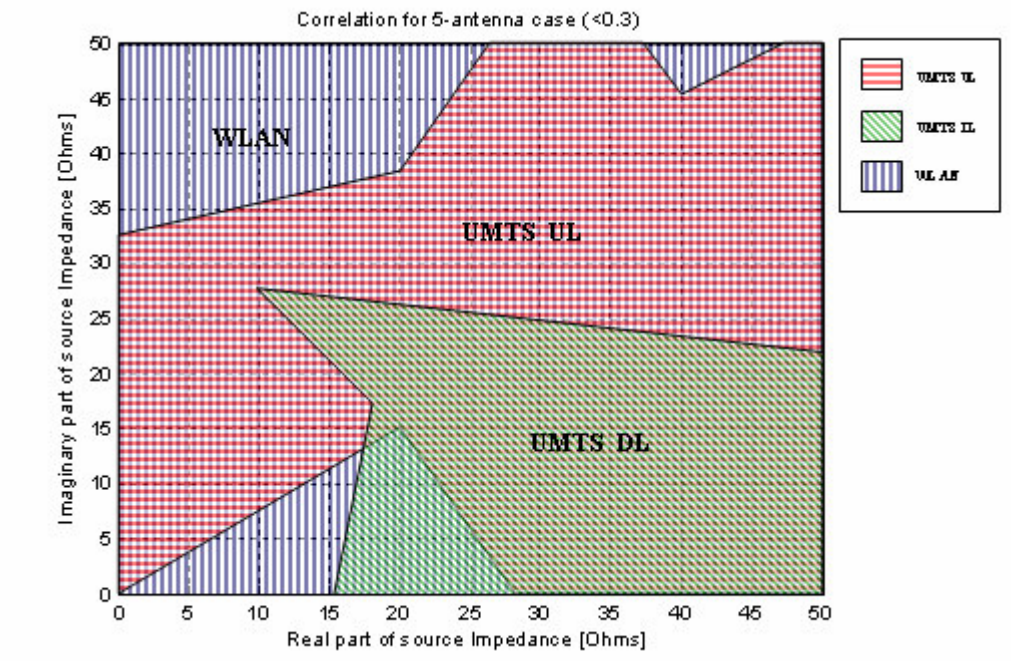

Figura 6.10: Representación de la correlación mejor que 0.3 para el caso de 5 antenas

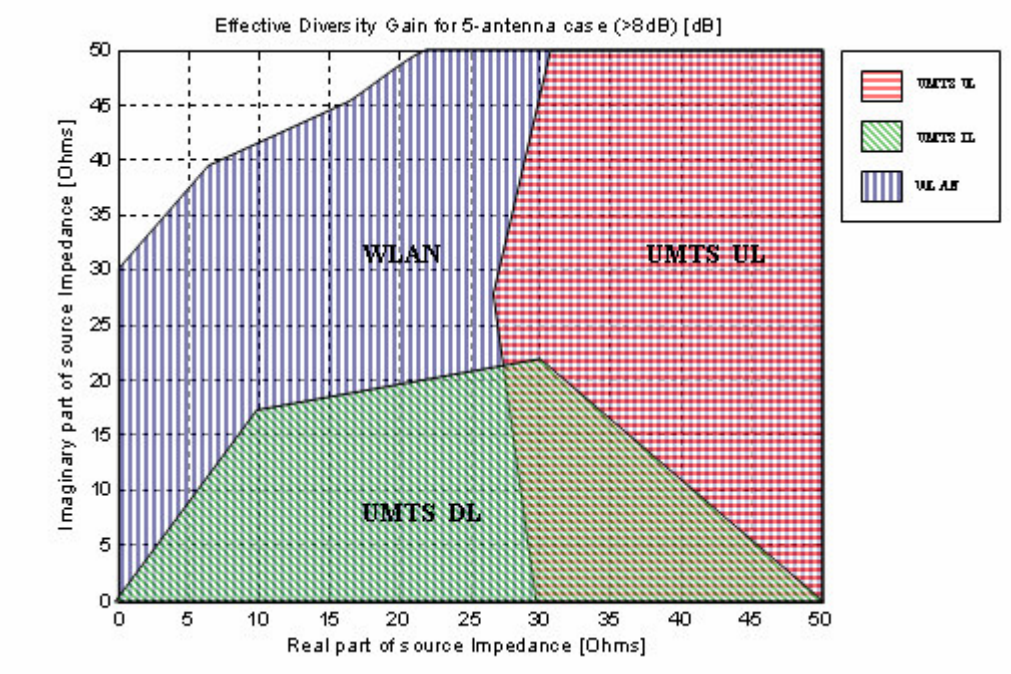

Figura 6.11: Representación de la ganancia efectiva obtenida por diversidad de muestras mayor que 8 dB para el caso de 5 antenas

D.2.1.2. Caso 3 antenas:

En este caso, las antenas están separadas tan sólo 1 cm y por tanto, existe un mayor acoplamiento entre los puertos, que influenciará a la correlación y a la eficiencia de las antenas. Es decir, como se comenta en la sección 6.1.2.1, para impedancias de entrada de 50 Ω, la correlación aumenta y la ganancia aparente obtenida por diversidad de muestras es menor que en el caso anterior.

Variando la impedancia de entrada de todos los puertos, y procediendo como en el caso anterior también podemos representar los intervalos para cada banda de frecuencia para los cuales el sistema cumple determinados requerimientos. En la Figura 6.20 se representan los intervalos de impedancia de entrada donde la eficiencia de radiación es mejor que -3 dB, para cada banda de frecuencias. Así, en la Figura 6.21 se representan los intervalos para cada banda de frecuencia donde la correlación es menor que 0.3 y al no existir región común, se permitirá una correlación menor que 0.4, Figura 6.22, donde aparece una región común entre las bandas WLAN y UMTS-UpLink. Sin embargo, en la banda de Down-Link, la correlación sigue siendo mayor que el límite establecido.

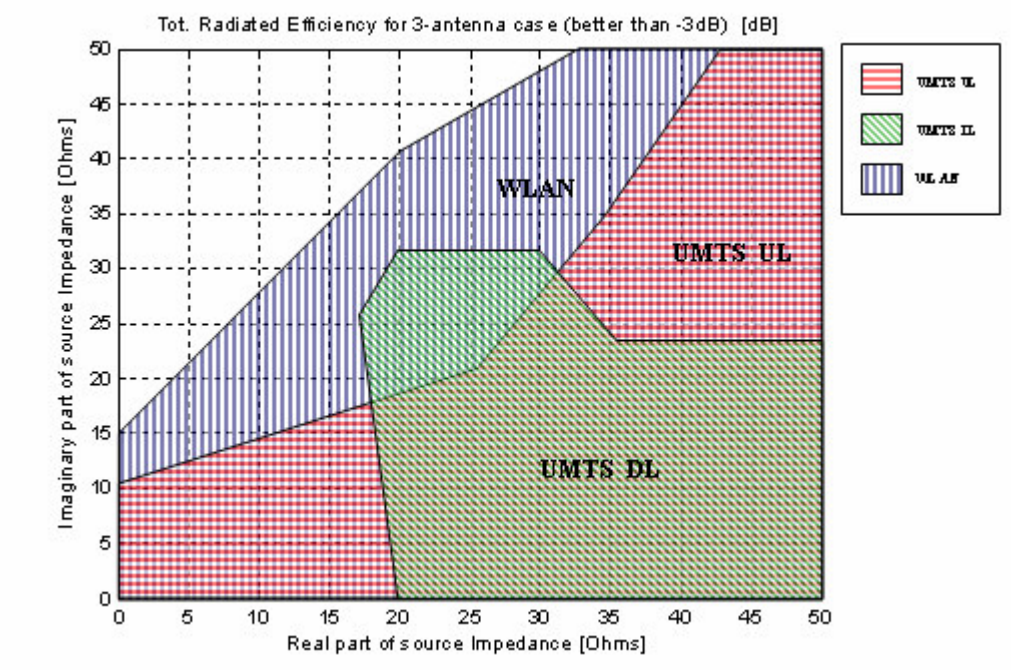

Figura 6.20: Representación de la eficiencia de radiación total mejor que -3 dB para el caso de 3 antenas

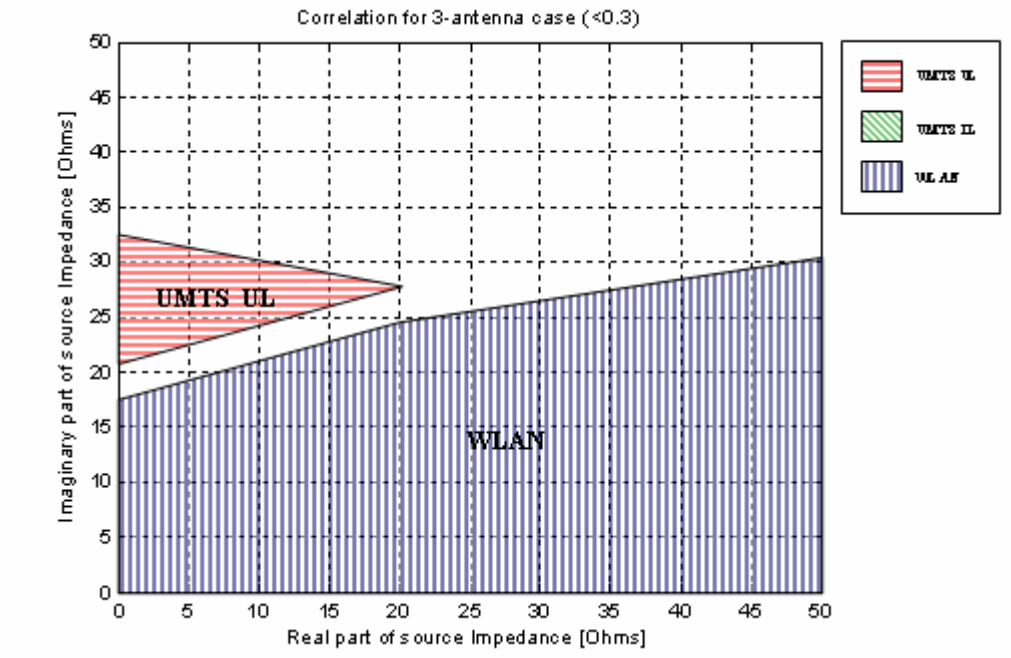

Figura 6.21: Representación de la correlación mejor que 0.3 para el caso de 3 antenas

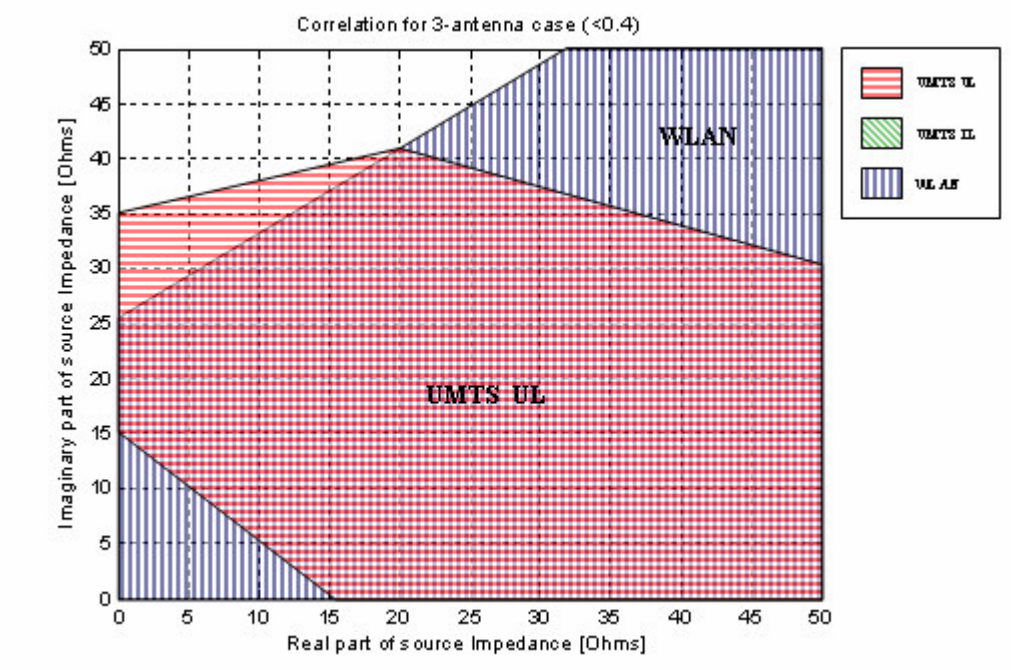

Figura 6.22: Representación de la correlación mejor que 0.4 para el caso de 3 antenas

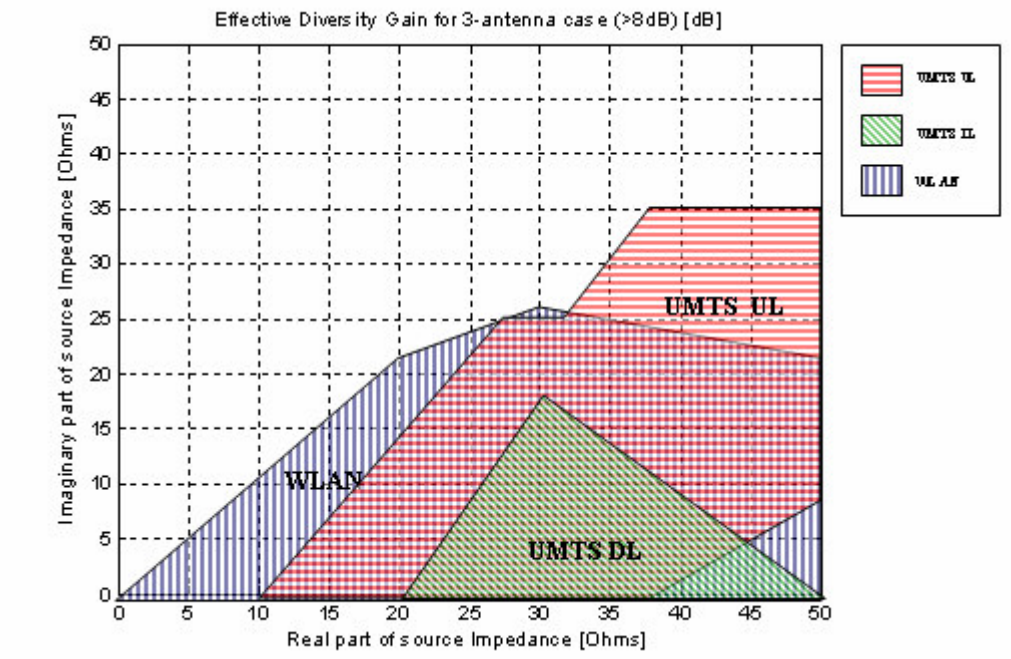

Figura 6.23: Representación de la ganancia efectiva obtenida por diversidad de muestras mayor que 8 dB para el caso de 3 antenas

D.2.2. Mediciones

En esta sección se incluyen algunos de los resultados medidos del modelo real utilizado, el cual incluye las 5 antenas colocadas en la parte superior del ordenador portátil separadas 2.8 cm. Debe tenerse en cuenta que para obtener resultados correctos del analizador de redes se modificaron ligeramente las dimensiones de las antenas simuladas, así se consigue un ajuste de los requerimientos en las bandas de frecuencia deseadas.

D.2.2.1. Analizador de redes:

El análisis del funcionamiento del modelo se realizará estudiando las antenas de dos en dos. Para ello, se conectarán los dos puertos del analizador de redes a dos de las antenas del portátil, terminando el resto de puertos con impedancias de 50 Ω. Obtendremos los parámetros S y representaremos los coeficientes de reflexión de los 5 puertos. Como era de esperar, para todas las frecuencias límite de las bandas estudiadas dicho coeficiente de reflexión es menor que -6 dB.

Otro parámetro interesante que podemos obtener es el acoplamiento entre pares de antenas. Como puede verse en las Figuras 6.25 a 6.29, el acoplamiento es mayor entre puertos vecinos, y en el caso de las antenas 4 y 5, dicho acoplamiento es mayor de -10 dB. Por tanto, para mejorar el funcionamiento del sistema conviene emplear el procedimiento empleado en la parte de simulaciones. Así, variando la impedancia de entrada podremos mejorar las prestaciones del sistema. En nuestro caso, no se incluyen resultados reales del procedimiento por falta de tiempo.

D.2.2.2. Cámara de reverberación:

Tras medir el modelo con las 5 antenas en la cámara de reverberación, se obtiene la eficiencia de radiación, la correlación y la ganancia efectiva obtenida por diversidad de muestras. Como puede verse en las tablas de la sección 6.2.2, la correlación entre cada par de puertos es pequeña, como esperábamos. Sin embargo, no podemos comparar directamente los valores simulados y los medidos ya que la correlación obtenida mediante medidas en la cámara de reverberación corresponde a la correlación en potencia, mientras que el valor obtenido mediante simulaciones corresponde a la amplitud de la correlación compleja. La relación que existe entre ambas puede encontrarse en la sección 2.1.7.

D.3. Conclusiones

Tras finalizar este proyecto, quisiera comentar en primer lugar que las antenas diseñadas no tienen aplicación comercial ya que fueron diseñadas e implementadas como un estudio para evaluar el procedimiento comentado. Dicho procedimiento puede ser empleado en el futuro en otros diseños reales para optimizar sus resultados. El método propuesto puede ayudar en el diseño de sistemas con diversidad espacial tan sólo variando la impedancia de entrada. Además, se puede aplicar como método para influenciar la correlación en sistemas MIMO.

Uno de los objetivos iniciales era probar el correcto funcionamiento del MPA usando los patrones de radiación en campo lejano importados de CST. Éste es el primer proyecto que integra ambos programas y además, el primero desarrollado empleando dicho software desarrollado en CHASE: MPA. Por ello, es importante mencionar el tiempo que se ha empleado comprobando la correcta funcionalidad del mismo, incluso colaborando en la depuración de algunos errores encontrados. Por otro lado, ha sido imposible emplear la herramienta de optimización que próximamente incluirá el MPA, ya que aún no funciona correctamente y por ello, durante el desarrollo de este proyecto se optó por implementar manualmente otro método de optimización.

Como hemos comprobado, el espacio entre las antenas afecta fuertemente al acoplamiento entre ellas y por tanto, a la eficiencia de radiación, a la correlación y a la ganancia efectiva obtenida por diversidad de muestras.

Para el caso de 5 antenas, no sólo se ha simulado su funcionamiento, sino que se ha implementado un modelo que ha podido medirse. Debido a que el cobre de las antenas no se ha cortado perfectamente, ni éstas eran exactamente iguales, que las soldaduras para añadir el puerto pueden introducir pérdidas y además el cable coaxial introduce algunas pérdidas de inserción, existen pequeñas variaciones entre los resultados simulados y medidos. Sin embargo, en ambos casos la correlación es baja entre todos los pares de antenas. En el caso de la eficiencia de radiación, la cámara de reverberación da información de los valores medios para todo el rango de frecuencia (de cada una de las bandas), mientras que los valores simulados son individuales para una determinada frecuencia, por ello, los resultados también pueden diferir de algún modo. Esta cámara de reverberación también continúa en fase de desarrollo y ofrecerá en el futuro mediciones de nuevos parámetros que hasta ahora son complicados de medir y que aportaran gran información para la simulación de antenas.

Las 5 antenas simuladas y medidas estaban separadas 2.8 cm y el acoplamiento entre ellas fue menor de lo esperado. Por tanto, variando la impedancia de entrada de los puertos y evaluando el funcionamiento del sistema, se ha podido comprobar que la eficiencia de radiación es el parámetro que más afecta a la ganancia efectiva obtenida por diversidad de muestras. Tomando como ejemplo los puertos 1 y 5 a 1.95 GHz y mirando la Figura A.12, puede verse que la correlación entre ellas es muy baja. Por tanto, fijándonos en la ganancia efectiva obtenida por diversidad de muestras, Figura A.13, podemos ver que está afectada por la eficiencia de radiación de ambos puertos (Figuras A.1 y A.2). Es decir, el área donde se obtiene el máximo de la ganancia efectiva obtenida por diversidad de muestras, corresponde con las zonas donde se encuentran los máximos valores de eficiencia de radiación de ambas antenas.

En las antenas de los extremos se observa un comportamiento diferente ya que dichas antenas sólo tienen un vecino. Por ello, para realizar el estudio de la ganancia efectiva obtenida por diversidad de muestras de dichas antenas se empleó la ecuación (2.5).

Tal y como se ha comentado en la sección anterior, estudiando todos los gráficos obtenidos, hemos conseguido encontrar regiones donde la variación de la impedancia de entrada permite un funcionamiento correcto del sistema según las especificaciones iniciales de las antenas. Es decir, que seleccionando uno de los valores incluidos en la región común a todas las bandas de frecuencia encontramos la optimización del sistema. Sin embargo, en ocasiones debe buscarse un compromiso entre los parámetros a optimizar, ya que quizás puede no ser viable optimizarlos todos a la vez.

En el segundo caso, simulando el modelo con 3 antenas separadas entre ellas 1 cm, el acoplamiento ha aumentado, así como la correlación, afectando también a la eficiencia de radiación. Si tomamos un valor de correlación de 0.3, se comprueba que no existe una región óptima que sea común a todas las bandas de frecuencia para los valores de impedancia de entrada estudiados. Por ello, debe decidirse la criticidad de la correlación y o bien aumentar el margen permitido de la misma o bien tratar de optimizar otros parámetros. Es decir, que incluso con una correlación mayor a 0.3 sí que encontramos regiones comunes a todas las bandas de frecuencia que ofrecen una ganancia efectiva obtenida por diversidad de muestras mayor que 8 dB para determinados valores de impedancia de entrada.

Por tanto, empleando el software mencionado hemos desarrollado un método que permite estudiar la influencia de la impedancia de entrada en la eficiencia de radiación, en la correlación y en la ganancia efectiva obtenida por diversidad de muestras. Si las antenas están situadas muy cerca unas de otras, quizás es deseable establecer un compromiso entre las especificaciones que se desean cubrir. Debe tenerse en cuanta, que como se ha visto, el parámetro limitante en la ganancia efectiva obtenida por diversidad de muestras es la eficiencia de radiación.

Cogiendo el ejemplo de la ganancia efectiva obtenida por diversidad de muestras, si la distancia entre las antenas se reduce, podemos tener aún así una ganancia aceptable modificando la impedancia de entrada de los puertos.

Como se ha explicado anteriormente, la máxima ganancia efectiva obtenida por diversidad de muestras aparece en diferentes áreas de las curvas de nivel calculadas para cada banda de frecuencia. En el caso de UMTS, podría ser útil separar el transmisor y el receptor para mejorar el funcionamiento de las antenas.

Este estudio ha establecido un método que puede aplicarse a otros muchos ejemplos y casos, que permitirían estudiar el funcionamiento de las antenas de diversos terminales móviles. Trabajando con simuladores electromagnéticos de 3D, como CST, podemos usar MPA para calcular de una forma rápida las características más importantes de las antenas incluidas en un diseño. Este software, aunque aún se encuentra en fase de desarrollo, permitirá ahorrar mucho tiempo a la hora de calcular eficientemente parámetros como los utilizados en este proyecto. En nuestro caso, el estudio de la influencia de la impedancia de entrada se ha realizado de forma manual, empleando Matlab para encontrar las regiones comunes que daban valores aceptables de funcionamiento. Los resultados simulados pueden compararse con los medidos de la cámara de reverberación que se emplea ofreciendo gran fiabilidad en las mediciones de terminales móviles. Para otros ejemplos, se puede seguir el mismo procedimiento modificando simplemente el modelo a evaluar.